A Neural Model of Human Prehension

Althea Ruth Iberall

Laboratory for Perceptual Robotics
Department of Computer and Information Science
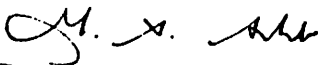University of Massachusetts
Amherst, Massachusetts 01003

ii

A Neural Model of Human Prehension

A Dissertation Presented

By

Althea Ruth Iberall
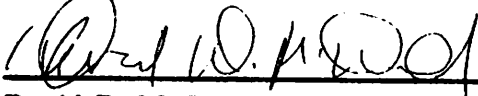
Approved as to style and content by:

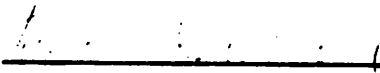Michael A. Arbib, Chairperson of Committee

---

Andrew G. Barto, Member

David D. McDonald, Member

Paul Herron, Outside Member

W. Richards Adrion, Department Head
Computer and Information Science

To my parents Arthur and Helene Iberall
who always said I could do it
Now I believe them

*"a hand before me
has experienced much—
silent and secret."*

-Japanese Haiku

ACKNOWLEDGEMENTS

ABSTRACT

A NEURAL MODEL OF HUMAN PREHENSION

FEBRUARY 1987

ALTHEA RUTH IBERALL, B.A., NEW YORK UNIVERSITY

M.S., BOSTON UNIVERSITY

Ph.D., UNIVERSITY OF MASSACHUSETTS

Directed by: Professor Michael A. Arbib

Behavioral studies have shown that as the human hand reaches out to grasp an object, it preshapes for the anticipated interaction. As it gets close to the object, it encloses it. In order to evaluate such studies, a model is needed which can be used to analyze grasping behavior characteristics as they relate to object and task properties. We present here a framework for studying human prehensile postures and movements, which is based on architectural features of the hand. While a grasping task will involve many fingers, we note that fingers group together to apply an opposing force against other fingers or against task torques. We call these groupings virtual fingers, and we call the coordinate frame in which they move an opposition space. This space provides a description of the ways virtual fingers can apply oppositions, as well as a method for defining the relevant object/task properties. In order to test this style of analysis, we performed behavioral experiments, and show here how our framework can be used by motor and sensory psychologists as an effective method for analyzing grasping behaviors.

To account for the coordination and control of these complex movements, we use schema theory. A perceptual schema must choose where to place the hand relative to the object. We show how such a choice could be performed by a neural network, simulated on a computer here using an Amari-Arbib cooperation/competition model. The preshape schema then drives the virtual fingers into general ballpark configurations, and the enclose schema fine tunes the virtual

It took Picasso's genius to capture a hand (the upper one) both pre-shaping and enclosing an object at the same moment in time.

TABLE OF CONTENTS

LIST OF FIGURES

xiii

LIST OF TABLES

CHAPTER I

INTRODUCTION

"The hand joins, in the same anatomical structures, the power of knowledge and action. It is both the origin of very precise information and the irreplaceable executor of the brain. The hand is the privileged messenger of thought."

— Raoul Tubiana

Over the last 30 years, artificial intelligence research has been trying to capture key aspects of higher cognitive thought [e.g., Quillian 1968, Schank and Colby 1973, Minsky 1974, Simon 1977, Minsky 1986]. By making explicit our human understanding of the world, these researchers look towards building machines which can reason and draw conclusions. In the human brain, complex skills such as language, conceptual thinking, and planning have evolved as the information processing capability of the neocortex increased [see, for example, Eccles 1977, Arbib 1972]. At the low end of the cerebral cortex, close to the periphery, sits motor cortex. In the neurophysiological literature, it has been noted that the control of fine, fractionated finger movements [Kuypers 1973] is permanently impaired in monkeys, apes, and man by ablation of motor cortex [Denny Brown 1960]. Brinkman and Kuypers [1972] have shown that after a pyramidotomy (which cuts the direct pathway from motor cortex to the motoneurons), a monkey cannot grasp small objects between its fingers or make isolated movements of its wrist. As a way of gaining insight into neocortical organization, we therefore look at primate hand movement, with the goal of being able to suggest algorithms which could also be at work at various levels of human intelligence.

1

A parallel, if not equivalent, concern of our research is to understand the human hand as a versatile model for the design of robot hands. With its over 25 degrees of freedom, the hand represents a level of complexity beyond the capacity of existing mechanical hands and their controllers. Its structure and adaptability have been a constant source of fascination to people for hundreds of years [Bell 1832, Wood Jones 1920, Bunnell 1944, Napier 1956, Brun 1963, Tubiana 1981, etc]. Currently, research is underway to attempt to duplicate some its capabilities, in three finger designs [Salisbury 1982, Okada 1982] and four finger ones [Jacobsen et al 1984]. We feel that a study of the human hand, in terms of its functionality within particular contexts, will offer insights for the design of future dextrous robot hands.

We focus our studies on one specific type of hand movement, that of *prehension*, or the grasping of objects [Napier 1956, 1961]. As a movement, we note its complexity, which is in part due to it involving some level of object recognition. As the hand reaches to grasp a visually observed object, it preshapes into a posture suitable for the interaction (see Figure 1, from [Jeannerod 1981]). When it has been moved close enough by the arm, the hand encloses the object. Although the object presents to the central nervous system (CNS) many sensations, only a few properties seem to effect these prehensile movements. Such focused, goal-directed motor behavior is an example of the action-perception cycle [Arbib 1972, Neisser 1976]: expectations of the interaction between hand, arm, and object drive the reach and preshape, leading to new sensations and perceptions, which in turn lead to further expectations. In the field of artificial intelligence, goal-directed algorithms have been put forth with notable successes [see, for example, Shortliffe 1976, Hayes-Roth and Lesser 1977, deKleer et al 1977]. We therefore direct our research to determining what properties might be being perceived, and how the CNS might be translating them into goals for prehensile movements.

This dissertation approaches these issues by looking first at the primate hand
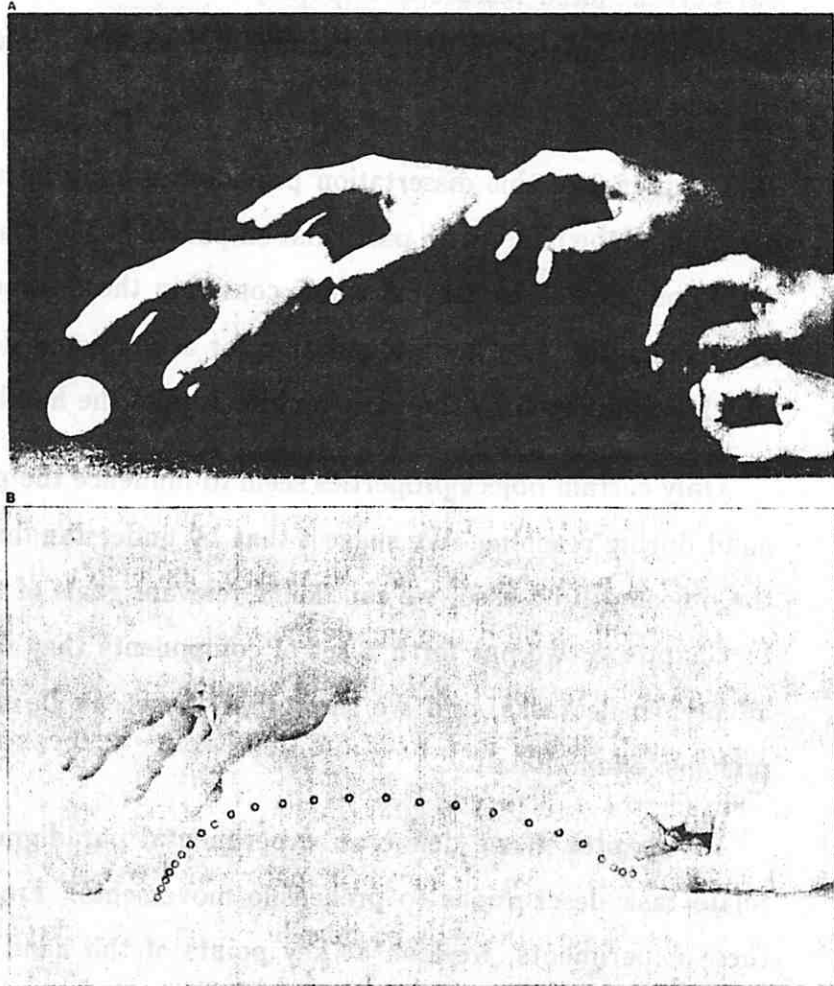
Figure 1: Reaching for a visually-perceived object [from Jeannerod 1981]

As the arm reaches for an object, the hand preshapes into a posture suitable for the interaction. The dots represent fixed time intervals, showing how the arm speeds up during the movement.

and then at the context within which it is used. Using a task-oriented approach, we focus on only a subset of the hand's features, creating a point of view for our current hand research. Hopefully in the future, we can relax some of the constraints imposed in this first study, and go on to look at other types of hand movements.

Chapter 2 of this dissertation provides an anatomical and physiological description of the hand, with particular emphasis on aspects that enhance prehensile functions, as well as aspects which constrain those same movements. The goal of this chapter is to lay a foundation for a functional description of prehension which is supported by the basic architecture of the hand.

Only certain object properties seem to influence the preshaped posture of the hand during reaching. We suggest that by understanding the task within which the object will be used, we can define relevant goals of the preshape movement. In Chapter 3, we put forth a set of components that we believe are generic to all prehensile tasks, and we show that these can be mapped into basic hand prehensile functionality.

In Chapter 4, we define an experimental paradigm which we are using to relate task descriptions to prehensile movements. From the data collected in these experiments, we look at key points of the hand's trajectory. This type of data can be used to quantify the mapping of object and task properties into hand configurations, in order to look at how constraints are imposed on the movements. We go on to suggest other experiments which could be performed by motor psychologists interested in studying prehensile movements.

Schema theory [Arbib 1981] provides a vocabulary for describing interactions between perceptual and motor structures. In Chapter 5, we describe a coordinated control program involving interacting schemas for prehensile tasks. As part of that coordinated control program, a model for a selector mechanism is described that is effective at determining prehensile goals.

Although somatotopic maps in various cortical and subcortical areas have been put forth as representations of the body within the environment, it is not yet clear what is the nature of the information being represented in these maps, what is transmitted between them, and how motor behavior emerges from such a representational scheme. A schema-theoretic approach to modelling the CNS offers a top down analysis to these questions. Instead of looking at cortical and subcortical areas individually, trying to glean their information processing contribution from an analysis of neuronal activity, Arbib suggests looking at the functional requirements of the system. After identifying functions, schemas as units of motor behavior are defined to account for the ability of the system to perform such functions. Multiple cortical and subcortical areas contribute to a given schema, and it is in the interaction of these schemas that the motor behavior emerges. The task, then, for the brain modeller is to not only identify potential schemas which constitute the motor behavior, but to also show how these schemas map into the known neural circuitry. In Chapter 6, we show how the models of Chapter 5, using the framework of Chapter 3, could possibly be laid out in the central nervous system. The plausibility of this scheme is supported by the neurophysiological literature through lesion and microstimulation studies. Neurophysiological experiments are suggested that would help to support the model.

Finally, in Chapter 7, we conclude by making suggestions as to how this study can be used by researchers from various fields. Neurophysiologists could help prove or disprove the models presented by trying the suggested experiments and looking at their data with our point of view. Psychologists and kinesiologists could use our framework in their experiments, helping to show its usefulness for addressing constraints acting on the hand. Roboticists developing dextrous robot hands might gain insight from this study, both for designing those hands as well as for controlling them. The human hand, represents a level of complexity beyond the capacity of mechanical hands and their controllers. Understanding

how the human hand works will both help in the design of future robots and in the understanding of the human brain.

CHAPTER II

WHAT IS THE HUMAN HAND?

"The functional architecture of the hand offers this organ multiple possibilities of adaptation, exploration, expression, and prehension."

— Raoul Tubiana

The human hand (Figure 2) consists of wrist bones (carpals), palm bones (metacarpals), and digit bones (phalanges) [see Kapandji 1982]. Joints between bones provide one or more degrees of freedom, or *dofs*. Examples include the distal interphalangeal joint (DIP), the proximal interphalangeal joint (PIP), the metacarpophalangeal joint (MP), and the carpometacarpal joint (CM). The number of *dofs* at each joint depends at least in part on the articular surfaces at the ends of the bones. Active movement at the joint is caused by both the extrinsic muscles in the forearm, which send tendons into the palm and digits, and the intrinsic muscles within the palm. Ligaments and sheaths around the bones make up the fibrous skeleton which both stabilize and restrain movement at the joints, while also guiding and containing the tendons. Movement is performed by tendons and muscles working together, developing a well-coordinated balance of forces around the joints, and preventing the ligaments and joint capsules from seeing excessive tension [Chao *et al* 1976].
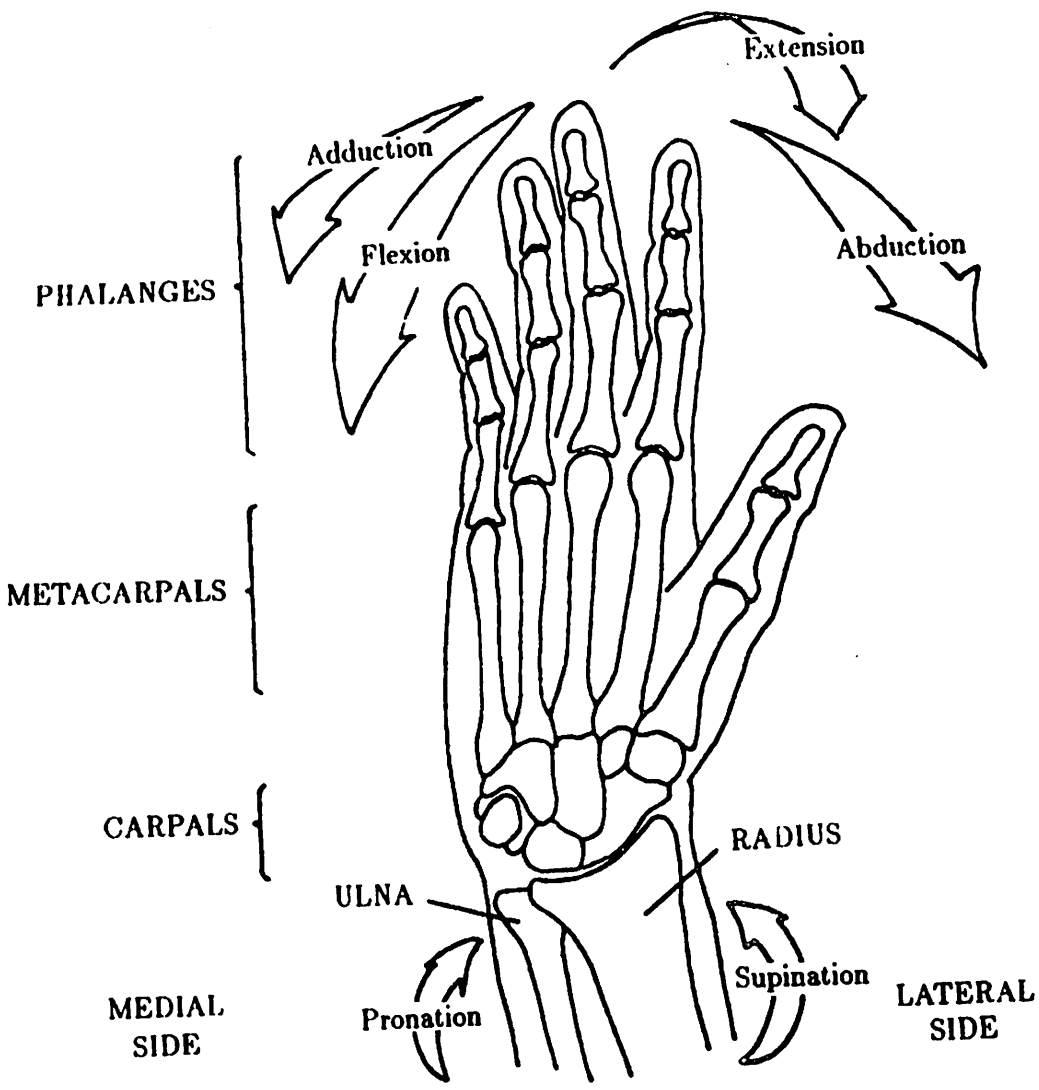
Figure 2: Structure and movements of the human hand

The digits of the human hand consist of bones called phalanges. The palm contains metacarpals, while the wrist contains eight small unevenly shaped bones called carpals. The surfaces between the bones, constrained by ligaments and tendons, allow various *dofs*, or movements in different directions.

§1. The Need for a Functional Prehensile Classification

When the human hand is used in prehension, particular styles of postures have been noted, as seen in Table 1. Schlesinger [1919] put forth a now classic taxonomy which tried to incorporate two critical notions, that of object shape and that of particular hand surfaces. McBride [1942] stressed the importance of which hand surfaces are being brought into play. Griffiths [1943] suggested a taxonomy based on the shape the hand takes on, while Slocum and Pratt [1946] strove for a simple description of postures. One of the most widely referenced taxonomies is that of Napier [1956]. Napier defined precision grip and power grip as basic prehensile postures, with the hook grip as a non-prehensile posture for grasping. Landsmeer [1962] extended Napier's concept of the precision grip to one of precision handling, thus bringing in the dynamic aspect of the movements during fine translations and rotations. In the robotics literature, Lyons [1985] suggests encompass grasp, lateral grasp, and precision grasp, and Cutkosky and Wright [1986] has further broken down precision grasping into 7 types and power grasping into 9 types. While these classifications are useful as broad general descriptions, they do not provide a useful mechanism for describing the goal of the prehensile posture. We define this goal to be *the bringing to bear of functionally effective forces against an object for a given task consonant with the hand's anatomical constraints* [Iberall, Bingham, Arbib 1986].

In our own first attempt at a prehensile classification [Iberall and Lyons 1984, 1985], we suggested six postures, searching for a way to capture the issue that hand postures are not as discrete as most classifications suggest. Objects are not as regular as Schlesinger or Griffiths presume, and yet the hand can pick up a vast range of object shapes. Cutkosky and Wright [1986], in an extremely thorough analysis of tool usage, attempt to solve these problems by making even more explicit the object shape and size, and the way the hand applies the forces. But forces are subtly applied at multiple places around an object, indicating

Schlesinger 1919	cylindrical grasp spherical grasp hook prehension	palmar prehension tip prehension lateral pinch
McBride 1942	whole hand grasping palm, digits grasping	thumb, finger grasping
Griffiths 1943	cylinder grip ball grip ring grip	pincer grip pliers grip
Slocum and Pratt 1946	grasp pinch	hook
Napier 1956	power grasp precision grasp	hook grasp
Landsmeer 1962	power grasp precision handling	hook grasp
Iberall and Lyons 1984	basic power modified power basic precision/power	basic precision modified precision/power fortified precision/power
Lyons 1985	encompass grasp precision grasp	lateral grasp
Cutkosky and Wright 1986	sm diam. heavy wrap lrg diam. heavy wrap medium wrap adducted thumb wrap light tool wrap disk power spherical power hook	5 finger precision 4 finger precision 3 finger precision 2 finger precision disk precision spherical precision tripod prec sion lateral pinc a

Table 1: Prehensile classifications

Within various disciplines taxonomies have been developed to describe human hand postures. These include anthropology, biomechanics, hand surgery, and robotics.

to us that more than one type of grip is being used at a time, instead of the either/or nature of these classifications. Even Napier stated that 'although in most prehensile activities either precision or power is the dominant characteristic, the two concepts are not mutually exclusive' [Napier 1956, p 906].

These various taxonomies attempt to capture the complex dexterity of a human hand used in prehensile tasks. They all fail in their inability to explain all the exceptions which usually occur due to task constraints. They also lack a mechanism for describing the complete grasping process, from perceiving an object, to preshaping the hand, to enclosing the object, to lifting, and to manipulating the object. We feel that a classification is needed that describes a prehensile posture in goal-directed terms; i.e., in terms of how many forces are needed in the task, in what direction they are to be applied, and at what strength they must be applied. The style of posture chosen must then match the task requirements (or the forces and degrees of freedom needed) with the hand's capabilities (the forces and degrees of freedom available).

However, while we find these classifications lacking in their ability to describe task constraints and the complete prehensile movement, we note their commonality. The very fact that classifications of this type can be made, describing prehensile postures in stereotypical and limited terms, suggests to us that there are anatomical and physiological constraints in the hand-object interaction, which the CNS in turn uses. Thus, we turn to an architectural study of the hand.

§2.   Architectural Analysis of the Human Hand

Basic postures seem to be stereotypical and limited in number, and so we would suggest (as argued by [Chao *et al* 1976]) that the chosen postures will likely be ones where joints are stabilized and where forces can be applied opti-

mally without undue stress and strain on the ligaments, tendons, and muscles. One such posture is an equilibrium position between the agonist and antagonist muscles, called the *position of function* [Kapandji 1982]. An example of a position of function is seen when the fingers are naturally relaxed, with the metacarpophalangeal joint being flexed to about 40°, in what is called the position of rest [Tubiana 1981].

Another stress-limiting posture is when articular surfaces are coadapted, an example of which is seen when the wrist is approximately 30° adducted (also, when 40° extended). In these positions, the articular surfaces of the proximal row of carpals and the radius are coadapted, thus allowing any force directed at the wrist to be directly transferred into the radius. In this position, little active force is needed to maintain contact between these two surfaces. Such an attitude is typically seen as people grasp objects, as noted in the literature [Napier 1956, Kapandji 1982].

Articular support can either enhance or hinder prehensile movements. The carpals form an arch (see Figure 3a), allowing the tendons of the extrinsic flexors into the hand. This arch creates three basic columnar supports as seen in Figure 3b: one for the thumb and index finger, one for the middle finger, and one for the ring and little fingers [Kapandji 1982]. The advantage is two-fold: first, the hand is smaller since fewer muscles reside in it [Tubiana 1981], and secondly, the arch acts as a strong base for finger movement [Kapandji 1982]. While the lateral column branches into two subcolumns in the distal row of carpals, the medial column does not. Differentiated strength is given to the thumb, index, and middle fingers, with little articular differentiation at the carpal level provided to the ring and little fingers. However, a disadvantage exists in this scheme because the position of the wrist affects the tension of the tendons, and thus the force output of the extrinsic muscles.

In Table 2, the relative amount of force available in various wrist positions
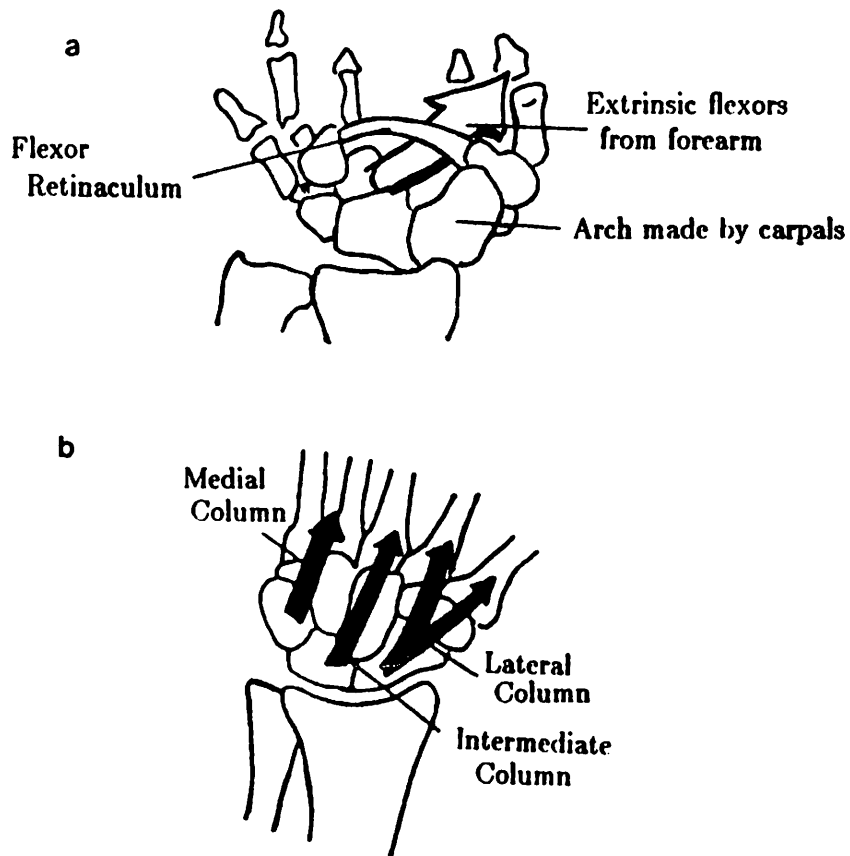
Figure 3: Architectural features of the human hand

(a) The carpals are oriented in such a way to let tendons of the flexor muscles to enter the hand from the forearm. The *flexor retinaculum* ligament acts as a band to contain the flexors. (b) The carpals provide support for the metacarpals. Due to their uneven structure and most likely, evolutionary pressures, three basic columns are noted. See text.

	Neut.	Ext.	Add.	Flex.	Abd.
Bunnell 1942		best (20°)	best (10°)		
Anderson 1965	best				
Slovly 1967			best (30°)		
Kraft and Detels 1972	best	best		least	
Hazelton et al 1975	2nd (0°)	3rd-4th (< 60°)	best (21°)	least (< 45°)	3rd-4th (14°)
Pryce 1980		best (0 − 15°)	best (0 − 15°)		

Table 2: Influence of wrist positions on relative force output

Various researchers have studied the influence of wrist position on the amount of force available at the fingers. Two of the wrist's *dofs* (flexion/extension and adduction/abduction) provide four different directions it can be moved. The angles at which the measurements were taken are noted in the parentheses. Hazelton *et al* did not use a fixed angle, but let each subject use a different angle, within the range noted. The general conclusion is that more force is available at the fingers if the wrist is slightly extended (dorsiflexed) and/or slightly adducted.

is summarized. Wrist positions in this table were measured as angles (noted in parentheses) relative to the position when the hand is sticking straight out, aligned with the forearm. Although these experiments were all carried out using different wrist angles, it is obvious from the table that in dorsiflexion (wrist extension) and/or ulnar deviation (wrist adduction), the amount of force that the fingers are able to apply is greater than in other positions. Hazelton *et al* [1975] note that the relative amount of force available at each finger remains constant across wrist positions (25% at the index, 33.5% at the long finger, 25% at the ring finger, and 16.5% at the little finger).

The long extensors (*extensor digitorum communis*) have a common origin within the forearm, as do the long flexors of the fingers (*flexor digitorum sublimis* and the *flexor digitorum profundus*) thus causing movements of the fingers to be interdependent. Of the fingers, only the index and the little fingers have additional individual extensors (*extensor proprius indicis* and *extensor digiti minimi*), thus allowing some measure of independence. The little finger also has an individual extrinsic flexor (*flexor digiti minimi*), which moves synergisticly with the *abductor digiti minimi* to abduct it. The index finger, on its own carpal subcolumn, has more independence than the little finger which is on a column with the ring finger. Movement of the little finger allows the cupping of the palm around an object (using the *opponens digiti minimi*), allowing a finer control of the molding of the hand's shape to the object. This cupping movement is enhanced by the extra degree of freedom the little finger has at the carpometacarpal joint. The thumb can be moved in different directions during flexion, allowing it to fit around a variety of object shapes [Kapandji 1982]. However, when the fingers are fully flexed, an interesting interaction occurs between tendons and ligaments; the ligaments are tensed up and no longer allow sideways movements (adduction/abduction) of the fingers. It is this sideways movement which gives the hand the ability to grasp larger objects.

The palm gives the fingers leverage, separating the thumb from the fingers. It lets the thumb move into a position of opposition to the fingers, due to the thumb's lower position on the palm, its articular surfaces, and smaller stature. As a result of this movement of the thumb (caused by four muscles, the *abductor pollicis longus*, the *abductor pollicis brevis*, the *opponens pollicis*, and the *flexor pollicis brevis*), the size and shape of the palm are changed, which affects the directionality of the forces applicable to objects through the palm. We note, however, that stabilization of the thumb is quite different from the rest of the fingers and quite complex [Kapandji 1982]. At the carpometacarpal joint of the thumb, four ligaments and muscles maintain articular contact by axial compression. The style of forces acting at the carpometacarpal joint is much like balancing a tent pole from external rigging [Kapandji 1982].

Movement of both the fingers and thumb tend to bring the pads into the same plane. These pads are highly specialized for prehension, in that they provide friction, due to the epidermal ridges, sticky self-lubricating excretions through the tops of the ridges, and their ability to comply [Quilliam 1978, Glicenstein and Dardour 1981]. Being padded, these surfaces have a good measure of elastic compliance, which tends to increase the amount of friction between the hand surface and the surfaces of objects grasped. This automatically supplies a force sufficient to counteract small amplitude perturbations of the object, useful in stable grasping [Hanafusa and Asada 1982, Moore 1972, Fearing 1983, 1986]. The lubricant is greasy, having good adhesive qualities at low shear velocities, enhanced by the hills and valleys of the ridged surface which extends the total shearing surface area [Moore 1972, 1975]. At high shear velocities, friction is reduced, thus minimizing wear and tear of the hand surface.

Comaish and Bottoms [1971] analyzed the coefficient of friction between skin and various materials in order to determine if it obeys Coulomb's law, which states that the tangential force of friction is constrained to be no greater than the

product of the normal force with the coefficient of static friction [Amontons 1699]. They found that the frictional force is not proportional to the load, and that, for some materials, the static coefficient of friction increased with the area. While their data showed a proportional response for loads over 100 grams for *in vitro* skin, the data for *in vivo* skin was definitely non-linear. Skin has been shown to be visco-elastic [Wilkes *et al* 1973], meaning that it is capable of both deformation and flow in response to an applied load. Thus, as Coulomb's law holds for plastic deformations between materials, living skin does not obey Coulomb's law.

The pulps of the fingers also have numerous tactile receptors, more so than most other parts of the body, thus giving the CNS much information about the object with which they come into contact [Johansson and Vallbo 1983]. The trajectory of the pads of the thumb and fingers is highly complex, changing direction as the digits move. This is due to the metacarpophalangeal and interphalangeal articulations and the ligaments [Kapandji 1982], which as a result couple finger interphalangeal joint movements. So, while each finger has four *dofs*, they are highly coupled. As a result, it takes more effort on the part of the muscles, and the CNS controlling them, to not bring the finger pads toward the thumb.

In conclusion, the shape the hand takes on during prehension depends on a large variety of architectural issues. The different types and orientations of the articular surfaces of the bones affect how they can be used to minimize stresses and strains on ligaments, tendons, and muscles. Forces are directed by muscles and tendons to apply leverage in such a way as to get the maximum mechanical advantage at some minimized level of stress and strain. Subtle couplings between articular surfaces, tendons, and ligaments either enhance or detract from the independent use of available *dofs*, thus constraining the way forces can be brought to bear. The frictional component of force is enhanced by directing pad surfaces towards the object, which also increases the amount of information supplied to the CNS. Thus, stereotypical postures, seen by so many researchers, are likely a

result of these, among other, architectural issues.

The hand of *Homo Sapiens Sapiens* represents millions of years of evolutionary pressures and changes [see, for example, LeGros-Clark 1959, Abbott 1970, Musgrave 1971, Phillips 1971, Lewis 1977, Marzke 1983]. LeGros-Clark [1959] notes the development of the pentadactyl (five-fingered) hand, the replacement of claws by nails, and the specialization of the finger pads. Other signs of refined functionality have been noted due to changes in tendon insertions [Abbott 1970], the remodelling of joints [Lewis 1977, Marzke 1983], and intradigital proportions between phalanges [Musgrave 1971]. While the study of evolutionary pressures presents one method for understanding human hand functionality, we suggest that clues for this research might be discovered by looking deeper into stereotypical postures. We note, however, that under degenerate conditions, when fingers are either totally or partially missing, different postures emerge, as the CNS modifies its strategical use of the hand. We suggest that it is not the posture that matters as much as the problem that the posture is addressing. As Wood Jones notes, "The difference between the hand of a man and the hand of a monkey lies not so much in the movements which the arrangement of muscles, bones and joints makes it possible for either animal to perform, but in the purposive volitional movements which under ordinary circumstances the animal habitually exercises" [Wood Jones 1920]. It is therefore our goal to understand what problem this posture is a solution of.

CHAPTER   III

FUNCTIONAL ANALYSIS OF PREHENSILE MOVEMENT

*"Our hands become extensions of the intellect, for by hand movements
the dumb converse, with the specialized fingertips the blind read; and
through the written word we learn from the past and transmit to the
future."*

- Sterling Bunnell

Prehension involves applying opposition to the forces arising during interaction with an object, and stable prehension adds the requirement that opposition is applied by hand surfaces directed against other hand surfaces [Iberall, Bingham, Arbib 1986]. We call the applications of forces between hand surfaces *oppositions*, and will note below that there are only a few basic ways humans apply oppositions. Preshaping the hand to grasp an object sets up the required oppositions for the task. Enclosing the hand around an object works within the area defined by the preshape. It involves increasingly flexing the fingers and thumb until they contact the object and can apply the required force. What determines the shape the hand takes on during these processes, and how is preshaping and enclosing achieved?

§1.   Virtual Fingers

To gain some intuition into this question, we initially observed three tasks [Arbib, Iberall, Lyons 1985; Iberall, Bingham, Arbib 1986]. In the first task, which was to pick up different size mugs by their handles (see Figure 4), we noted

19

that three basic forces were being applied: one to provide a downward force from above the handle, one to provide an upward force from within the handle and, if necessary, a third force to stabilize the handle from below. We hypothesized that each of these functions could be represented as the task of a *virtual finger* [Arbib, Iberall, Lyons 1985]. The real fingers move in conjunction within a virtual finger, which has the same characteristics as real fingers. This both limits the degrees of freedom to those needed for a given task, and also provides an organizing principle for task representation at higher levels in the CNS. It is then a subtask at a lower-level to perform the actual mapping to real fingers, making task implementation somewhat "tool-free".

Figure 4 shows an example of the use of virtual fingers. In the four examples, the thumb, mapped into the first virtual finger or VF1, provides a force from above the handle. For a teacup with a very small handle (Figure 4a), only one finger will fit inside the handle. During the preshaping, only the index finger is mapped into the second virtual finger VF2, which provides an upward force from within the handle, and which opposes the force applied by VF1. The rest of the fingers map into VF3, which provides support for cup stabilization. For a coffee mug of the kind pictured in Figure 4b, two fingers will fit within the handle to form VF2, with the other two fingers becoming VF3. For the mug of Figure 4c, VF2 will comprise three fingers, while Figure 4d demonstrates the case in which all four fingers are mapped into VF2, with an empty mapping to VF3.

§2. Task Requirements

In [Iberall, Bingham, Arbib 1986], we looked at how the hand preshapes for the same object used in two different tasks, and saw that the way the object will be used also affects the preshape. The object was a medium sized cylinder standing on its base. The first task (Figure 5a-c) was to grasp the cylinder, pick
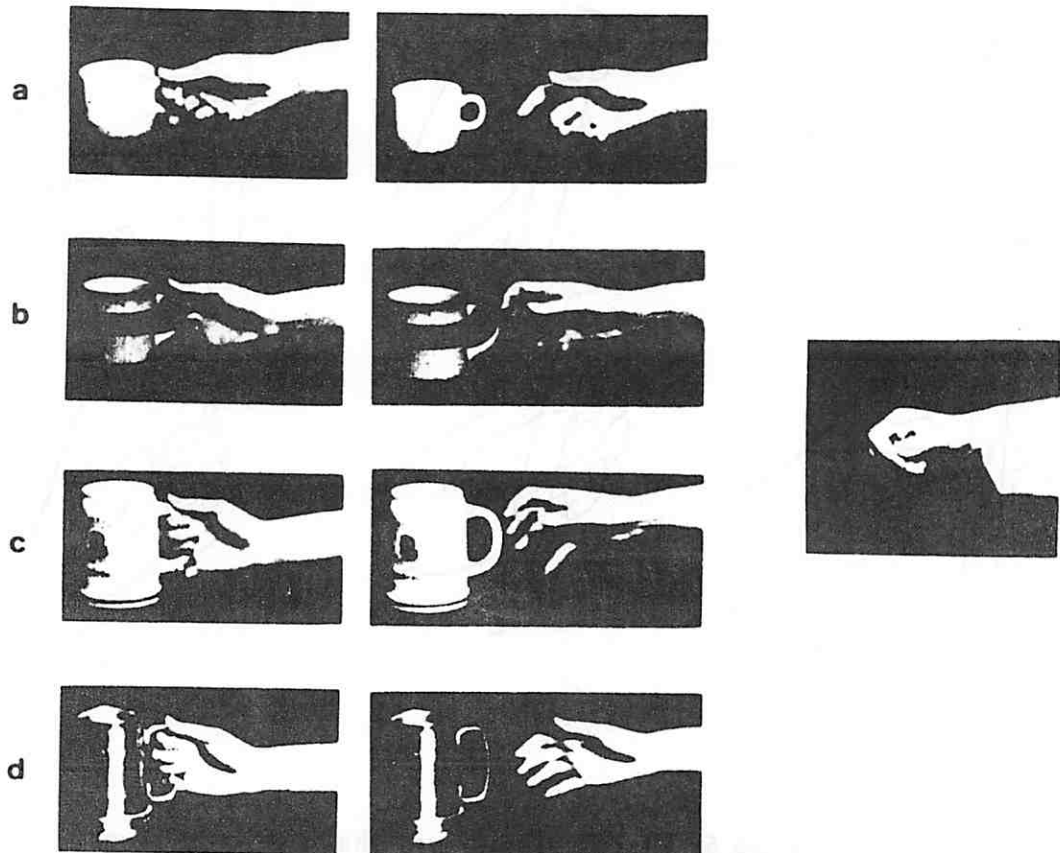
Figure 4: Preshaping and grasping mug using virtual fingers.

The number of real fingers which map into the second virtual finger (VF2) varies, depending on the size of the handle. In (a), the index finger maps into VF2. In (b), the index and middle fingers map into VF2. In (c), the first three fingers, and in (d), all four fingers.
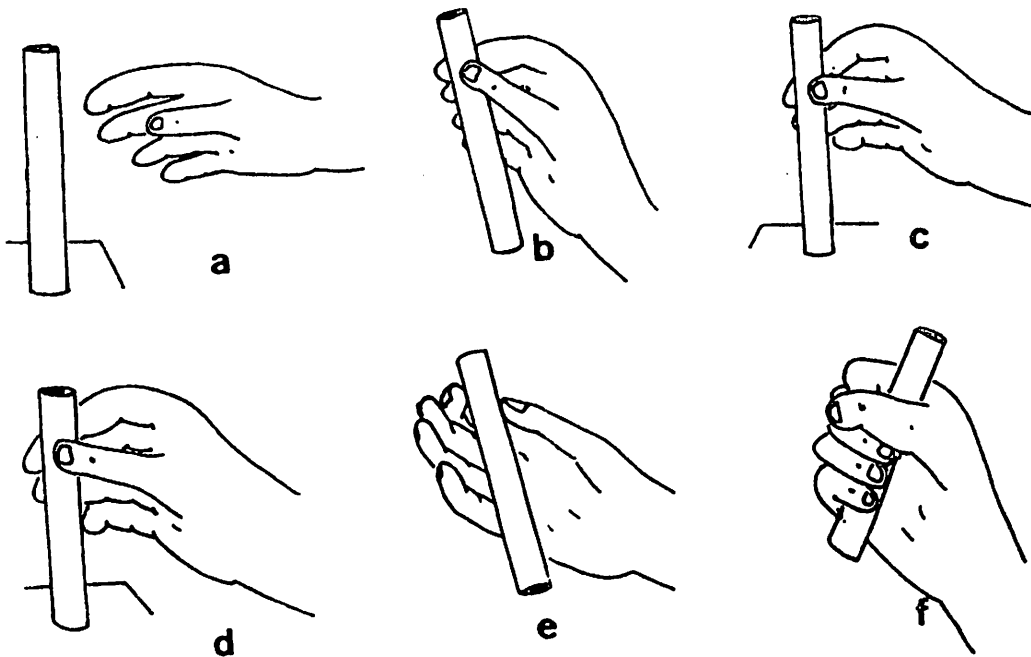
Figure 5: Place cylinder vs. shake cylinder task

(a-c) Place Cylinder Task. The hand preshapes into a precision grasp as the arm reaches toward the cylinder. It is lifted, carried to the target location, and placed on the circle. (d-f) Shake Cylinder Task. The cylinder is picked up in the same precision grasp. It is then rotated in the hand, clasped into a power grasp, and then shook.

it up, and set it onto a circle on which it could just fit (the "place cylinder" task). The cylinder, providing two opposing surfaces which were pinched between the thumb (VF1) and finger pads (VF2), was lifted (Figure 5b) and carefully guided onto the circle (Figure 5c). Typically, this precision grasp [Napier 1956] allows the object to be translated or rotated in the fingers and thumb so that fitting the cylinder onto the circle could be more easily and accurately accomplished. Such fine control is better effected by the fingers, a low mass system, than by the arm with its greater structural mass. The second task (Figure 5d-f) was to grasp the cylinder, pick it up, and shake it vigorously two or three times along its long axis (the "shake cylinder" task). The cylinder was initially grasped (Figure 5d) using the same precision grasp between thumb (VF1) and finger pads (VF2) as described above. However, once the object was securely lifted in the hand, a transition in grasping postures occurred (Figure 5e). Using an axis between thumb and index, the object was allowed to be rotated by gravity into the palm where first the ring and little fingers and then the middle and index fingers and thumb wrapped it in a secure grip against the palm (Figure 5f). This latter grasp, a power grasp [Napier 1956], provides a strong and stable grasp to counteract the forces that developed during the shaking task. The cylinder body again provided opposing surfaces to grasp, but this time the palm (VF1) and digits (VF2) were used. The thumb, pressing against VF2, secures the object.

It was our goal in this analysis to observe how the preshaping for stereotypical postures emerged. By using the same object under different conditions, we could begin to pinpoint which components of the task affected the shaping of the hand. We had hypothesized that these two tasks would lead to the distinct use of the precision grasp in the place cylinder task and of the power grasp in the shake cylinder task. We were surprised that it was not the case. The power grasp did not emerge in the initial hand preshape for the shake cylinder task.

We concluded that a task has multiple components. We called the group

of them the *task requirements* and noted that they consist of both functional constraints and physical constraints. Functional constraints are not so much a property of the object to be grasped, but more a property of how the object will be used within the task. A fundamental functional constraint on most prehensile tasks require that the object will not dropped. The posture used by the hand during the task must be able to overcome the anticipated forces acting on the object. Initially, during the lifting phase of a task, this is likely to just be the weight of the object. Later, during the actual task, there are likely additional inertial and/or coupling forces. Another functional constraint in some tasks, for example the place cylinder task, is to maintain the ability to stably manipulate the object.

However, underlying these functional constraints are physical constraints, based on properties of the object and on properties of the hand. From the object, these include such properties as surface compliance, texture, surface sizes, etc[1]. From the hand, different postures present different degrees of available force and of available *dofs*. Therefore, the shape that the hand takes on reflects these anticipated task requirements.

While it is not our goal to model how the CNS might do it, we suggest that perception of the object involves extracting a set of properties relevant to the person's *intent* for the use of the object in the task [Iberall 1986]. The perceived task requirements, which help determine the shape of the hand, consist, as noted above, of both functional constraints and physical constraints. As a first approximation toward quantifying these, we list a working set of task properties, as related to objects to be (see Figure 6):

---

[1] Some objects, such as a pair of scissors, have an internal *dof* as a property. Only single rigid bodies are being discussed here.

Opposable surfaces
length
radius of curvature
surface compliance

Opposition Vector
magnitude
angle (wrt approach vector)

Functional DOFs
direction of movement
range of movement
resolution of movement

Anticipated Forces
weight
inertial forces
torques at opposition vector
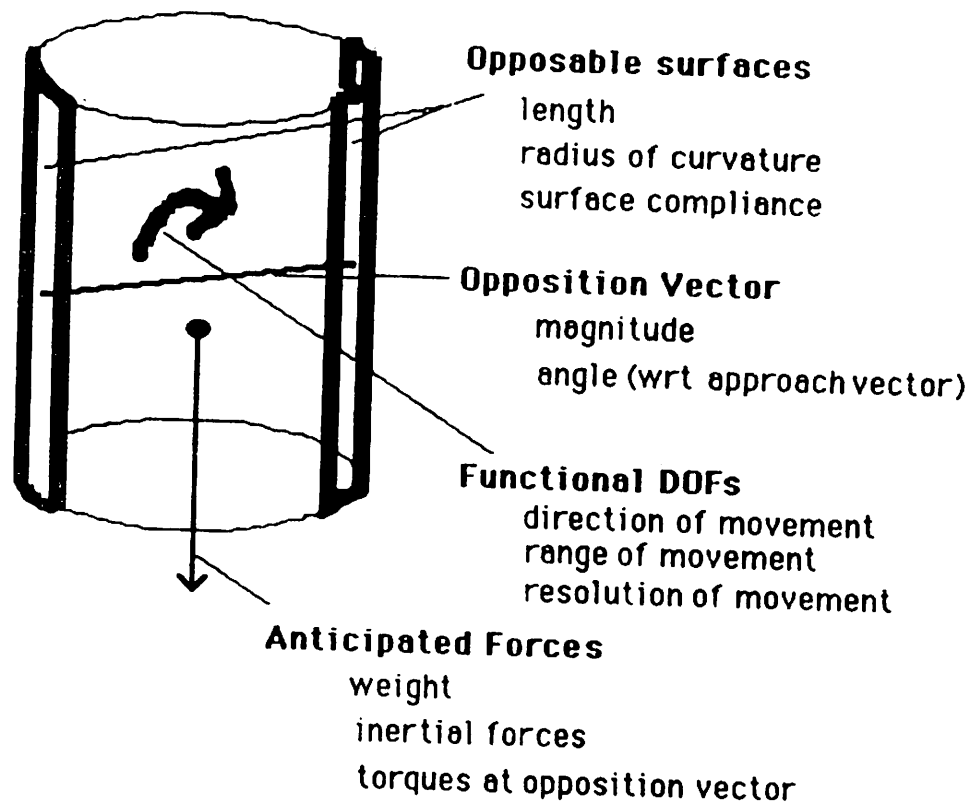
Figure 6: Task requirements

An object has features which are useful to prehensile tasks. These include opposition vectors, opposable surfaces, and a weight. A task defines how the object will be used; and features particular to the task include the *dofs* of the movement and forces that will arise during the task. A person's intention can be captured by representing the anticipated used of the object within the task.

- a set of opposable surfaces

  - length of each opposable surface
  - radius of curvature of surface
  - surface compliance

- an opposition vector V between pairs of opposable surfaces

  - magnitude of opposition vector V
  - orientation of opposition vector V, relative to the approach vector A

- functional degrees of freedom *dofs* about the opposition vector V

  - direction of movement
  - range of movement (how far is movement needed along *dof*)
  - resolution of control (how coarse can the movement be)

- a set of anticipated forces

  - object weight vector
  - inertial force vector
  - torques at opposition vector

Objects have many properties, but we suggest that for prehensile movements, an object is perceived by a limited number of properties. Between every two task-relevant opposable surfaces exists an opposition vector. The mug, for example, having a cylindrical body and a curved cylindrical handle, has an infinite number of possible opposition vectors between the infinite number of points along its surfaces. But, due to its construction and due to the person's intent of drinking from the top opening, it provides at least three solutions in terms of task requirements:

1. an opposition vector, between body surfaces slightly above the center of mass, will allow the task-related rotation (i.e., drinking from the opening) of that opposition vector while stably overcoming the object's weight vector. By choosing the particular opposition vector that has its origin near the proximal surface of the mug and placing the thumb there, the object's (changing) weight vector will be opposed by the thumb as the mug is tilted to the lips.

2. an opposition vector, between the top and bottom body surfaces, will also allow the task-related rotation. It is, however, off the center of mass, and has smaller opposable surfaces, and is usually blocked by other obstacles, such as the table. (This of course focuses on the fact that other issues, missing in this first approximation, are at work; these include object temperature, obstacles, etc).

3. two opposition vectors, one through the top of the handle and one through the side of the handle, will also allow the task-related rotation. By choosing two particular opposition vectors, one with an origin on the top of the handle and one on the distal surface of the handle, the object's (changing) weight vector can be overcome by accounting for the torque caused by being off the center of mass. While these opposition vectors are off the center of mass and the surfaces smaller, they provide a solution to the temperature problem.

In the grasp mug task of Figure 4, when the subject was told to 'Pick up the mug to drink out of it', she chose the third solution in each case.

Similar representational schemes for object features are noted in the robotics literature in terms of general feature extraction [Aggarwal *et al.* 1981] or in terms of object features for robot planning issues [Popplestone *et al.* 1980, Lozano-Perez and Winston 1977, Brooks 1981, Lyons 1985, Vijaykumar and Arbib 1986]. These systems address the larger issue of representing an object in a general way, and not just for prehensile tasks. They also address the issue of designing a system that selects the correct object features which can then be mapped into a robot hand posture [Lozano-Perez and Winston 1977, Popplestone *et al* 1980, Lyons 1985, Cutkosky and Wright 1986]. This is most likely a reasonable approach for serial task planning for a robot gripper with limited abilities, but it would not do justice to the flexibility seen in primate prehensile behaviors. Current dextrous robot hands with many *dofs*, such as the JPL/Stanford hand [Salisbury 1982] and the Utah/MIT hand [Jacobsen *et al* 1984], have been developed by researchers who are exploring control issues, and not task requirements (see [Hollerbach 1982] for a discussion of these issues).

§3. Oppositions

Prehensile postures are constrained by the way the hand can apply opposing forces around an object for a given task [Iberall, Bingham, Arbib 1986]. From our analysis of the prehensile classification literature, we suggest that these can be classified into three basic methods. As seen in Figure 7a, *pad opposition* between the finger pads (VF2) and the thumb pad (VF1) occurs along an axis roughly parallel to the palm. Opposition at the digit pads offers greater flexibility in finely controlled manipulations of an object at the expense of stability and maximum force. *Palm opposition*, between the digits (VF2) and the palm (VF1), sacrifices flexibility in favor of stability. Essentially the object is fixed in hand coordinates (see Figure 7b), along an axis roughly normal to the palm of the hand. Greater stability is achieved by a combination of factors [Thomine 1981]: the larger palmar surface area providing more friction, greater forces available from proximal finger areas [Hazelton et al. 1975, Chao et al. 1976], the ability to passively cancel torques, and the use of the thumb against the fingers for adding force and changing the size of the palm. Finally, *side opposition* (either between the thumb pad (VF1) and the side of the index finger (VF2), or else between the sides of the fingers) is a compromise between flexibility and stability (see Figure 7c). Its opposition axis occurs primarily along a transverse axis. The thumb, due to the orientation of its articular surfaces, has its pad oriented toward the sides of the other digits, giving side opposition using the thumb the extra frictional component. Side opposition between fingers is stronger (but less flexible) if the object is held proximally in the fingers, and weaker (but more flexible) if held more distally.

We suggest that the shape the hand takes on during the grasp reflects the use of one or more of these oppositions. The place cylinder task used pad opposition. The shake cylinder task started with pad opposition, but changed to palm opposition, with an intermediate step of opposition to the torque arising while switching. The grasp mug task used both palm opposition and side oppo-

a) Pad Opposition

b) Palm Opposition
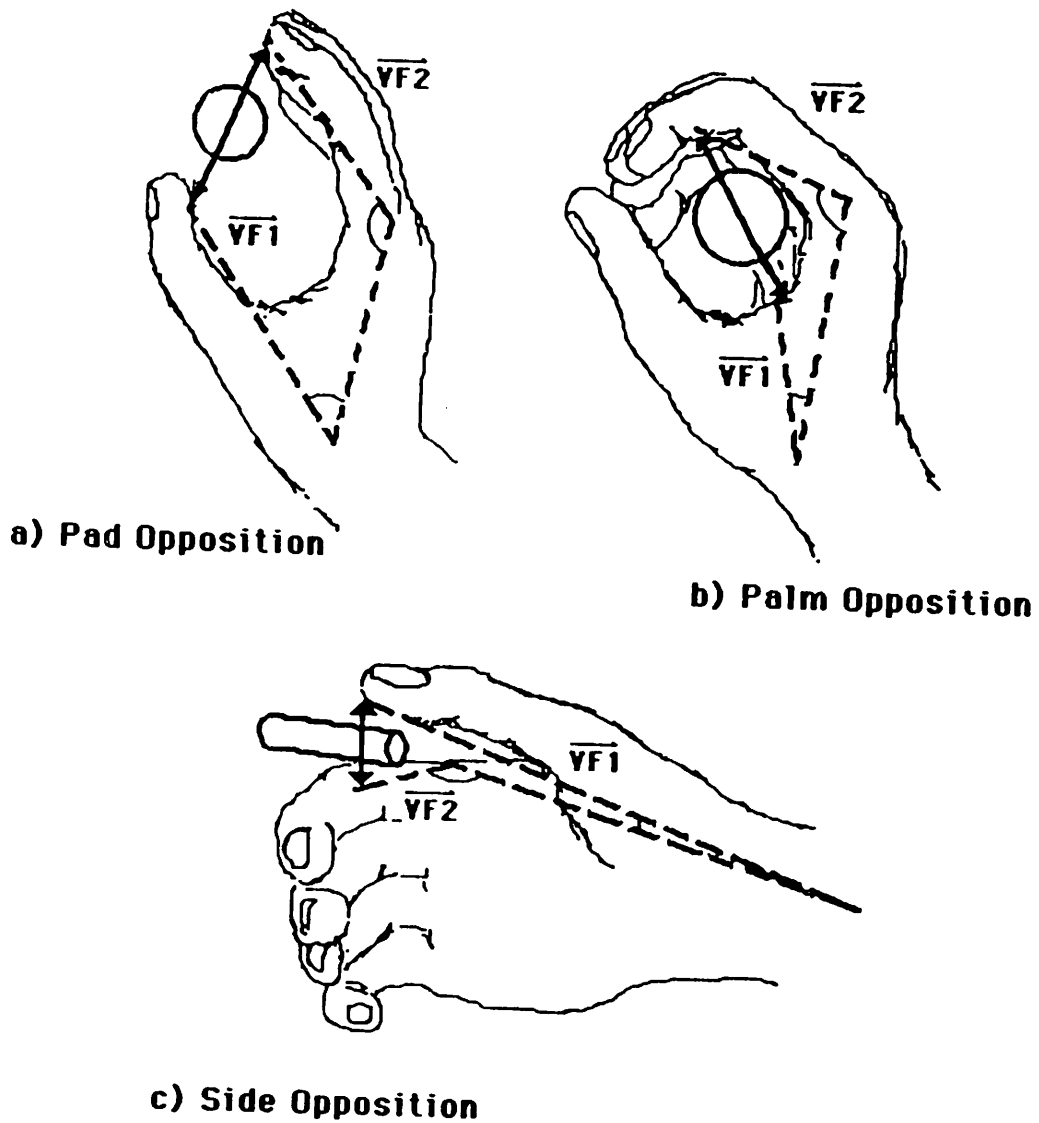
c) Side Opposition

Figure 7: The basic oppositions that make up human prehension

(a) Pad opposition along axis generally parallel to palm (b) Palm opposition along axis generally normal to palm (c) Side opposition along axis generally transverse to palm. Solid lines show axis of opposition, dashed lines show virtual finger vectors $VF1$ and $VF2$.

sition. Since the mug is grasped off-center from its center of mass, VF3 applies an opposition to the torque which brings the mug into the hand.

Due to the asymmetries of the hand, such mixing of oppositions is commonplace and simple [Tubiana 1981]. A functional classification of prehension must be able to describe composite use of oppositions, both during the actual grip and during the preshape. A complete functional description of each opposition would discuss:

- the direction of the applied force,

- the magnitude of the applied force as related to the number of real fingers involved (in terms of minimal, maximal, and mean forces),

- the direction of available movement (*dofs*),

- the range of available movement, and

- the amount of control over those movements.

A task is a composite set of subtasks, as the task requirements change from the lifting phase, to the actual task phases, to the replacing of the object phase. A complete functional description of prehensile movement would show how these three oppositions are seen and functionally used in the emergent postures, relative to the phases of a task, described in terms of task requirements.

Using oppositions to describe prehensile postures, the classic taxonomies can be reanalyzed. In Tables 3 - 5, we show the type or types of oppositions that each posture is using and the mapping for VF1 and VF2. In the first column, we list the grasp, and in the second column we show which opposition or oppositions make up that grasp. In the third column, we show the VF1 mapping. We define two generic areas of the hand for VF1: the 'thumb' refers to the pad or tip of the thumb, and the 'palm' refers to the palmar surface of the hand, including the volar surfaces of the fingers and thumb. The fourth column contains the possible mappings of real fingers for VF2. The numbers refer to the digits; 2-5 denotes

Posture	Opp. Type	VF1 Mapping	VF2 Mappings
cylindrical grasp	palm	palm	2-5, 2-4, 2-3
spherical grasp	palm	palm	2-5, 2-4, 2-3
hook grasp	palm	palm	2-5, 2-4, 2-3, 2
palmar prehension	pad	thumb	2-5, 2-4, 2-3, 2
tip prehension	pad	thumb	2-5, 2-4, 2-3, 2
lateral pinch	side	thumb	2

Table 3: Relationship of Oppositions to Schlesinger [1919] Classification

Posture	Opp. Type	VF1 Mapping	VF2 Mappings
power grasp-a	palm	palm	2-5, 2-4, 2-3
power grasp-b	palm	palm	2-5, 2-4, 2-3
	side	thumb	2
precision grasp	pad	thumb	2-5, 2-4, 2-3, 2
hook grasp	palm	palm	2-5, 2-4, 2-3, 2

Table 4: Relationship of Oppositions to Napier [1956] Classification

the use of all four fingers (digits 2 through 5) in VF2, 2-4 denotes that digits 2 through 4 are used instead, and so on.

We see in Table 3 that Schlesinger's cylindrical and spherical grasps are palm oppositions between the 'palm' and volar surfaces of the fingers. The hook grasp is also a palm opposition, because its opposition axis occurs perpendicular to the palm. Tip and palmar prehension are seen as pad opposition, between the thumb pad and one or more finger pads. The number of real fingers mapping into VF2 varies. While Schlesinger's classification cannot precisely describe this issue, our classification using virtual fingers does. The lateral pinch is seen as side opposition.

A similar analysis is seen for Napier's taxonomy in Table 4. Analyzing his power grasp in terms of oppositions, we see that we can clearly explain the dif-

Posture	Opp. Type	VF1 Mapping	VF2 Mappings
sm diam. heavy wrap	palm	palm	2-5
lrg diam. heavy wrap	palm	palm	2-5
medium wrap	palm	palm	2-5
adduct. thumb wrap	palm	palm	2-5
	side	thumb	2
light tool wrap	palm	palm	3-5
	pad	thumb	2
disk power	palm	palm	2-5
spherical power	palm	palm	2-5
hook	palm	palm	2-5
5 finger precision	pad	thumb	2-5
4 finger precision	pad	thumb	2-4
3 finger precision	pad	thumb	2-3
2 finger precision	pad	thumb	2
disk precision	pad	thumb	2-5
spherical precision	pad	thumb	2-5
tripod precision	pad	thumb	2-3
lateral pinch	side	thumb	2
	palm	palm	2-5

Table 5: Relationship of Oppositions to Cutkosky and Wright [1986] Classification

ference between his two types of power grasps. Power grasp-a involves palm opposition between the palm and two or more fingers, while power grasp-b involves side opposition as well as palm opposition. This is the grasp where the thumb rests along side the tool, as was seen in Figures 8b and 10a. The precision grasp involves pad opposition between the thumb and one or more fingers, and the hook grasp again is seen to be palm opposition.

In Cutkosky's classification (see Table 5), the heavy and medium wraps can be seen as palm opposition between the palm and four fingers. The adducted thumb wrap adds side opposition to the palm opposition. The light tool wrap adds pad opposition instead of side opposition. The disk and spherical power grasps are seen as palm oppositions. All precision grasps are shown as pad opposition

between the thumb pad and various numbers of real fingers mapped into VF2. The lateral pinch is side opposition and palm opposition.

§4. Opposition Spaces

Using the concept of virtual fingers, and noting how the hand can apply forces through oppositions, we define an *opposition space* [Iberall, Bingham, Arbib 1986] as providing the coordinates within which opposition can take place between virtual fingers; specifically, an opposition space defines *the functional capabilities of the hand for executing a stable grasp and object manipulation*. The goal was to develop a method for mapping from task requirements formulated in terms of object degrees of freedom into a functionally constrained space of manipulator degrees of freedom. To completely characterize an opposition space, we therefore need to specify:

1. a description of the task-relevant object features, or *task requirements*;

2. a coordinate frame with relevant grasping parameters, or *opposition space*;

3. a mapping between the task requirements and opposition space.

In Section 2, we defined a working set of task requirements that can be used for describing the task. In order to match the task requirements to the hand's capabilities, a coordinate system is needed that:

1. accounts for the anatomical constraints of the hand;

2. allows a way to map between the object's space and the hand's grasping space;

3. accounts for the three postures of prehension: pad opposition, palm opposition, and side opposition;

4. describes movements in terms of virtual fingers;

5. describes both preshaping and enclosing movements.

A useful coordinate system for the three oppositions is shown by the dashed lines in Figure 7. The dark line indicates the opposition vector along which the opposition is occurring. In pad opposition (Figure 7a), the dashed line $VF1$ describes where the thumb pad is, as it extends and flexes through its 'workspace', relative to the palm vector. It represents the complex movement of the three thumb joints, the carpometacarpal joint, the metacarpophalangeal joint, and interphalangeal joint. The virtual finger vector $VF2$ similarly describes where the finger pads are, relative to the palm vector, taking into account the movement of the metacarpophalangeal joint and the two interphalangeal joints as well. This vector also increases and decreases in length and orientation as the fingers extend and flex. $VF2$ also has a width, depending on the number of real fingers mapped into it.

For palm opposition (Figure 7b), $VF1$ ends anywhere on the palmar surface, and can include the palmar, or volar, surface of the thumb and even the volar surfaces of the fingers. $VF2$ ends anywhere on the volar surface of the fingers above the metacarpophalangeal joint, but is generally shorter than the $VF2$ of pad opposition. In side opposition (Figure 7c), $VF2$ stops at the proximal interphalangeal joint of the index finger, but $VF1$ is still the vector between the thumb pad and the opposition origin.

The movement of the finger *dofs* is highly coupled [Tubiana 1981, Kapandji 1982, Becker et al. 1986], although a complete study analyzing the coupling has yet to be performed. Becker et al. [1986] plot the relationship between the proximal interphalangeal joint angle and the metacarpophalangeal joint, showing the independence of these two joints. However, the interphalangeal joints are coupled by a complex n+1 tendon arrangement using the retinacular ligaments to passively help [Tubiana 1981]. In a biomechanical study of the middle finger, Fischer [1969] shows the distal interphalangeal joint angle depending on the proximal interphalangeal joint angle. One eventual goal of this research is to map these VF

vectors onto real finger configurations, using a reasonable model of the intrinsic and extrinsic muscle contributions to finger movements. One such model [Wells *et al* 1985] is currently being examined for this eventual study. However, since it is a non-linear mapping, understanding the contribution of all the task requirements is a necessary prerequisite for performing the mapping.

Examples of these coordinate systems being used in a composite grips are seen in Figures 8- 10 on various tools of differing sizes. In Figure 8a, the object is a small screwdriver, and it is perceived with one opposition vector. The thumb maps into VF1 which opposes the index finger (VF2) in pad opposition, thus allowing fine control of the object. Pad opposition is seen being formed in the preshape on the left between VF1 and VF2, and then seen again in the grasp itself on the right. Possible use of the palm as a third virtual finger is seen opposing a task related force. In Figure 8b, the object is a medium size screwdriver. The fact that there are two opposition vectors anticipates the need for two types of oppositions, thus capturing the two characteristics of the task (i.e., power and control). The lengths of opposable surfaces for each of the opposition vectors are longer than the hand is wide, and so do not present a virtual finger size constraint. The magnitude, or width, of the opposition vectors are not particularly big, indicating that the object is not particularly heavy. The anticipated task torque (rotating the screwdriver against the screw) indicates the need for palm opposition, using as many fingers as possible in VF2. However, during the first part of the task (fitting the screwdriver blade into the screw), some control is needed. This, along with the fact that only coarse resolution of control over the task *dofs* (turning the screwdriver) is needed, indicates that side opposition would be more useful than pad opposition for the second opposition, with the index finger mapped into VF2 and the thumb into VF1. This allows all four fingers to map into VF2 and the palm into VF1 for the palm opposition. In Figure 8c, the large screwdriver is part of a task that requires more strength and less control.

Figure 8: Examples of grasps using opposition spaces on screwdrivers

(a) Grasping a small screwdriver involves fine control, thus pad opposition is used between VF1 and VF2. Using the palm as VF3 opposes a task related force. (b) Grasping a medium-sized screwdriver involves both power and control, using side opposition between thumb (VF1) and index finger (VF2), and palm opposition between palm (VF1) and four fingers (VF2). (c) Grasping a large screwdriver involves power, using palm opposition between palm (VF1) and four fingers (VF2). The thumb helps VF2 press against VF1.

Preshape   Grasp

a

b

c
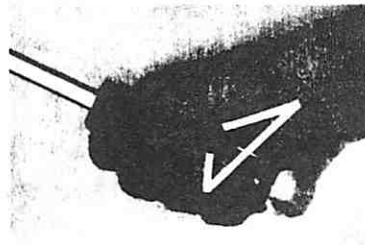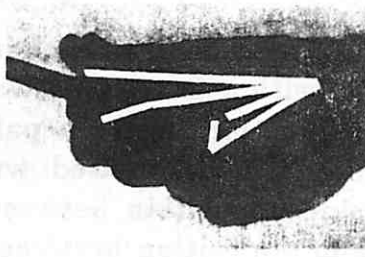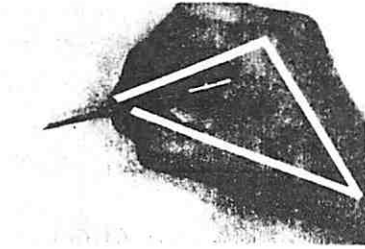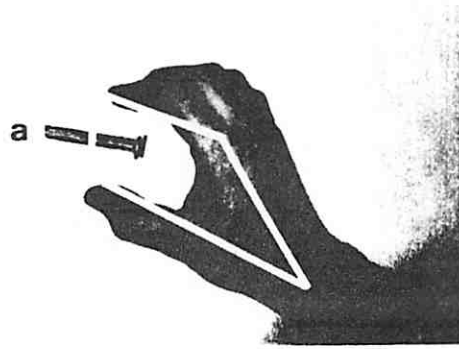
Figure 9: Examples of grasps using opposition spaces on wrenches

(a) Grasping a small wrench involves both fine control and some power. Pad opposition is seen between thumb (VF1) and index (VF2), and palm opposition between palm (VF1) and three fingers (VF2). (b) Grasping a medium-sized wrench involves both power and control, using side opposition between thumb (VF1) and index finger (VF2), and palm opposition between palm (VF1) and four fingers (VF2). (c) Grasping a large wrench involves power, using palm opposition between palm (VF1) and four fingers (VF2). The thumb helps VF2 press against VF1.

39

Preshape   Grasp

a

b

c

Figure 11: Coordinated control program for reaching (from Arbib, Iberall, Lyons 1985)

Control of the movements for a prehensile task can be described as the behavior of interacting perceptual and motor schemas. Visual location of the target is performed by three perceptual schemas. Control of the arm movements is done by two motor schemas (on the bottom left) and control of the finger and wrist movements is done by three motor schemas (bottom right).

useful motor behavior. Schema theory [Arbib 1981] provides a vocabulary for describing interactions between motor and perceptual structures. A coordinated control program, as seen in Figure 11, can be used to describe the overall behavior of perceptual and motor schemas interacting to perform a motor task, such as reaching and grasping [Arbib, Iberall, Lyons 1985]. Each box represents a schema, those at the top are perceptual schemas, and those at the bottom, motor schemas. In the figure, perceptual schemas extract task requirements from the visual image, based on previous knowledge. In this case, knowledge about the location of the object is needed for driving the arm to the correct location. Knowledge about the size of the object is needed for the finger adjustment, which is the preshaping of the virtual fingers. Finally, knowledge about the orientation of the object is needed to orient the hand correctly.

We suggest that the information extracted by the perceptual schemas can be respecified in terms of the task opposition vector and opposable surfaces. The reaching schemas would care about the location of the chosen opposition vector, and the Preshape Schema would care about its magnitude. The Orient Schema would care about the opposition vector's orientation. The mapping, then, from task requirements to opposition space, would specify the virtual finger configurations which would solve these requirements.

Driving the virtual fingers to goal locations can be characterized as an inverse kinematic problem, in the sense that the Preshape Schema must determine the correct angles for $VF1$ and $VF2$ given a particular opposition vector. However, the inverse kinematics do not necessarily give a unique solution [Paul 1981], and therefore a further analysis of the problem is needed.

We turn to a study of pad opposition as a way of looking at this problem. By looking at a functional description of pad opposition, based on the list in Section 3, we can then suggest a more accurate picture of the mapping between task requirements and opposition space.

When grasping objects in pad opposition, the direction of the applied force is through the pads, generally aligning a normal through them with each other and with the opposition vector [2]. The amount of available force to apply against the object, using the fingers and especially the finger pads as we saw in the place cylinder task, is not great. In fact, studies by Johansson and Westling [Johansson and Westling 1984, Westling and Johansson 1984] have shown that, in pad opposition, the grip force mirrors the slip force, the amount of force below which the object will slip out of the fingers. In their experiments, a subject uses pad opposition to pick up objects of unknown weight and under a variety of friction conditions. The subject holds the object for a certain amount of time, and then slowly relaxes his or her grip until the object begins to slip. The relative safety margin between the grip force and slip force measures the safety margin, which protects the object from slipping out of the grasp, in percent of the grip force [Westling and Johansson 1984]. They show that this relative safety margin remains constant (and small) over changes in object weight and also in changes in grasping conditions.

In terms of relating force to the number of real fingers in a virtual finger, we find guidelines from [Hazelton *et al.* 1975]. The index finger, as noted previously, contributes approximately 25%, the middle finger 33%, the ring finger 25%, and the little finger 16%. However, we note, from Table 2, that different amounts of available force arise for different wrist positions [Bunnell 1942, Hazelton et al. 1975, Pryce 1980, etc]. While Napier [1956] suggests that the wrist extends and adducts in precision grasping, the best wrist position for pad opposition has yet to be empirically tested.

In terms of *dofs*, pad opposition offers translational stability, the amount of which depends on the number of real fingers contributing to VF2 [Iberall, Bing-

---

[2]This is a simplification of the more precise notion of a cone of friction, which would define the tolerance for being generally aligned [Fearing 1983, Mason 1982].

ham, Arbib 1986]. Rotating the opposition vector in either direction is somewhat stable, but rotations through the opposition vector are unstable. Ranges of movements are limited by the size of the phalanges and the tension and insertions of the ligaments, although fine gradations of movements are possible along these *dofs.*

Within these capabilities for pad opposition, we suggest the following list as a working set of goals, useful to a pad opposition schema:

1. satisfy kinematic constraints, based on desired locations for the pads of the virtual fingers, taking into account the limitations on virtual finger postures.

2. align pad normals (co-linear and opposite) within some tolerance

3. minimize magnitude of force based on some criteria (don't apply more force than necessary for the task, as exemplified by the relative safety margin),

4. minimize finger movement (final posture is close to current hand posture)

5. maximize available *dof* based on some criteria

Kinematic constraints can be determined by analyzing the possible configurations of $VF1$ and $VF2$. VF endpoints must be $|V|$ apart (the magnitude of the opposition vector), and the opposition vector within the range of the VF vectors. As a first approximation toward looking at the other goals, we can just look at the direction of a normal through the index finger and thumb pad, and see how they vary as the finger and thumb move within their anatomically-constrained 'workspace'. The workspace of a VF is the area within which each can move, and the workspace of the pads is further limited to those areas where the pads can reach.

In order to get some general idea of these workspaces, we built a simple measuring device (see Figure 12) and measured the workspace (the darker line in Figure 13) of the index finger (VF2) and the workspace (the lighter line in Figure 13) of the thumb (VF1). We fixed the palm vector relative to the forearm
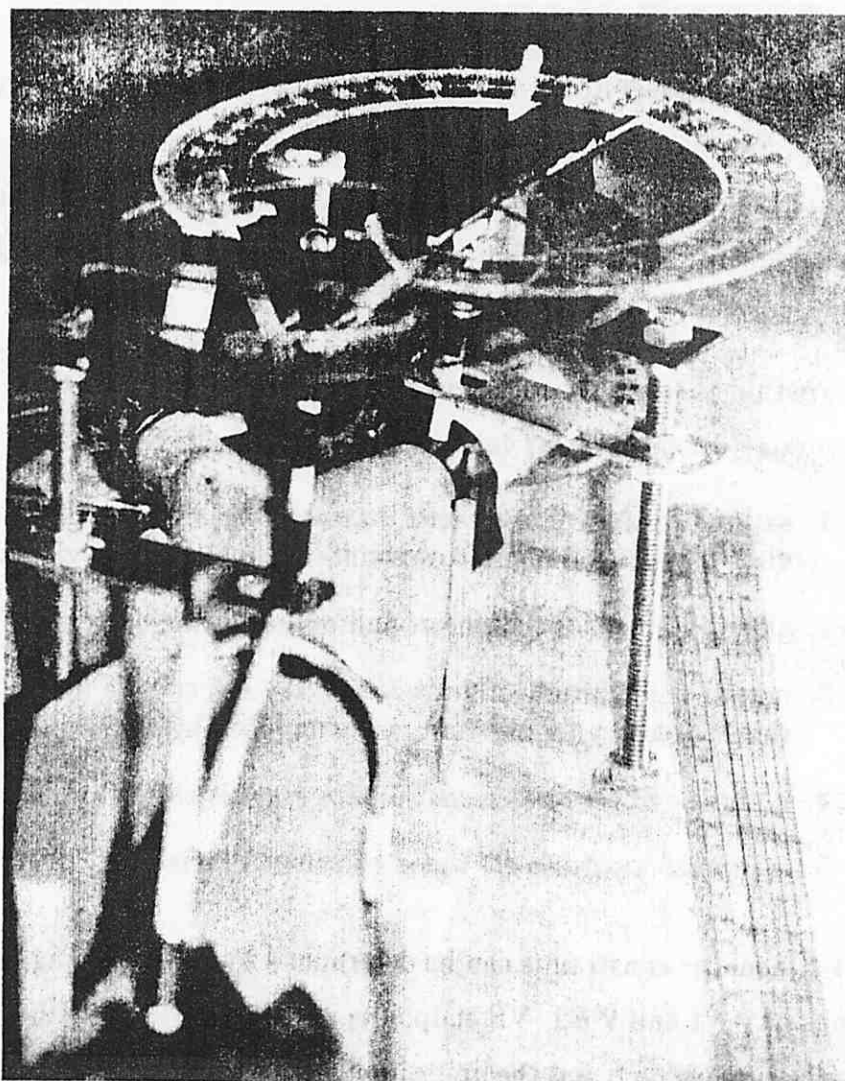
Figure 12: Workspace of a pad opposition being measured.

Using a simple measuring device, we were able to measure the length of $VF1$ (from the thumb CM joint to the thumb pad) and the length of $VF2$ (from the MP joint to the index pad). We measured the angles the vectors made with the palm as well.
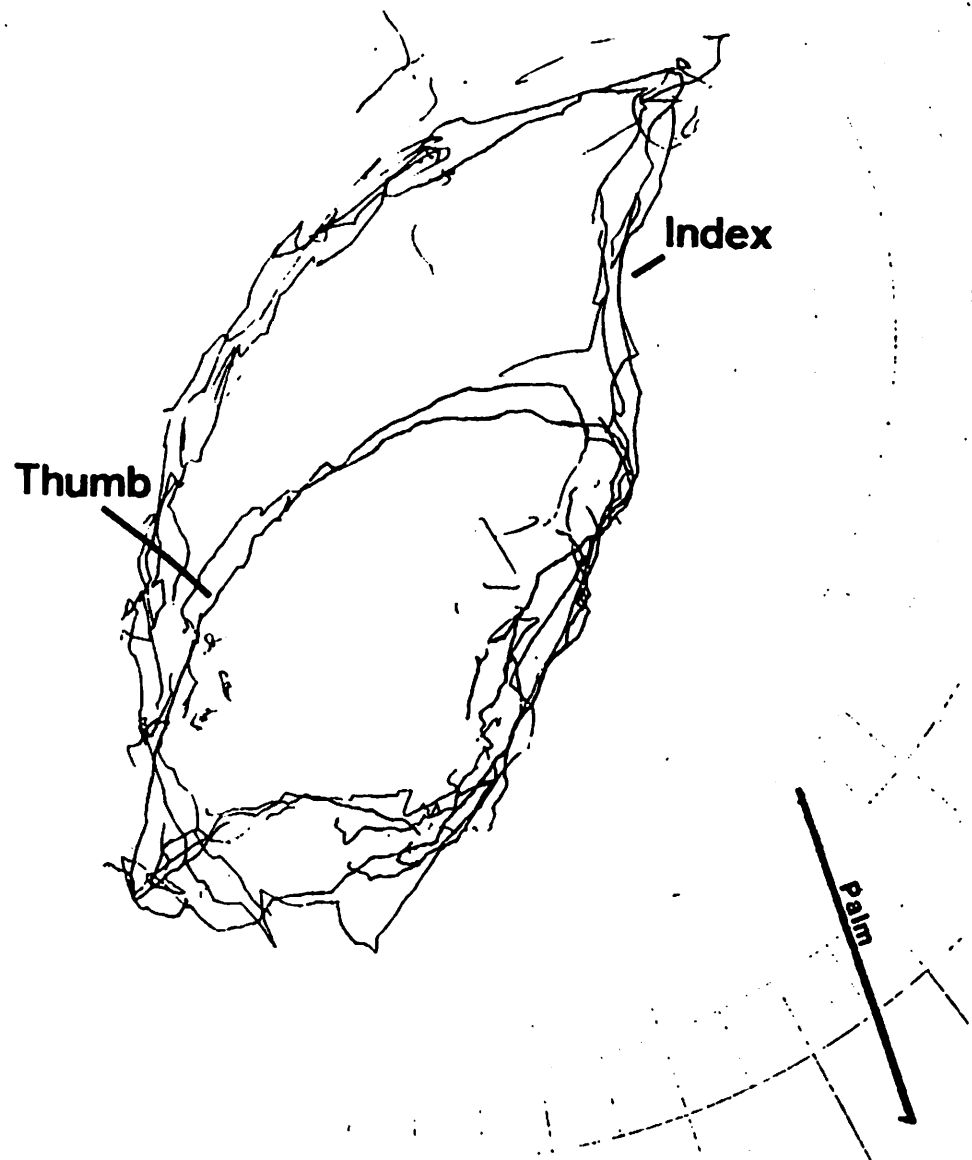
Figure 13: Sample workspace traced by index and thumb

As the index finger and thumb each flex and extend, there are only limited places that they can go, based on the length of the phalanges, the articular surfaces between the phalanges and the metacarpals, the ligaments attaching the bones together, and the excursion range of the tendons. By attaching a pen to the index finger (the larger area) and then to the thumb (the smaller area), we were able to get a sense of the size and shape of those areas.
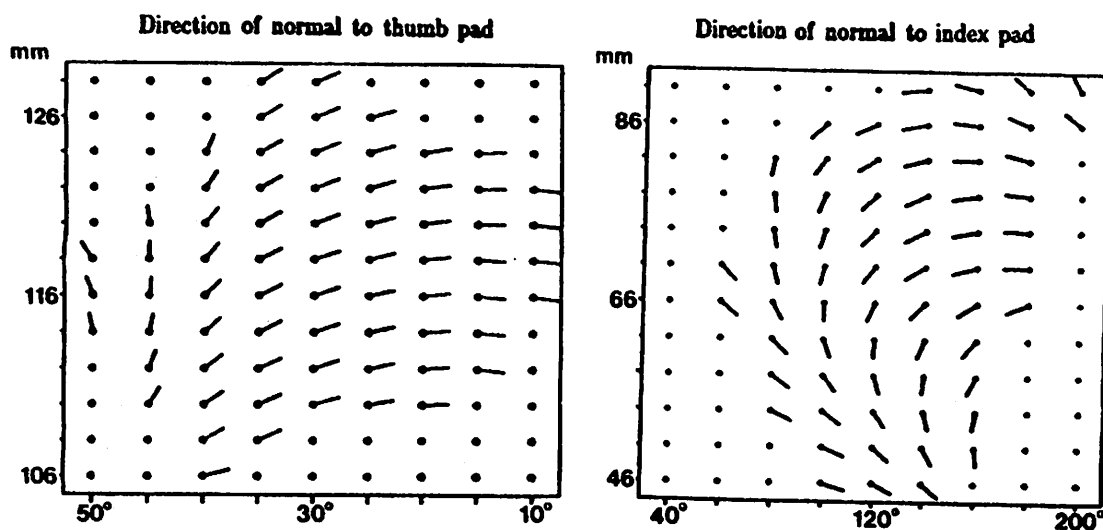
Figure 14: Opposition space for pad opposition between thumb and index finger.

As a virtual finger vector changes orientation (abscissa) and length (ordinate), the direction that the pad is pointing also changes. On the left, the angle $VF1$ makes with the palm is plotted versus the length of $VF1$, showing the direction of the thumb pad normal at a given vector configuration. On the right, the angle $VF2$ makes with the palm is seen versus the length of $VF2$, showing the index finger pad normal. The abscissas are opposite in direction, reflecting the opposability of the thumb and index.

vector at a constant dorsal wrist angle of 150° (or 30° from the forearm axis). We took some sample data points for the opposition space vectors $VF1$ and $VF2$, and then did a linear interpolation to produce the plot seen in Figure 14. Each small vector shows the direction of a normal with respect to the pad. On the left side of the figure, the magnitude of the thumb vector $VF1$ is plotted against its angle. On the right side of the figure, the magnitude of the index finger vector $VF2$ is plotted against its angle. These two plots show how the direction of the pad normals change as the fingers and thumb open and close. Each vector shows the direction of a normal with respect to the pad, when the thumb vector $VF1$ (on the left side of the figure) or the index finger vector $VF2$ (on the right side of the figure) is at a given angle and length. The dots are areas outside the workspaces. The abscissa values are in opposite direction, thus graphically showing how the normals become co-linear but opposite at various locations in the workspaces. Such a description of the workspace of VF1 and VF2 provides a first attempt at quantifying pad opposition space and its functionality.

In summary, we have put forth hypotheses about perceived object properties, task requirements, hand prehensile functionality, and control of prehensile movement. We have suggested some of the constraints acting on the hand during prehensile tasks that arise as a result of these task requirements and hand capabilities. From this analysis, it seems clear that prehensile tasks involve the balancing of two key issues: affixing the object in the hand, and gathering information about forces acting on the object during the task. To provide affixment, enough force must be used to counteract the emergent task forces. In terms of information, contact against the hand's sensors must be maintained with the object in order to determine the state of the object (location, forces acting on it, etc.) during the task.

These two aspects are balanced through combinations of three basic methods of applying oppositions around objects. In this sense, it is as if the human hand

were really three hands in one. One or more of these hands is selected for use during the task, depending on the requirements of the task. The mapping from virtual fingers into real fingers is thus effected by the constraints on how these three hands can cooperatively use the fingers, palm, and thumb to apply the necessary oppositions.

In order to test these hypotheses and go on to develop a neural model of prehension, we found it necessary to look at this mapping of task requirements to opposition space empirically. Using the results of the empirical studies, we can then go on to construct a neural model which might account for these movements within a distributed somatotopically organized system.

Chapter IV

Quantifying Opposition Space Parameters for Pad Opposition

"Just grasp it one more time, Cloud, just one more time."

– T. Iberall

The coordinated control program of Figure 11 shows how interacting schemas can produce a mapping from task requirements to virtual finger configurations, placing the wrist at a useful distance from the object and the fingers in a useful location within an opposition space. The coordinated control program separated the arm reaching, or transport, component of the movement from the hand, or grasping, component, a separation based on the research of Jeannerod and colleagues [Jeannerod 1981, Jeannerod and Biguer 1982]. In Jeannerod's experiments [1981], subjects were asked to reach along the frontal medial plane for an object, starting with their thumb pad touching their finger pads. The object was either a cylinder (10 cm long by 5.5 cm in diameter) or a skinny rod (10 cm long by 2 mm in diameter). Jeannerod noted that the grip aperture between the thumb and index finger pads increased, until it reached some peak, and then the fingers closed in toward the object until contact. He noted a bell-shaped plot in the arm transport velocity profile, which quickly rose to some peak value, and then decreased as the arm slowed down. In the descent phase, a change in the velocity was noted, which correlated with the beginning of finger closure. This led Jeannerod to hypothesize that reaching and grasping movements can be separated into two phases: an initial, faster arm movement during which the fingers

---

preshape, and a later, slower arm movement during which the fingers capture the object. Jeannerod then went on to show that the point at which the peak aperture occurs in the trajectory is within 70-80% of the movement's duration, irrespective of how fast the movement was [Jeannerod 1984].

Wing and colleagues [Wing and Fraser 1983; Wing, Turton, and Fraser, in press] argue that a stronger relationship exists between the transport component and the grasping component of the movement. In their experiments, subjects reached toward and grasped, using pad opposition, a dowel standing on its end, a paradigm similar to our cylinder studies [Iberall, Bingham, Arbib 1986]. The movement direction was in the sagittal plane either through the shoulder [Wing, Turton, and Fraser, in press] or through the midline [Wing and Fraser 1983]. By measuring the distance that the thumb pad and index finger pad moved in a Cartesian coordinate system, they noted that the thumb tended to move less than the index finger, especially after the peak aperture. Their conclusion was that this relative invariance of the thumb allows a simplified visual monitoring of the relationship between the object and a part of the hand involved in the grasp. In [Wing, Turton, and Fraser, in press], they suggest that this might be due to the greater range of movement of the fingers, relative to the thumb.

Arbib, Iberall, Lyons [1985] suggest that the initial phase of reaching movements is being used to get the fingers and the arm into a 'ballpark' location relative to the final goal. They hypothesized that the arm movement is under the control of the $Move_{fast}$ Schema; it is activated with a Preshape Schema, and both schemas serve to get the arm and the fingers into the 'right ballpark'. The second phase of the movement is then controlled by the $Move_{slow}$ Schema and the Enclose Schema, which bring the arm and hand into contact with the object. They note the advantage of assuming a small buffer factor $\pm\delta$ for movements involving contact with objects, as seen in Figure 15. For the first phase of a movement, adding δ_1 to the goal position A would prevent accidental contact

A+δ₁ → $A+\delta_1$

(a)

$A-\delta_2$

enter

exit if
'wrong'
contact
made

$\bar{C}$ MOVE(B,T,C) C

exit if
contact
C made

B

exit if
move
"completed"

(b)

enter

enter

$\bar{C}$ | $A+\delta_1$ T fast C | C → success or failure?

$A+\delta_1$

$\bar{C}$ | $A-\delta_2$ T slow C | C

$A-\delta_2$

failure exit   normal exit

(c)
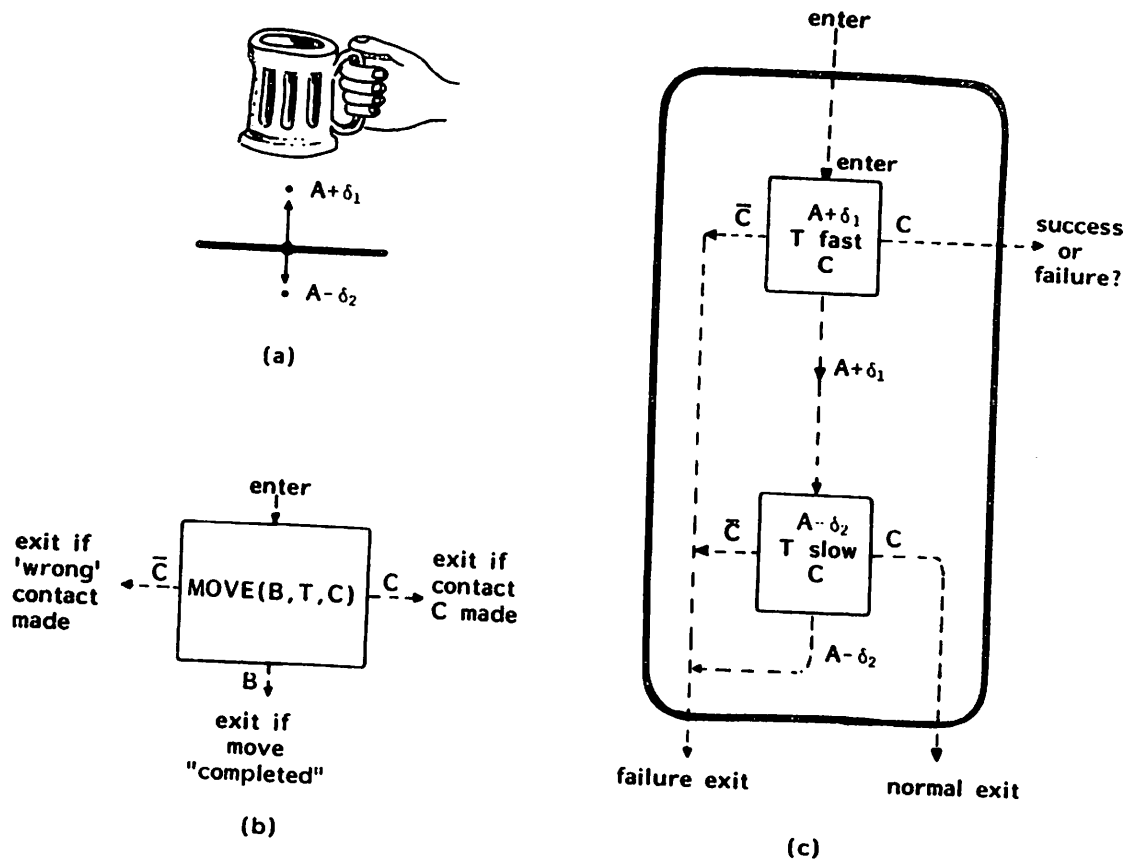
Figure 15: Move Schema describing 'ballpark' movements (from [Arbib, Iberall, Lyons 1985])

(a) As mug is brought toward table during fast movement, the goal is actually $A + \delta_1$. As it lowers onto table during the slow movement, the goal is $A - \delta_2$. (b) Hypothetical move schema (c) Two phase fast and slow movement

with the object; for the second phase of a movement, subtracting δ_2 would ensure contact, as the goal of the movement would actually be inside the object. In this way, errors in depth perception can be overcome. Wing, Turton and Fraser [in press] show that in fast movements and in blind movements, the peak aperture is larger than in slow movements and in visible movements, thus providing evidence for an increased δ_1 value at the finger level to avoid accidental contact.

Our concern with these studies is that they only begin to characterize prehensile movements. Their emphasize has been on teasing out the temporal and spatial interactions between the arm and hand components of reaching and grasping. It is our hope to extend their research by more precisely quantifying particular prehensile events, such as the grip peak aperture, 'ballpark' values for arm and hand movements, differential contributions of thumb vs fingers, and preshaping for goal-directed movements. By this quantification, we hope to get at the underlying constraints on prehensile movements, adding to knowledge about constraints on aiming movements in general [see MacKenzie and Marteniuk 1985, MacKenzie et al, in press].

In the previous chapter we presented opposition space as a way of functionally analyzing prehensile movements. We represented it as combinations of virtual finger vectors and suggested that task requirements can be mapped into opposition spaces. To relate this characterization of prehensile postures with actual reaching and grasping tasks, we embarked on an empirical study of opposition space and the effect of task requirements on preshaping and enclosing the hand. The study described here is limited to looking only at pad opposition between the thumb and index finger, focusing on the effect of the opposition vector of a small, light object. Virtual finger vectors were captured by tracking infrared light emitting diodes (IREDs), placed at vector origins. The question we are initially asking is how the notion of getting into the right 'ballpark' can be more explicitly characterized. By looking at the relationship between the opposition vector and the

wrist, we hoped to quantize a ballpark concept for the arm transport component of the arm. By looking at the angle and length of the two virtual finger vectors, we hoped to do the same thing for the grasping component of the hand. We were concerned about positional and postural effects on our movement parameters, so we varied as many of these as we could.

A secondary concern involves the nature of the measures that researchers use in studying hand movements. We feel it is important to use intrinsic coordinate systems, ones that are related to the natural architecture of the hand. The issue is to search for physical hand and arm features which could be involved in goal-directed motor behavior. A polar coordinate system style of analysis for hand movements is more intrinsic than any arbitrary x-y-z coordinate system.

§1. Methods and Procedure

Our one participant in the experiment was a right handed subject, a graduate student, who sat in front of a table, with his right hand resting on the table (see Figure 16). He was asked to pick up a light wooden dowel, 1.2 cm in diameter, between his thumb and index finger pad. Two different dowels were used, one 4 cm in length (approx. 6.3g in mass) and one 8 cm in length (approx. 10.3g in mass). The dowel rested horizontally 11 cm above the table on a small platform, allowing unconstrained access to the ends. The dowel was 45 cm from the edge of the table, either directly in front of the subject at his midline or directly in front of him at his shoulder (in front of the acromion protuberance of the scapula). The subject always began each trial with the IRED on his index finger (VF2) positioned above a marker on the table. In the conditions where both his starting position and ending position were in the same sagittal plane, the center of the dowel was 30 cm from the marker. In the conditions where the object was placed diagonal to this plane, the center of the dowel was more than 30 cm from the

dowel on side: length 4 or 8 cm

45° or 90°

end on table top in front
of midline or shoulder

30 cm

hand initially
relaxed or index pad
touching thumb pad

start on table top in front
of midline or shoulder

(only 2 starting locations,
so distance hand travels on
diagonal is larger than 30cm)

IRED placement

VF2

VF1
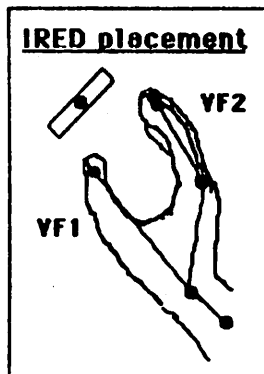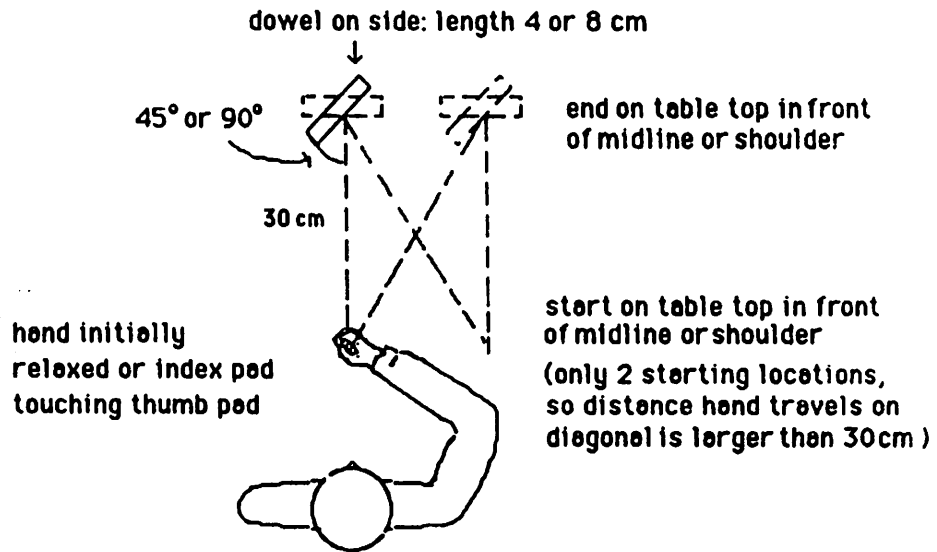
Figure 16: Experimental paradigm in Waterloo grasping studies

Five variables were tested, resulting in 32 different conditions. The
object was a small light dowel, resting on its side. Variables include
the length of the dowel, its orientation to the subject, the starting
position of his hand, the ending position of his hand, and the starting
posture of his hand. Placement of the infrared light emitting diodes
(IREDs) is shown.

marker. In the conditions where the subject was instructed to begin with a relaxed posture, he comfortably rested his hand on the table, making sure the index IRED was placed above the marker. In the touching conditions, he held his thumb (VF1) and index finger (VF2) pinched together, again with the index IRED positioned above the marker. The subject was told to wait for a 'ready' command, and, on the 'go' command, he was to reach for and grasp the dowel by its ends with the index finger and thumb, lift it a few inches off the platform and hold it until the 'ok' command. No mention of speed was made in the instructions to the subject. The subject was instructed to move comfortably and naturally.

The parameters that varied during the task included: the length of the dowel (4 cm vs 8 cm), the angle of the dowel with respect to the sagittal plane (making a 90° angle vs a 45° angle), the location of the dowel (45 cm in front of the midline or 45 cm in front of the right shoulder), the initial starting location of the hand (15 cm in front of the midline or 15 cm in front of the right shoulder), and the initial posture of the hand (finger pad touching thumb pad, or hand relaxed). Each condition included 10 trials, although only the last five were recorded. The order of the 32 conditions was randomized.

§2. Recording System

Using a WATSMART data collection system [WATSMART 1985] driven by an IBM-AT computer, we were able to track the hand using infrared light emitting diodes, which were monitored by two solid state cameras. The subject was fitted with five IREDs, positioned as follows (see Figure 16): at the index finger, positioned at the lateral lower corner of the nail; at the thumb, positioned at the medial lower corner of the nail; at the proximolateral edge of the metacarpophalangeal joint of the index finger; at the wrist, on the radius, even with the head of the ulnar bone; and on the forearm, proximal to the wrist IRED along

the radial bone. In addition, an IRED has placed on the objects center. The X and Y positions of each IRED were sampled at a frequency of 200 Hz by the two cameras placed at about 50° to each other and about 2 m from the working space. The absolute accuracy of each camera over the field of view was 1/200 while the relative accuracy was 1/4000. Strobing of the IREDs, collection time and sampling rate were controlled by the IBM-AT. The total collection time for each trial was two and one half seconds.

§3. Data Analysis

For each trial the 2D data recorded from the two cameras were reconstructed into trajectories of 3D coordinates, which were then filtered at a cutoff frequency of 10 Hz. To minimize distortion of the movement, the program used a second order Butterworth filter with a dual pass, thus eliminating phase lag. The filtered data were analyzed to define when in the two and one half seconds the movement actually began and ended. An interactive program which graphically represented the non-normalized resultant velocity profile was used to determine the start and end of the movement. The start was determined by finding where the resultant velocity began to continuously increase, and then we took the lowest, non-repeating velocity value as the start of the movement. The end of the movement was defined as the point in the non-normalized velocity profile where all IREDs began to exhibit the same general velocity. (See [Marteniuk *et al*, in press] for a general discussion of this approach toward movement analysis.) This part of the data was then extracted and normalized across 100 time units. Thus, the times of occurrence for particular movement features could then be compared in terms of a percentage of the total duration of the movement.

Orientation (degrees)	Starting Position	End Position	Peak Value (mm)	Time (%)
45°	M	M	87.88±3.26	75.6±2.88
		S	88.17±1.43	61.0±10.65
	S	M	84.58±2.02	74.6±0.89
		S	95.91±2.96	70.6±3.85
90°	M	M	82.83±2.33	71.8±4.27
		S	90.32±3.85	86.2±3.63
	S	M	82.93±2.41	73.4±5.46
		S	83.96±2.70	72.0±5.24

Table 6: **Effect on peak aperture and time of occurrence by object orientation (45 or 90 degrees), starting position (Midline or Shoulder) and end position (Midline or Shoulder).**

For the eight conditions, we extracted the frame at which the peak aperture occurs. Since this was done on data normalized to 100 time units, this frame indicates the percentage of total movement time at which this feature occurs.

§4. Results

For this first study, we look only at the conditions where the hand began in a relaxed position (R) and the object was four (4) centimeters in length. We therefore limit this analysis to looking at the effects of only three variables, starting position (midline M or shoulder S), ending position (midline M or shoulder S), and object orientation (45° to sagittal plane or 90° to sagittal plane). Our dependent variables fall into two categories: those related to the arm transport component, and those related to the grasping component. The former include the object's distance and orientation relative to the wrist and arm, and the latter include the grip aperture and the angle and length of $VF1$ and $VF2$.

§4.1 Aperture Trajectory

The distance between the thumb IRED and the index finger IRED, or the aperture of the grip, changes during the preshaping and closing of the hand as it reaches for an object. Aperture over time profiles can be seen in Figure 17 (see end of chapter) for all the analyzed movements. Time is represented along the abscissas as normalized time, showing the total movement time as 100 time units, or frames. Distance between the IREDs in mm is plotted on the ordinate. The upper left plot in Figure 17 shows how the aperture changed for the five trials when the object was at 45° to the sagittal plane, and the subject's hand started and ended in front of the midline (relaxed 'midline to midline' reaches for the 4 cm object, or R-4-45-MM). The next lower left plot in Figure 17 is the changing aperture for trials where the object orientation was similar but the hand started in front of the shoulder and reached for the object which was in line with the midline (relaxed 'shoulder to midline' reaches, or R-4-45-SM). In the upper right plot are the 'midline to shoulder' reaches, or R-4-45-MS; in the next lower right are the 'shoulder to shoulder' reaches, or R-4-45-SS.

The bottom four plots in Figure 17 shows the aperture for the four conditions when the object was oriented at 90° to the subject's sagittal plane. In the third row on the left are the 'midline to midline' reaches, or R-4-90-MM; in the lower left are the 'shoulder to midline' reaches, or R-4-90-SM). In the third row on the right are the 'midline to shoulder' reaches, or R-4-90-MS; in the lower right are the 'shoulder to shoulder' reaches, or R-4-90-SS.

We note in looking at these plots of the relaxed conditions, that the aperture between the index and thumb shows an initial decrease, then an increase to a peak aperture, and then a decrease as the fingers close in on the dowel. This result is somewhat different from Jeannerod's results, which did not show as distinct, if at all, an initial decrease in the aperture as these plots show. This could be attributed to the difference in starting posture: his subjects start with the finger

and thumb pads touching, where our subject started with his index finger and thumb in a posture that was closer to the rest position of the hand.

The time of occurrence of the peak aperture in our data tends to be in agreement with Jeannerod [1981], in that the peak aperture occurs within 70% to 80% of the total duration. In Table 6, we show the mean value for the peak aperture and its time of occurrence for all eight conditions. The time of occurrence in the two midline to shoulder movements tends to be at the extremes of the range suggested by Jeannerod. When the object is oriented at a 45° to the sagittal plane, the peak occurs at 61.0%±10.65 of the normalized time, suggesting that the peak aperture happens earlier and with more variability for this movement. When the object is oriented at a 90°, the peak aperture occurs at 86.2%±3.63 of the normalized time, which is later than the other movements. However, if one looks at the plots (in Figure 17), one can see by visual inspection that the aperture against time profile for midline to shoulder movements is different from the other movements. For the object oriented at 45° (first row on the right in Figure 17), the profile is quite flat, and it is even questionable if there is a distinct peak aperture. In the 90° orientation (third row on the right in Figure 17), the second half of the profile is flat, again making the exact time for the peak aperture questionable.

Finally, in Table 6, we note an effect of object orientation in the sagittal movements (midline to midline, and shoulder to shoulder). The aperture is larger for the object at the 45° orientation (87.88±3.26 mm and 95.91±2.96 mm) than for the object at the 90° orientation (82.83±2.33 mm and 83.96±2.70 mm).

§4.2 Object Properties

As the hand reaches for the object, it orients and moves closer to the object. We call the vector between the opposition vector and the wrist the *approach*

Orient. (deg.)	Start. Pos.	End Pos.	At Initial Frame	At Peak Frame	At Final Frame
45°	M	M	0.69±0.06	0.96±0.04	0.96±0.04
		S	0.25±0.13	0.60±0.18	0.66±0.11
	S	M	0.95±0.08	0.91±0.06	0.91±0.07
		S	0.39±0.06	0.68±0.06	0.72±0.06
90°	M	M	1.04±0.02	1.04±0.04	1.04±0.04
		S	0.81±0.09	1.04±0.07	1.05±0.07
	S	M	1.41±0.08	1.15±0.06	1.09±0.08
		S	1.05±0.10	1.03±0.11	1.01±0.10

Table 8: Effect on angle between opposition vector and approach vector by object orientation, starting position and end position.

The angle between opposition vector and approach vector is measured in radians. See Tables 6 and 7 for explanation.

In Figure 19, the angle ϕ that the opposition vector makes with the approach vector is plotted. We calculated ϕ using an estimate of the orientation in space of the opposition vector, as we did not have two IREDs on the object. This was done by using the distance r (the difference between the wrist IRED and the object IRED) and estimating the opposition vector (the difference between the thumb IRED in the last frame and the object IRED). The orientation ϕ of the approach vector is then the angle between these two vectors. In Figure 19, we note less change in the angle ϕ after peak aperture than before. This is also seen in Table 8, where we have extracted the same three snapshots of the changing object orientation parameter. In comparing the amount of change before the peak aperture and after the peak aperture, we note less change after the peak aperture than before. We can also see that in the sagittal movements the wrist is not initially positioned the same, as one might expect. In the R-4-45-MM condition, the wrist is reasonably close to a line between the subject's midline and the center of the object. However, in the R-4-45-SS condition, the wrist is twisted in toward his midline and not in line between the shoulder and the center of the object.

Orient. (deg.)	Start. Pos.	End Pos.	At Initial Frame	At Peak Frame	At Final Frame
45°	M	M	2.92±0.08	2.62±0.05	2.62±0.06
		S	2.87±0.07	2.78±0.07	2.82±0.03
	S	M	2.96±0.03	2.71±0.06	2.65±0.05
		S	2.87±0.12	2.68±0.04	2.63±0.06
90°	M	M	2.32±0.13	2.44±0.03	2.43±0.02
		S	2.76±0.04	2.66±0.01	2.63±0.03
	S	M	2.94±0.04	2.43±0.05	2.41±0.04
		S	3.01±0.07	2.52±0.05	2.51±0.08

Table 9: Effect on dorsal wrist angle between palm vector and forearm vector by object orientation, starting position and end position at three points in the trajectory. Measured in radians. See Tables 6 and 7 for explanation

While we did not use enough IREDs to observe all the kinematic constraints on arm transport, our study in Chapter 2 showed the importance of the proper wrist angle. In Figure 20, we plot the angle at the wrist between the forearm and back, or dorsal, side of the palm as it changes over time. We note that after about frame 60 in all the conditions, the wrist has taken on a standard value in the range of 2.4 – 2.8 radians (137° – 160°). In Table 9, we can see the values for the dorsal wrist angle at the initial, peak, and final frames, and note that the wrist angle at the peak aperture is generally within 0.17 radians of its value at the end of the movement.

§4.3 VF Parameters

We look at hand movement in terms of the changing virtual finger configurations, represented as two vectors. In Figures 21 and 22, we plot the $VF1$ (thumb) parameters, which are the length and angle of the $VF1$ vector. In Figures 23 and 24, we plot the $VF2$ (index finger) parameters.

Orient. (deg.)	Start. Pos.	End Pos.	At Initial Frame	At Peak Frame	At Final Frame
45°	M	M	139.25±2.94	132.24±2.44	136.02±2.80
		S	132.23±1.91	138.02±2.79	139.15±2.33
	S	M	143.86±3.12	133.26±1.52	136.10±1.21
		S	140.19±3.03	127.43±1.78	130.35±1.16
90°	M	M	141.14±4.62	135.14±1.13	139.11±0.71
		S	143.14±2.87	140.88±2.12	142.16±1.80
	S	M	144.61±1.53	132.01±1.83	137.85±1.08
		S	140.01±3.93	132.12±1.71	138.78±1.77

Table 10: Effect on VF1 length between thumb IRED and wrist IRED by object orientation, starting position and end position at three points in the trajectory.

Length measured in mm. See Tables 6 and 7 for explanation.

Orient. (deg.)	Start. Pos.	End Pos.	At Initial Frame	At Peak Frame	At Final Frame
45°	M	M	0.45±0.10	0.40±0.03	0.44±0.03
		S	0.28±0.06	0.34±0.01	0.33±0.02
	S	M	0.38±0.05	0.36±0.01	0.42±0.03
		S	0.53±0.12	0.35±0.03	0.38±0.04
90°	M	M	0.34±0.07	0.43±0.01	0.50±0.02
		S	0.47±0.05	0.36±0.01	0.39±0.02
	S	M	0.51±0.10	0.43±0.02	0.47±0.01
		S	0.41±0.11	0.38±0.03	0.43±0.04

Table 11: Effect on VF1 angle between thumb vector and palm vector by object orientation, starting position and end position at three points in the trajectory.

Angle measured in radians. See Tables 6 and 7 for explanation.

Orient. (deg.)	Start. Pos.	End Pos.	At Initial Frame	At Peak Frame	At Final Frame
45°	M	M	133.72±2.27	122.74±0.54	121.57±1.59
		S	129.10±5.21	117.49±5.14	116.69±1.45
	S	M	122.65±3.3	121.51±1.98	121.50±2.03
		S	128.43±4.92	121.09±1.77	122.56±1.16
90°	M	M	134.96±2.81	120.03±1.42	118.82±1.52
		S	135.03±2.28	125.51±2.55	125.26±2.16
	S	M	131.00±4.46	121.46±2.74	118.04±1.22
		S	125.69±4.42	123.21±1.27	124.53±1.75

Table 12: Effect on VF2 length between index finger IRED and metacarpophalangeal IRED by object orientation, starting position and end position at three points in the trajectory.

Length measured in mm. See Tables 6 and 7 for explanation.

Orient. (deg.)	Start. Pos.	End Pos.	At Initial Frame	At Peak Frame	At Final Frame
45°	M	M	2.21±0.08	2.31±0.04	2.28±0.07
		S	2.37±0.11	2.72±0.17	2.96±0.05
	S	M	2.56±0.10	2.36±0.09	2.29±0.06
		S	2.30±0.55	2.66±0.10	2.67±0.10
90°	M	M	2.53±0.09	2.37±0.09	2.34±0.11
		S	2.27±0.05	3.08±0.04	3.07±0.06
	S	M	2.33±0.15	2.35±0.09	2.36±0.08
		S	2.43±0.12	2.60±0.12	2.78±0.21

Table 13: Effect on VF2 angle between index finger vector and palm vector by object orientation, starting position and end position at three points in the trajectory.

Angle measured in radians. See Tables 6 and 7 for explanation.

In Figure 21, we see a bell shaped curve in about the first third of all movement, and then a slow increase in value. After the peak aperture, the length changes less than before the peak aperture occurs. How much is seen in Table 10, where we can compare the value of $VF1$ length at the peak aperture and at the final frame. In all cases, we note that the $VF1$ length is smaller at the peak aperture than at the final frame, which is the result of the slow rise seen in all the trials in Figure 21.

In Figure 22, we plot the changing angle of $VF1$. We note that it changes very little within any trial (less than 0.2 radians). After the peak aperture, there is even less change (less than 0.1 radians). While there is variability in the first part of the plots for all the movements, we note that the $VF1$ angle is smaller than its value at the final frame, in all cases except the R-4-45-MS movement. This is shown in Table 11, where the means and standard deviations are seen for the initial, peak aperture, and final frame.

In Figure 23, we see the time profiles for the changing $VF2$ length. The curves show much variability, however, again, there is generally less change after the peak aperture than before. Comparing these plots to Figure 17, one can see that the $VF2$ length tends to be decreasing in value through the frame of the peak aperture, reaching some low value after the peak aperture, and then slightly increasing until contact. In Table 12, we see the length values for the three points in the trajectory, and note that the general similarity of the values at peak aperture and at the final frame. In six out of the eight conditions, the $VF2$ length tends to be slightly less in the final frame, while in the shoulder to shoulder moves, it tends to be slightly higher.

In Figure 24, we plot the changing angle of $VF2$. By visual inspection, one can see similarities in the trajectories across object orientation: the R-4-45-MM trials are similar to the R-4-90-MM trials, the R-4-45-SM trials are similar to the R-4-90-SM trials, and so on. Overall, there is again more change within trials

over time before the peak aperture than before. This is even more pronounced in the movements toward the midline (all the plots on the left side of Figure 24). The actual values of the means at the three points in the trajectory are seen in Table 13. General similarity is seen between the value at the peak aperture and at the final frame, without change in a pronounced direction.

§5.   Discussion

Preshaping the hand during the grasping process indicates that the CNS has chosen some particular object features, and adjusts the hand posture accordingly in preparation to interact with the object. We note that the chosen posture is task-specific [Jeannerod 1981, 1984; Arbib, Iberall, Lyons 1985]. Not only does it reflect the perception of particular object properties, but it also incorporates the subject's intention of how the object will be used in the task. The posture chosen in the mug task of Chapter 3 allows the person to comfortably rotate mug toward the mouth to drink from it. In Figure 8, the hand preshapes to grasp the screwdriver so that an axis through the screwdriver is aligned with the forearm and rotation of the wrist will cause the correct rotation of the tool. The object could be grasped in other ways, but many of those ways would not be useful for task performance.

If the chosen posture depends on task-specific object properties, we should be able to selectively vary those object properties and then see their effect on the chosen posture. The problem with this approach is to determine a correct description of human hand postures and object properties. As a first approximation, we have chosen to characterize human hand postures based on the intrinsic coordinate frames described in Chapter 3. We have chosen to characterize the object/task with the task requirements also listed in Chapter 3. With these characterizations, we attempt to look at the virtual finger parameters and the changing relationship

between the hand and the object.

In this study, we narrowed our goals to mapping one specific prehensile posture. By using small, light dowels, we forced the subject to use pad opposition, with the thumb as VF1 and the index as VF2. Infrared light emitting diodes were placed at the virtual finger vector origins of pad opposition, as was seen in Figure 16. In this way, we can look at how a limited set of task requirements (the opposition vector) map into the pad opposition space.

Jeannerod and colleagues [Jeannerod 1981, Jeannerod 1984, Jeannerod and Biguer 1982] looked at pad opposition in the context of visually-guided movement. They noted that the maximum aperture between thumb pad and finger pad occurs within 70-80% of the movement. We note in our study that this is generally true, but that movements from the midline out toward the shoulder were at the extremes of these ranges: reaches for the object oriented at 45° are at the low end, and reaches for the object oriented at 90° are at the high end. However, the flatness of these aperture against time profiles, especially in the second half of the movement, suggests that the concept of a peak aperture in this type of move might be invalid, and one should look at the kinematic and dynamic constraints on the complete arm to see what might be happening at the hand level.

In characterizing arm movements, Hollerbach and Flash [1982] describe planar arm movements as either a reaching action (change in the elbow and shoulder angles is in the opposite direction) or a whipping action (change in the elbow and shoulder angles is in the same direction). Midline to shoulder movements seem to be more in the category of whipping movements, while the others are reaching movements. As a result, it is possible that external forces at the hand level might be passively acting on the fingers. Evarts and Tanji [1974, Tanji and Evarts 1976] have shown that if an anticipated external force acting on the arm will do the same work that the muscles would have done, the CNS lets the external force do the work and doesn't activate the muscles. If this is happening at the hand level,

then in movements where inertial forces are anticipated to open the fingers, the observed movement parameters might be quite different than those times when the movement parameters are under more direct CNS control. Another cause might be due to the nature of the arm's geometry, which might make preshaping unnecessary when approaching an object in this way. Further experimentation is needed to more carefully detail the relationship between the grip aperture and the direction of the arm movements.

Jeannerod [1984] also noted that this peak aperture occurred at the peak deceleration of the arm transport component of the movement, where a break in the velocity profile occurs. Arbib, Iberall, and Lyons [1985] characterized this first part of the arm movement as the results of a $Move_{fast}$ Schema which gets the arm into the 'right ballpark'. The second phase of the movement, the $Move_{slow}$ Schema, allows the hand to track the object as it comes in close. We hypothesized in [Arbib, Iberall, Lyons 1985, in press] that the transport component is driving the wrist to a location offset from the object by some δ_1. Here, we have defined a polar coordinate system (r, ϕ), defining the relationship between the object and the wrist, to let us quantify what the 'right ballpark' means. In our data for this one subject, we note the similar values (0 – 0.06 radians) across conditions for ϕ at the end of the $Move_{fast}$ Schema and at the end of the $Move_{slow}$ Schema. We also note that, in movements in the two sagittal planes and in movements toward the midline, the distance r is within a small range (9 – 14 mm) of the value it will have at the end of the enclose phase. However, we find midline to shoulder movements to be different. First, finding the peak is difficult, due to the flatness of especially the second half of the aperture trajectory, a time during which the peak normally occurs. If our peak point is accurate, we note that in the 45° orientation of the object, the peak seems to occur earlier than most, and in the 90° orientation, it occurs later. We also found that the peak aperture in a shoulder to shoulder movement in the 45° orientation condition is larger than in other conditions.

A good experimental question to explore is how arm configurations affect the occurrence and size of the peak aperture. For example, some of the moves pose awkward reaching conditions on the arm, forcing the elbow to push against the body. The awkwardness of the R-4-90-MS movement might be a cause for the generally large peak aperture; however, this does not explain why the R-4-45-SS movement has as large, or even a larger, peak aperture. One indication of what the arm is doing is captured in the dorsal wrist angle. We note in Figure 20 that the wrist seems to get into a standard angle (2.4 - 2.8 radians, or 137-160°) about half way through movements under all conditions. These values for the dorsal wrist angle are within the range noted in the biomechanical data presented in Chapter 2 (which were measured from a different axis) as a optimal angle for the long tendons.

Wing and colleagues [Wing and Fraser 1983, Wing, Turton, and Fraser, in press] have suggested that the thumb moves less than the fingers, thus perhaps setting up a constraint for the total movement. The movements they studied were midline to midline movements and shoulder to shoulder movements. In their measurements, they calculated the differential contribution of the thumb and index finger to the changing aperture between them. They found the distance traveled by the thumb to be less than that of the index finger, especially after the peak aperture. We see that this is most likely demonstrated in our data by the larger angles that $VF2$ travels through, as seen in Figure 24 and Table 13. The length of $VF2$ changes very little during the enclose phase across all conditions, while the length of $VF1$ changes in three of the eight conditions: in R-4-90-xM and R-4-90-Sx movements (where x is either S or M). We see that the length of $VF1$ increases after the peak aperture, as does its angle.

We saw that the amount of finger movement between the initial frame and the frame of the peak aperture is generally larger than the amount of movement after the preshape phase. Just as the $Move_{fast}$ Schema gets the arm into the

correct 'ballpark', the Preshape Schema is doing this same function for the finger movements. The Preshape Schema shapes the virtual fingers into a posture larger than the object [Jeannerod 1981], and the Enclose Schema brings the virtual fingers together, trying to get the fingers 'into' the object (of course, the object surfaces stop the fingers at the appropriate time). The question, however, is what is the right ballpark, or, more formally, what is the size of the buffer δ_1 discussed in Figure 15? The data presented here, for this one subject, indicate prehensile movements can be characterized in terms of small buffers for the approach vector and for the virtual finger vectors. The distance r of the wrist at the end of the preshape phase is generally a predictable value away from the object. We denote this value as $\delta_{1,r}$, where the first subscript relates to the subscripts in Figure 15. The angle ϕ of the approach vector at the end of the preshape phase is within some small range $\pm\delta_{1,\phi}$ from its value at the end of the enclose. For the $VF1$ angle, the ballpark reached at the end of the preshape phase is some $\delta_{1,\theta_{VF_1}}$ smaller than the $VF1$ angle at the end of the enclose phase. For the length of $VF1$, it is some smaller $\delta_{1,l_{VF_1}}$. For the length and the angle of $VF2$, they are some $\pm\delta_{1,l_{VF_2}}$ and $\pm\delta_{1,\theta_{VF_2}}$ values, respectively. This could be possible evidence to the view [Wing and Fraser 1983] that the role of the thumb in the task sets up constraints on the moves: the length and angle of VF2 at peak aperture relative to their value at the end of the enclose phase is not as critical as the relative length and angle of VF1. Perhaps, the strategy of a thumb controller is to posture the thumb so that the $VF1$ parameters will be increasing during the enclose phase; the fingers, having more range of movement than the thumb, will then be adjusted accordingly in whichever direction is necessary as enclosing and then contact occurs. Experiments on more subjects are needed to see whether this hypothesis holds across subjects.

We note that there is a problem in doing inverse kinematic mappings in that they are non-unique [Paul 1981]. At the desired wrist location, there are possibly more than one virtual finger configuration solutions. However, we have seen that

there is a great deal of variability in reaching movements, especially at the peak aperture [Wing *et al.*, in press]. This could be indicative of a controller trying to maintain controlled variables within relative ranges of each other, instead of computing a perfect solution for each variable separately[1].

The coordinated control program shown in Figure 11 indicated certain relationships between aspects of the movements. Here, we show how using a natural coordinate system for studying prehensile movement can allow insights into describing prehensile postures. We have hypothesized some of the finer details of the relationships between task requirements and virtual finger parameters. Much experimentation remains to be done to see if these variables can be analyzed for further task-specific details, as well as to see if the results shown here hold across subjects. Other questions remain as to how they co-vary, in the time domain as well as in the space domain.

Experimentation is also needed to look at the other oppositions as well. We suggest the following experiments:

- Instead of a dowel, using a rectangular block would allow us to analyze the size of VF2. The length of the block would be varied to see how many real fingers map into VF2. We would also look for the transition between pad and palm opposition in preshaping for the task.

- Using a key-like object would allow us to analyze side opposition. The width of the object would be varied to see the effect on the VF parameters.

- Using an object with two opposition vectors would allow us to analyze combinations of oppositions. The widths of the opposition vectors would

---

[1]Of course, sometimes a great deal of accuracy is needed at the end (i.e., a specific solution is needed). In our task representation, we would specify this in the task requirement variable called resolution of control. In these experiments here, there was little resolution of control needed. This also gets into issues of Fitt's law, which relates the speed of the movement to its accurarcy [see MacKenzie *et al*, in press].

be varied to see the effect on the combination of side and palm opposition.

In Chapter 3, we hypothesized that the constraints on pad opposition involve satisfying kinematic constraints, aligning pad normals, minimizing a force magnitude, minimizing finger movement, and maximizing available *dofs*. Towards supporting that hypothesis, we have begun to look at some of the kinematic constraints across various movements and initial conditions. Within those constraints exists a solution space of virtual finger configurations (satisfying those constraints). We suggest that useful wrist locations, which a transport component controller would want to select as places to put the wrist, are locations where kinematic solutions (for now) exist for the chosen opposition. In these data, we see that kinematic constraints are (of course) satisfied when the object is picked up. More importantly, we also see that the virtual finger configurations at the peak aperture are within 'ballpark' values of these kinematically constrained configurations. This is true for the four virtual finger parameters (length and angle of VF1 and VF2).

These virtual finger solutions must be computed relative to the object, in either an object centered or a wrist centered space. As the controller doesn't know exactly where a visually-determined object is, and therefore doesn't know exactly where to put the wrist, we would argue that the preshaped posture should be a configuration which maximizes the chances of successful capture of the object. This would mean putting the wrist at a location where many solutions exist in the virtual finger solution space. The preshaped posture would then reflect not only 'ballpark' values for a particular kinematic solution, but 'ballpark' values for many kinematic solutions. In the next chapter, we show how to model a controller as a process which determines a virtual finger configuration by searching the VF kinematic solution space relative to the object. By looking for a wrist location in that space where many solutions exist, it maximizes the chances of successful capture of the object. Preshaping then becomes putting the fingers into

configurations which are in 'ballpark' ranges of those many kinematic solutions.
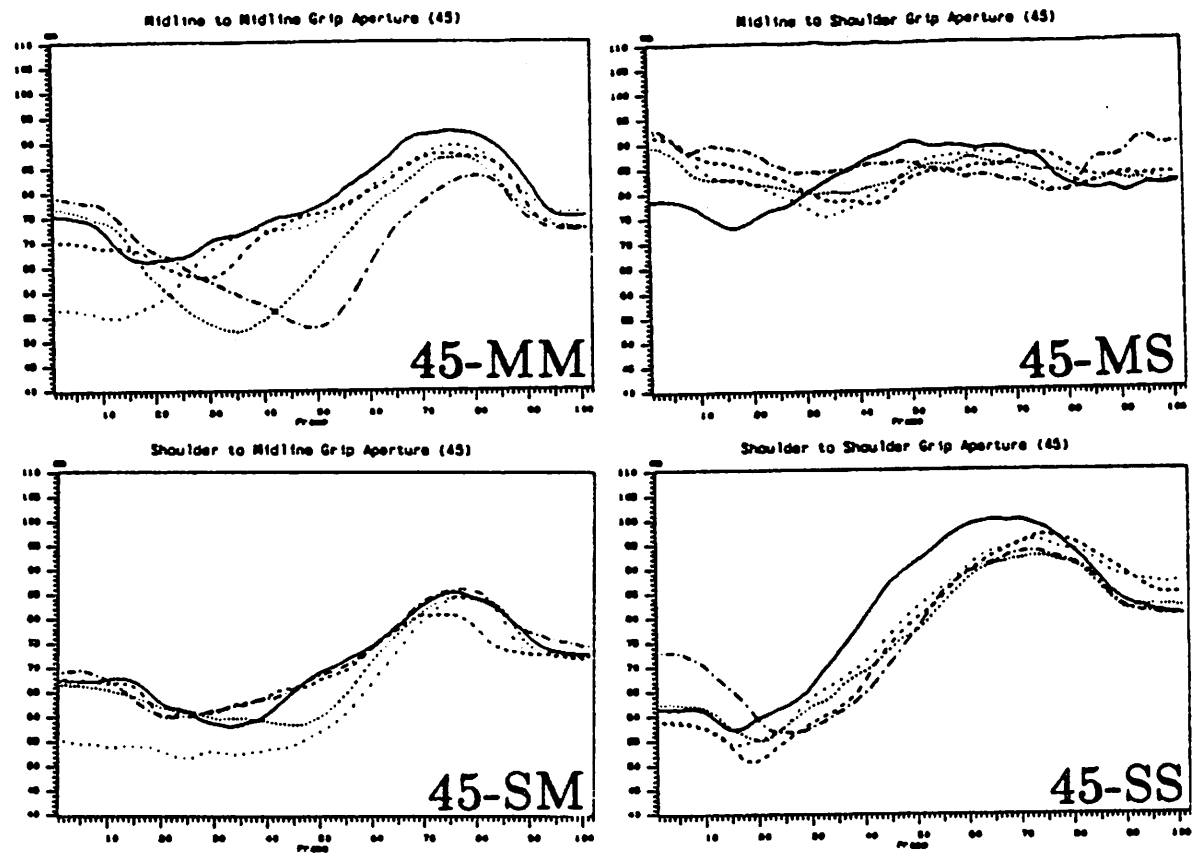
Figure 17: Aperture between the Thumb and Index Finger IREDs

The changing aperture between the thumb and index finger IREDs is shown over normalized time. All five trials of eight conditions are shown, as noted in the titles. Upper four plots are for the 45° orientation, and the lower four for the 90° orientation

90-MS

90-SS

90-MM

90-SM
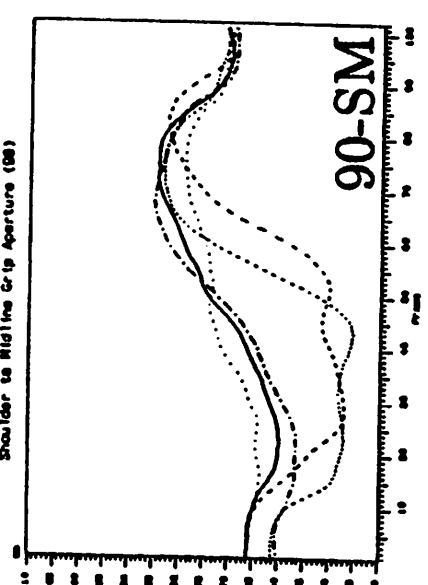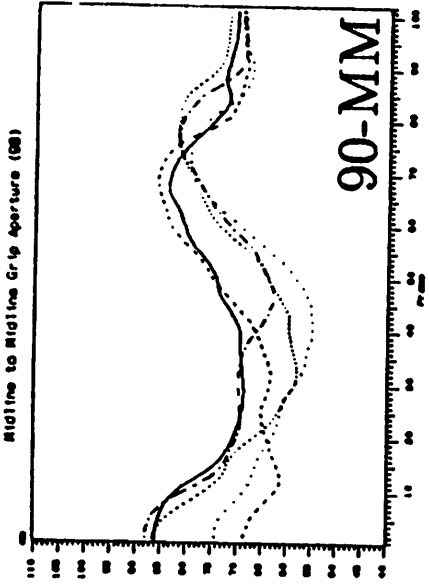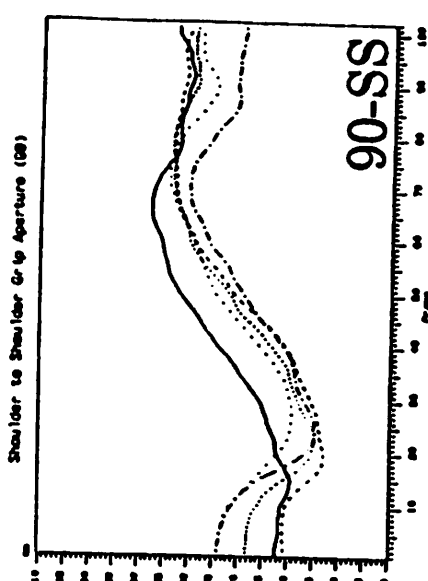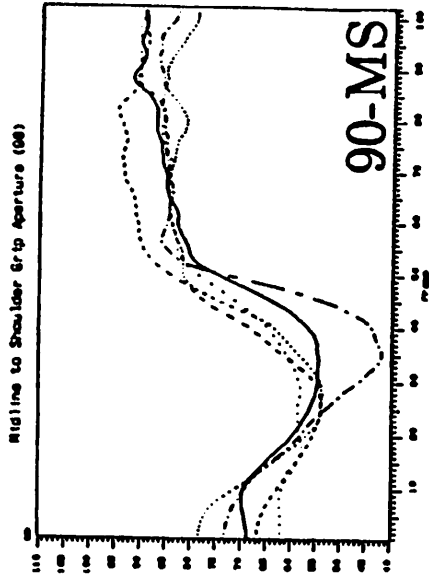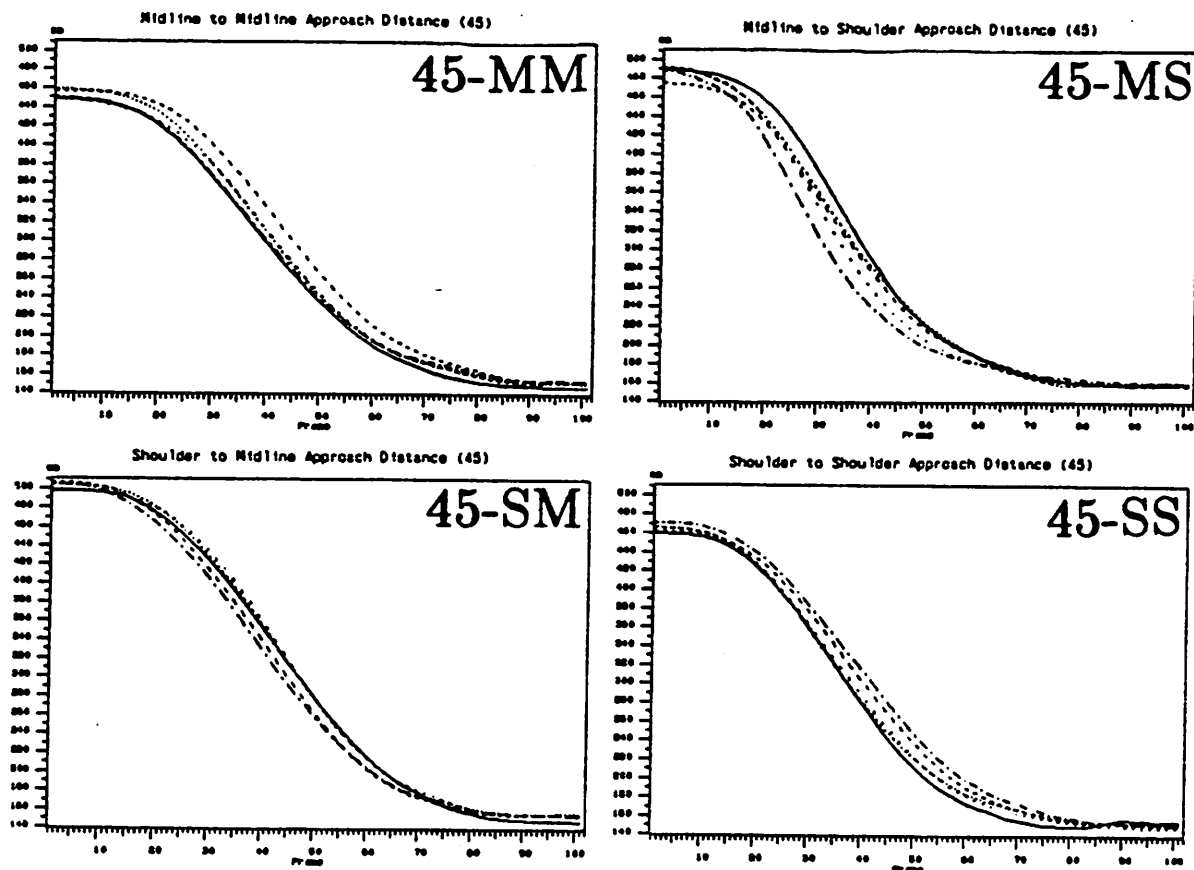
Figure 18: Object Distance *r* plotted over time

The distance between the object and the wrist is plotted over time, as
the wrist approaches the object, for all five trials of all eight conditions.
See Figure 17 for explanation.

Midline to Midline Approach Distance (90)   90-MM

Midline to Shoulder Approach Distance (90)   90-MS

Shoulder to Midline Approach Distance (90)   90-SM

Shoulder to Shoulder Approach Distance (90)   90-SS

80
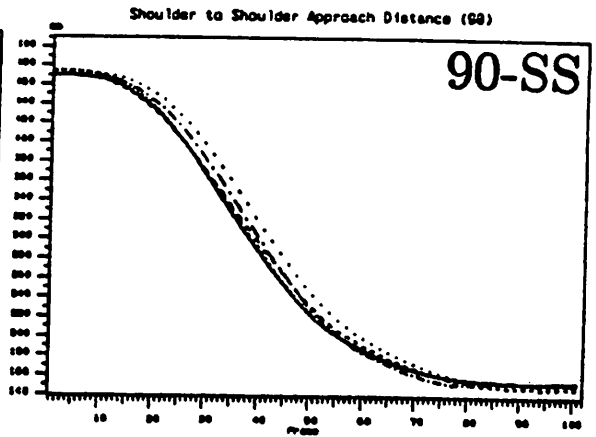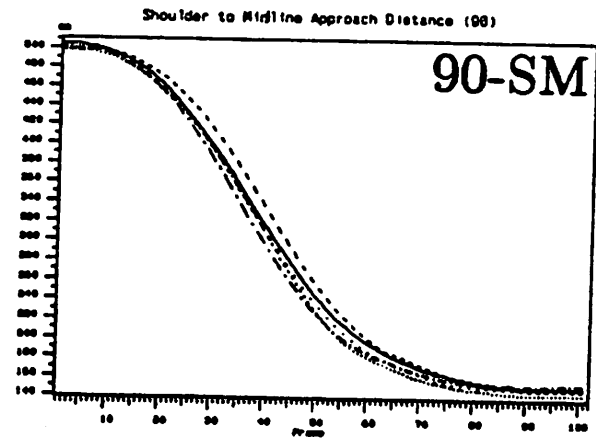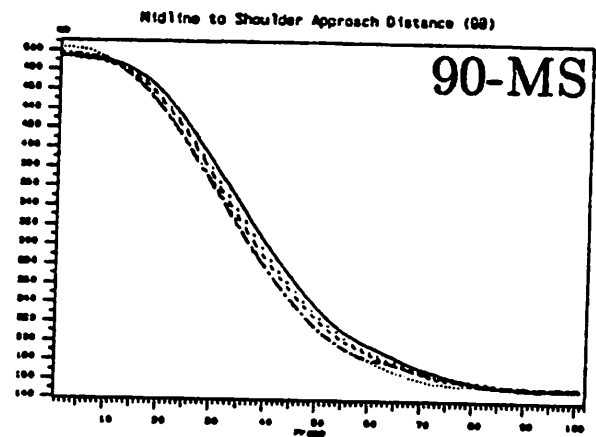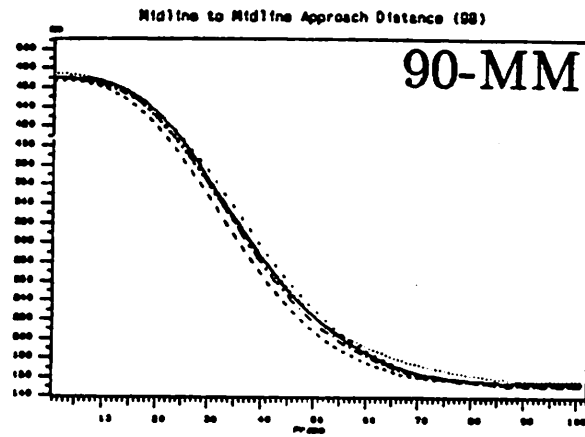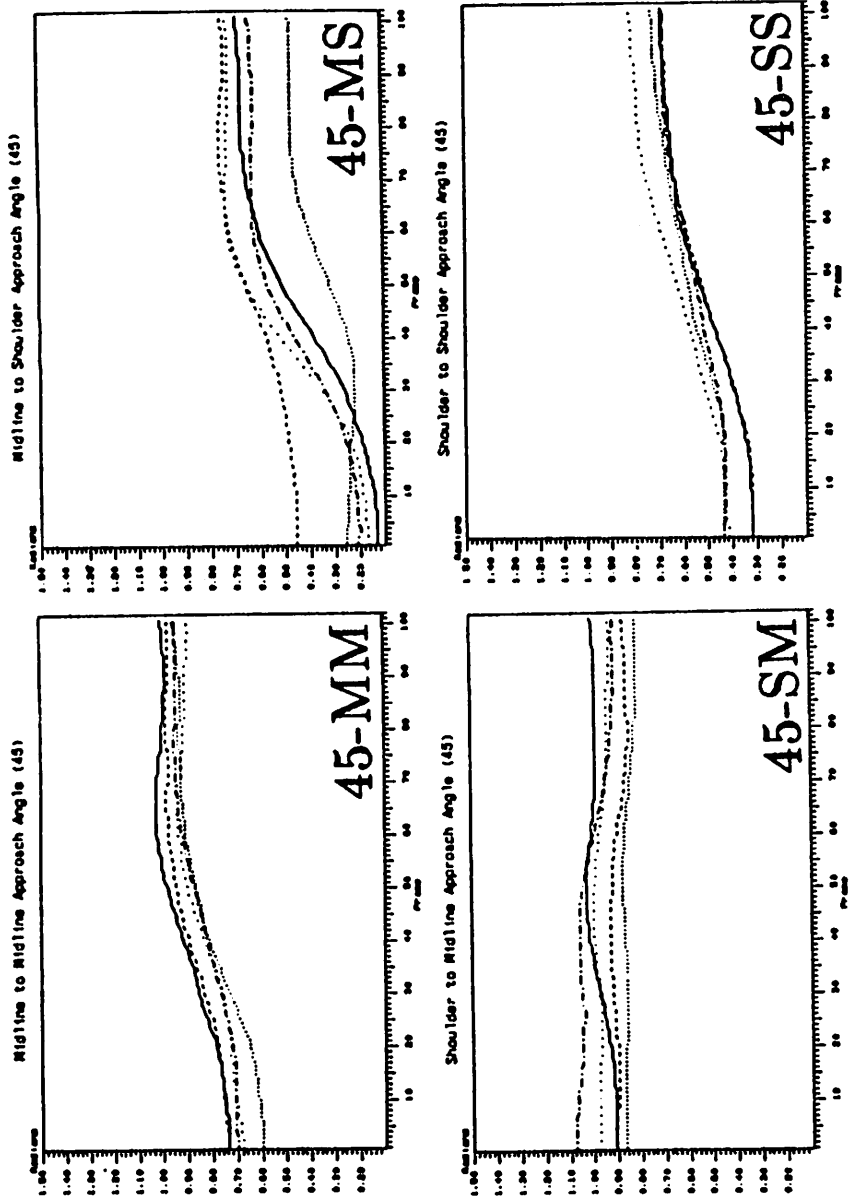
Figure 19: Object Orientation ϕ plotted over time

The orientation between the dowel's axis and the approach vector is plotted over time, as the wrist approaches the object, for all five trials of all eight conditions. See Figure 17 for explanation.

Midline to Shoulder Approach Angle (90)

90-MS

Shoulder to Shoulder Approach Angle (90)

90-SS

Midline to Midline Approach Angle (90)

90-MM

Shoulder to Midline Approach Angle (90)

90-SM

82
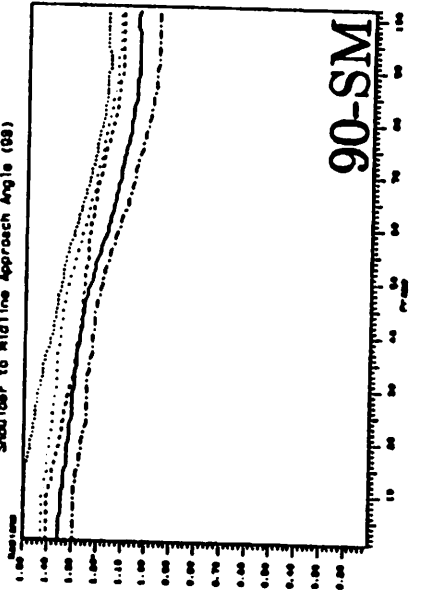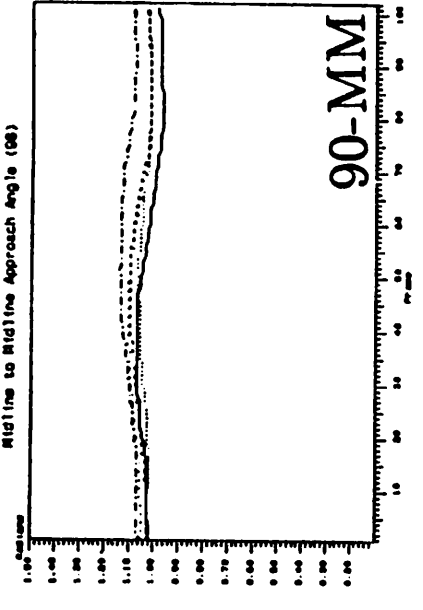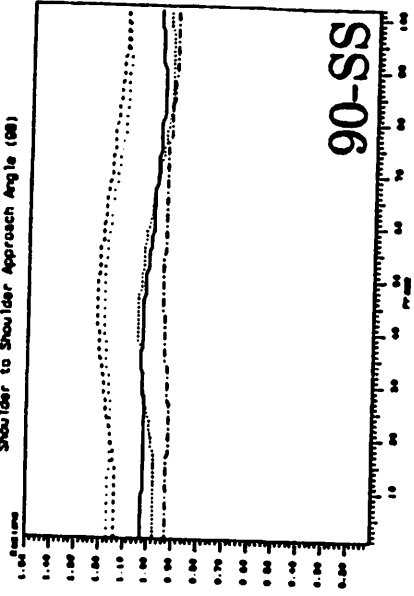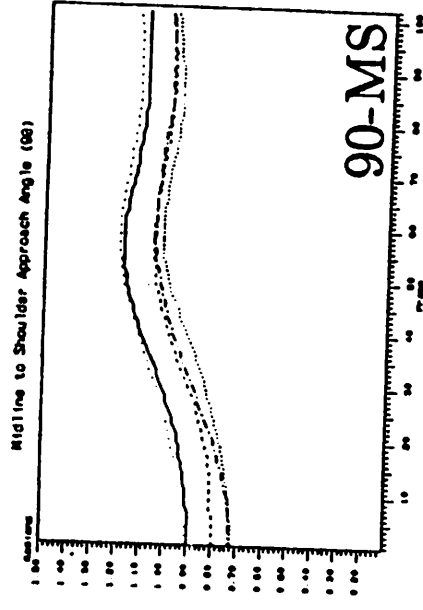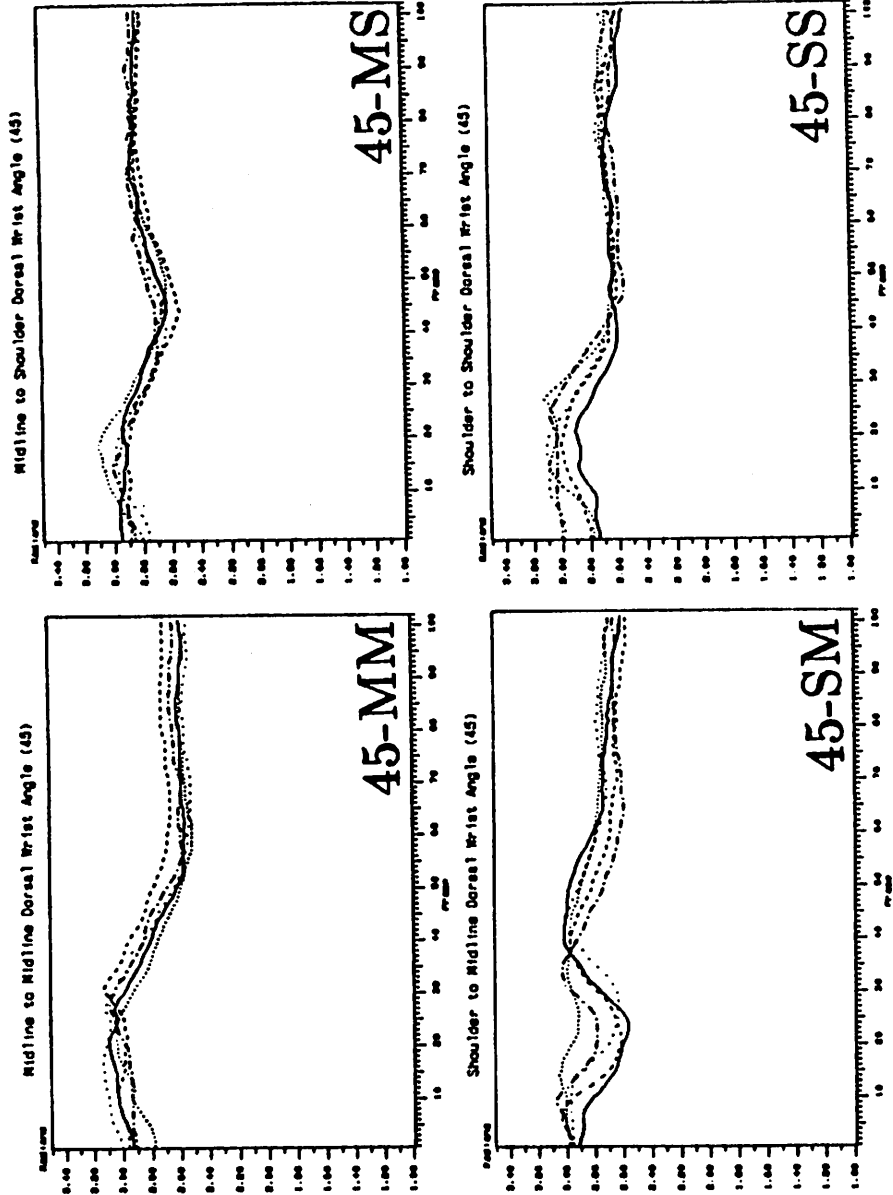
Figure 20: Dorsal Wrist Angle plotted over time

We plot the angle that the back of the hand makes with the forearm vector as it changes over time, as the hand preshapes and encloses the object. See Figure 17 for explanation.

90-MS
Midline to Shoulder Dorsal Wrist Angle (90)

90-SS
Shoulder to Shoulder Dorsal Wrist Angle (90)

90-MM
Midline to Midline Dorsal Wrist Angle (90)

90-SM
Shoulder to Midline Dorsal Wrist Angle (90)
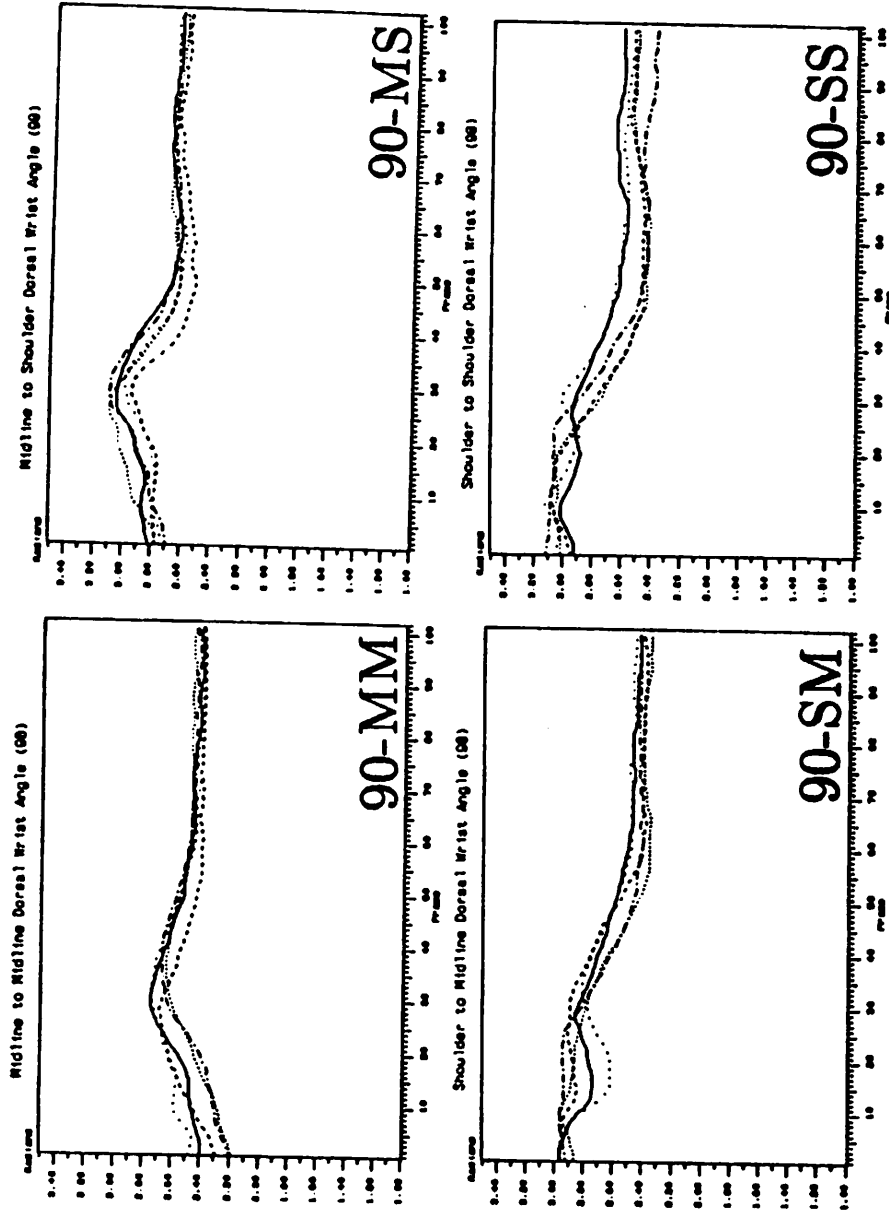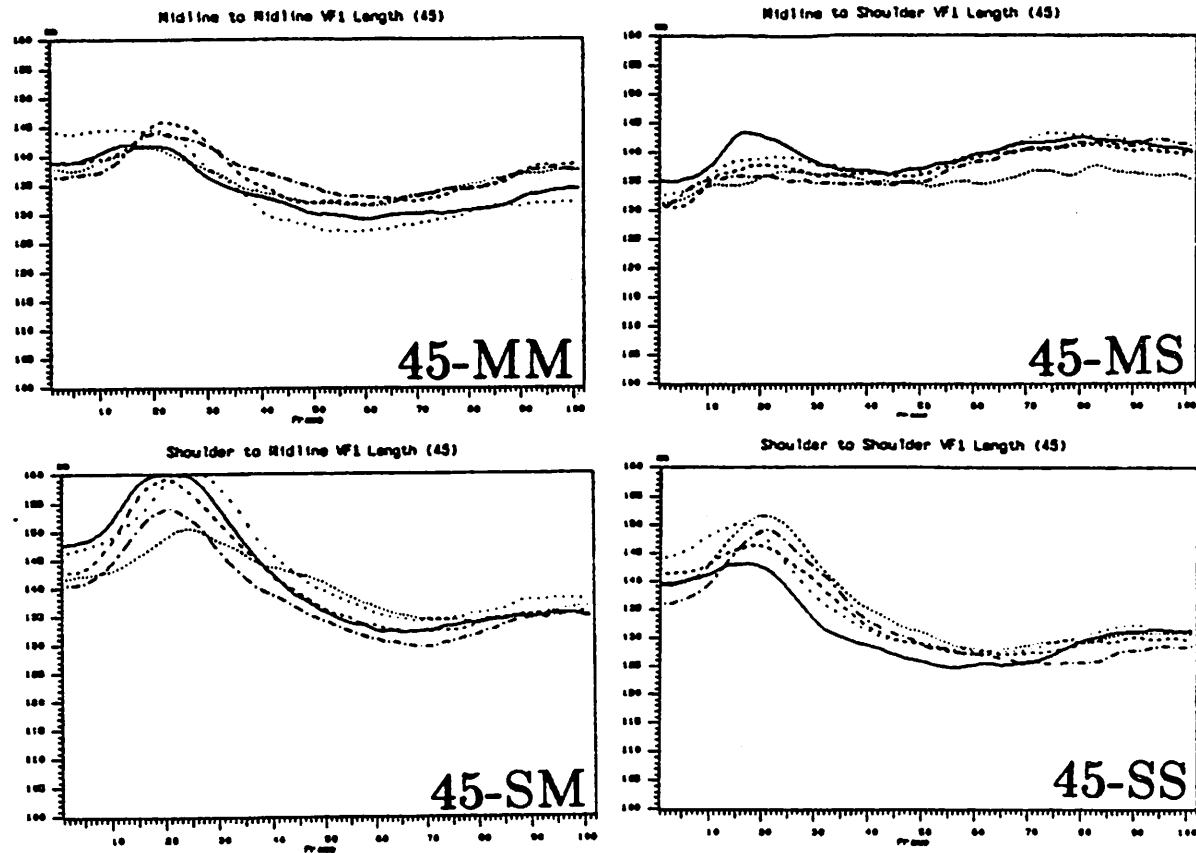
Figure 21: VF Parameters - VF1 length plotted over time

We plot the length of VF1 changing over time, as the hand preshapes and encloses the object. See Figure 17 for explanation.

90-MS — Midline to Shoulder VF1 Length (90)

90-SS — Shoulder to Shoulder VF1 Length (90)

90-MM — Midline to Midline VF1 Length (90)

90-SM — Shoulder to Midline VF1 Length (90)
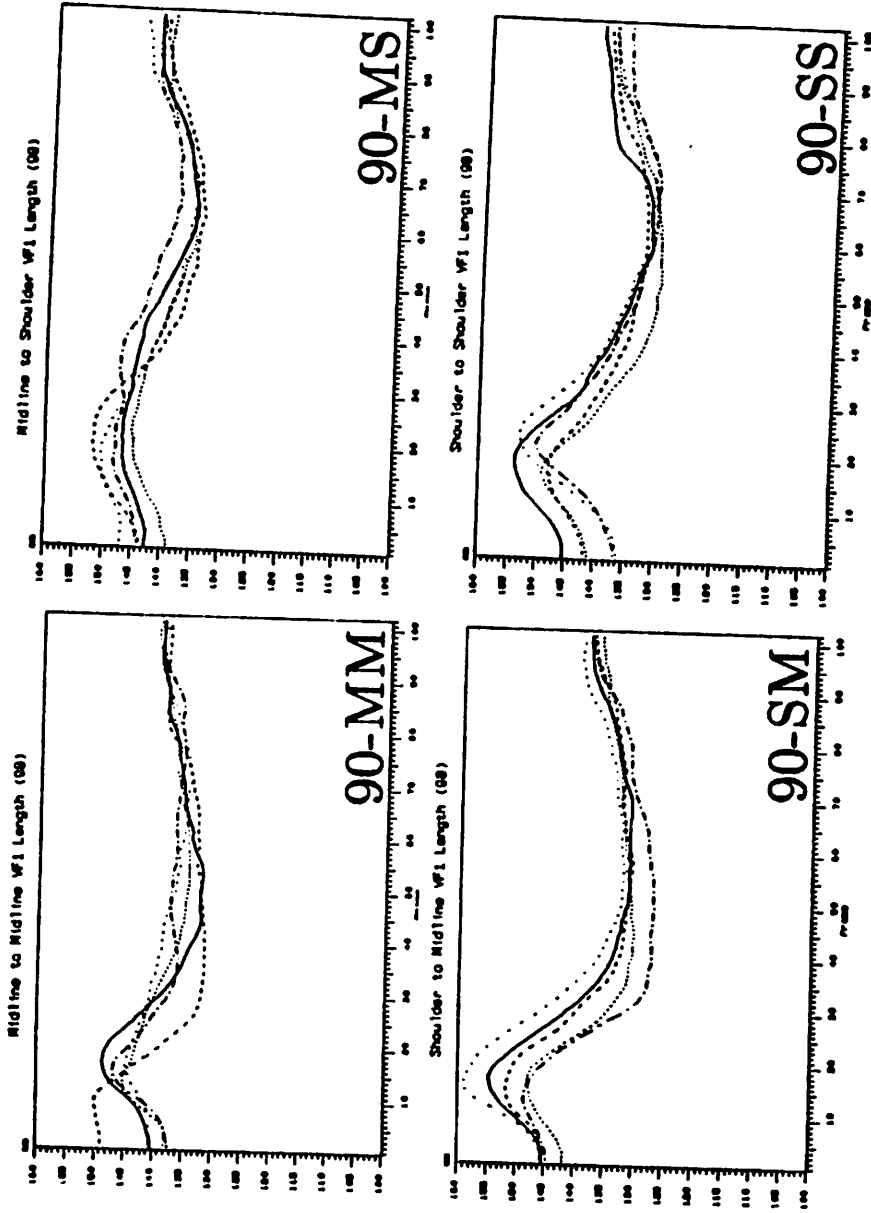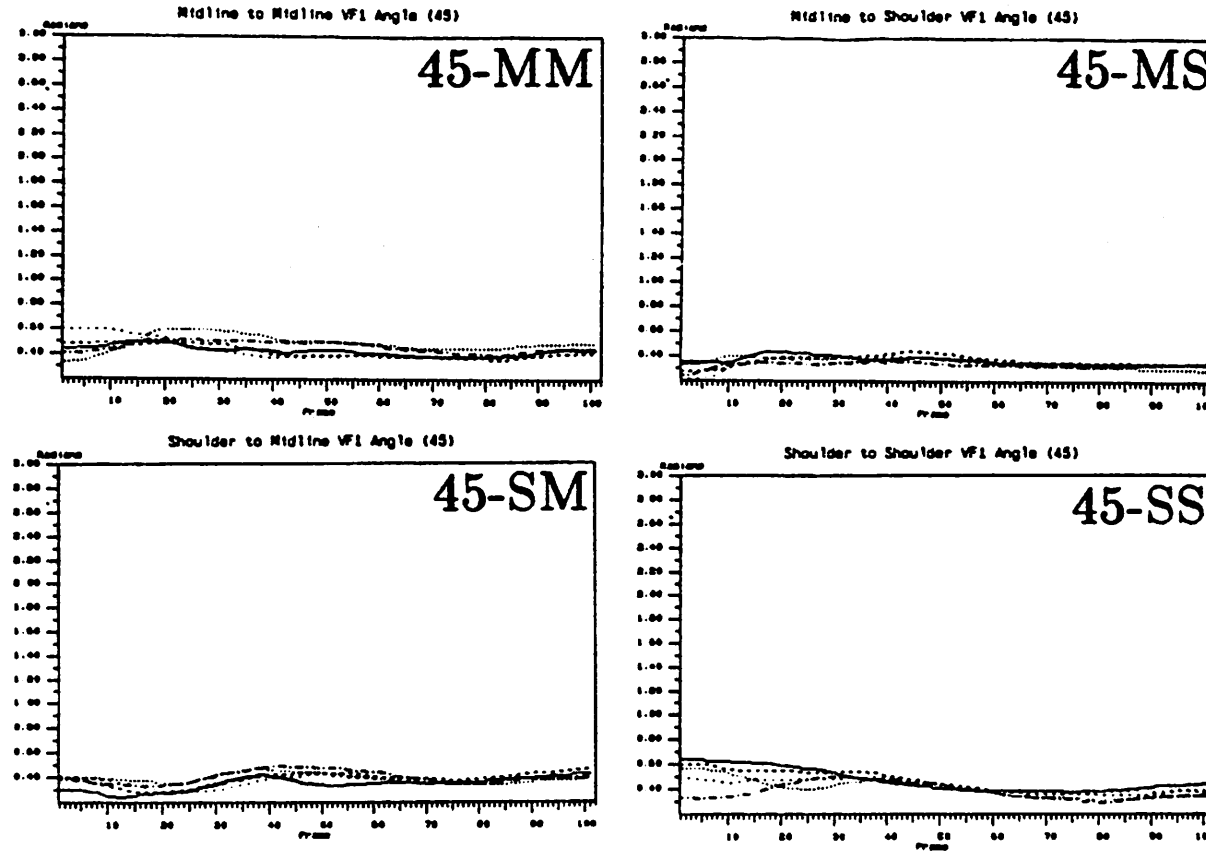
Figure 22: VF Parameters - VF1 angle plotted over time

We plot the angle that VF1 makes with the palm changing over time, as the hand preshapes and encloses the object. See Figure 17 for explanation.

Figure showing four plots labeled 90-MS, 90-MM, 90-SS, and 90-SM.
Plot labeled 90-MS: Midline to Shoulder VF1 Angle (99)
Plot labeled 90-MM: Midline to Midline VF1 Angle (99)
Plot labeled 90-SS: Shoulder to Shoulder VF1 Angle (99)
Plot labeled 90-SM: Shoulder to Midline VF1 Angle (99)
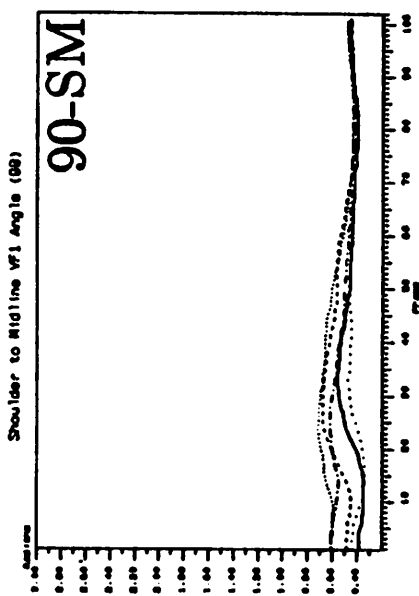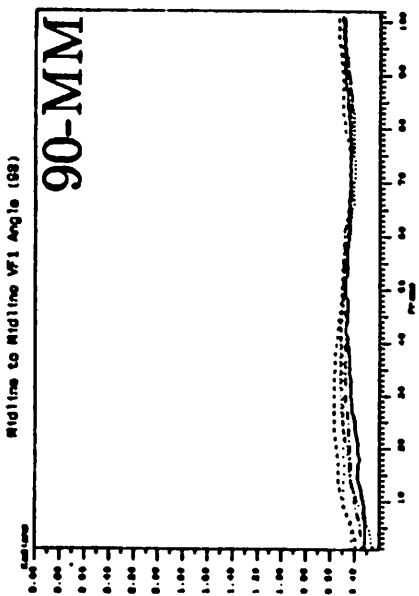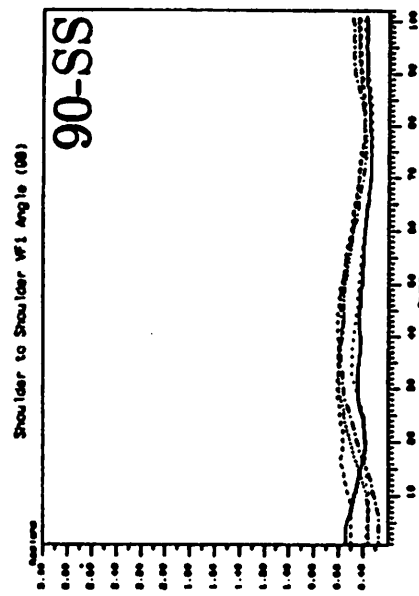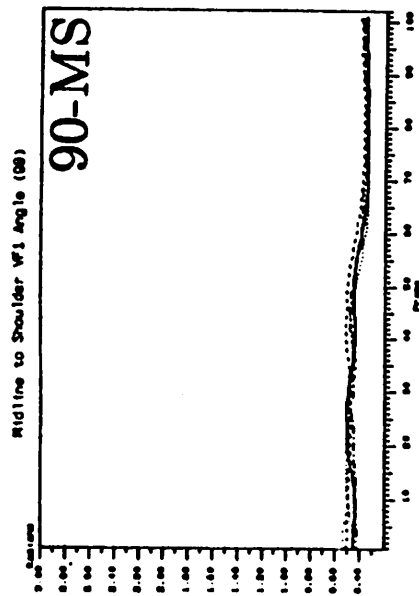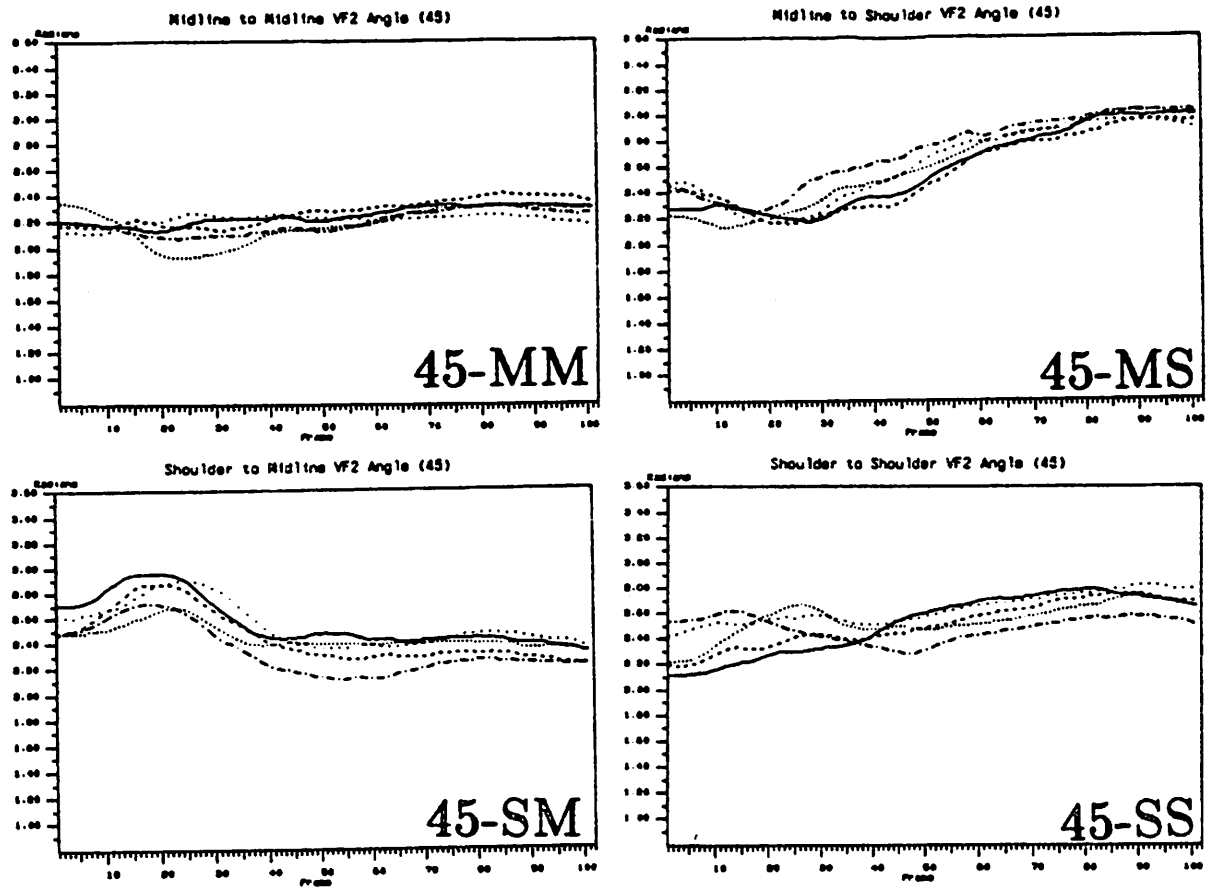
Figure 23: VF Parameters - VF2 length plotted over time

We plot the length of VF2 as it changing over time, as the hand pre-shapes and encloses the object. See Figure 17 for explanation.

SS-06

SM-06

Shoulder to Shoulder VF2 Angle (88)

Shoulder to Midline VF2 Angle (88)

MS-06

MM-06

Midline to Shoulder VF2 Angle (88)

Midline to Midline VF2 Angle (88)
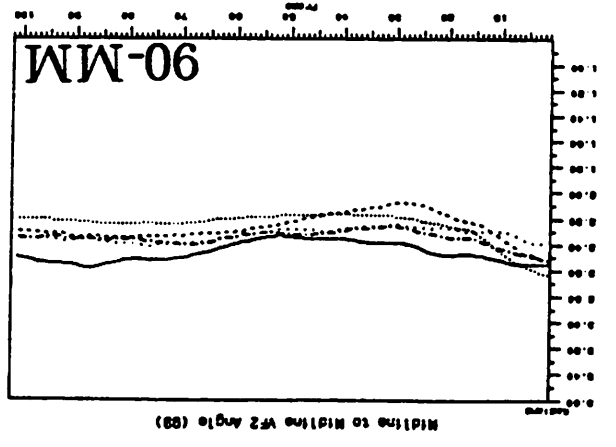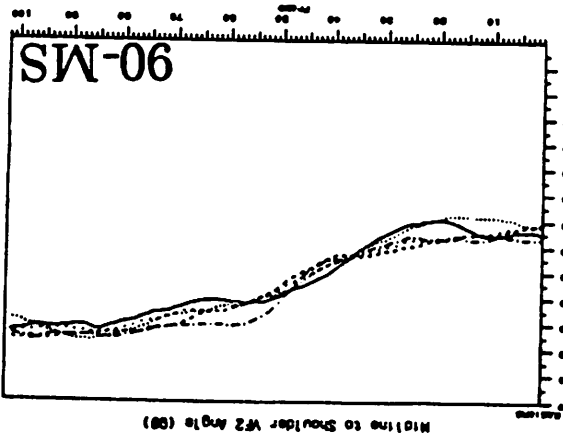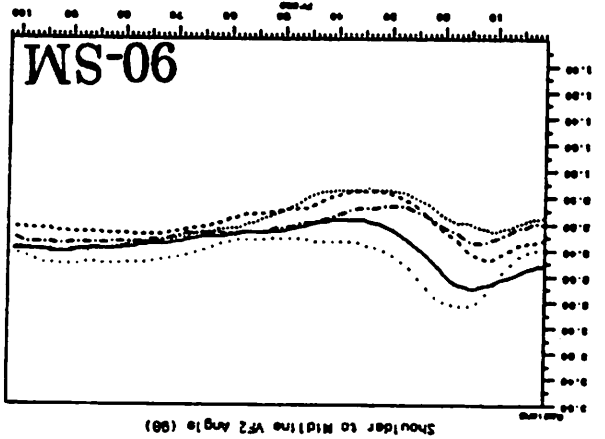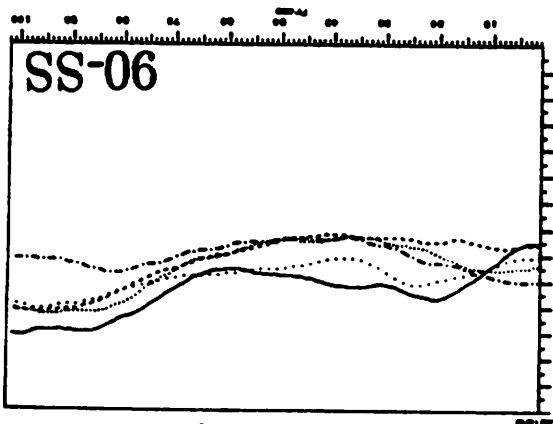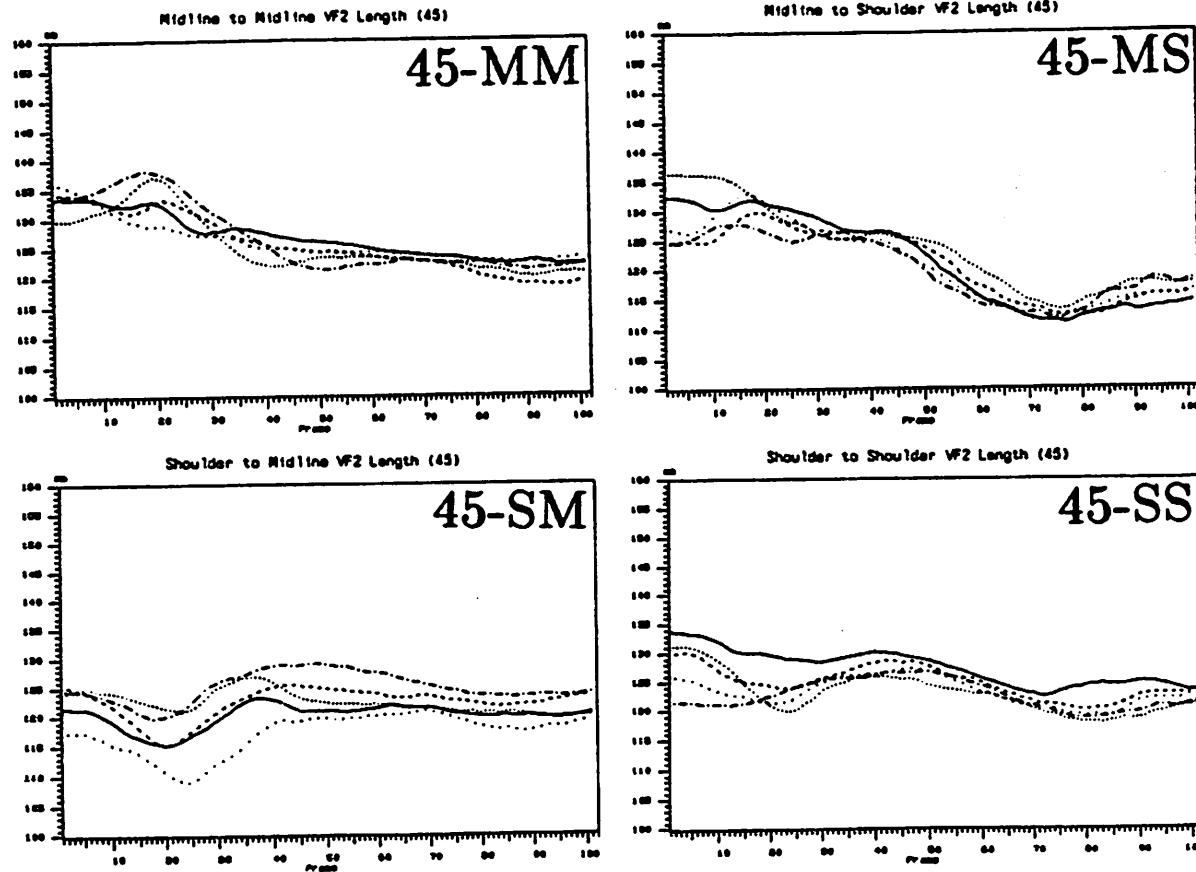
Figure 24: VF Parameters - VF2 angle plotted over time

We plot the angle that VF2 makes with the palm as it changes over time, as the hand preshapes and encloses the object. See Figure 17 for explanation.

90-MS
Midline to Shoulder VF2 Length (98)

90-SS
Shoulder to Shoulder VF2 Length (98)

90-MM
Midline to Midline VF2 Length (98)

90-SM
Shoulder to Midline VF2 Length (98)
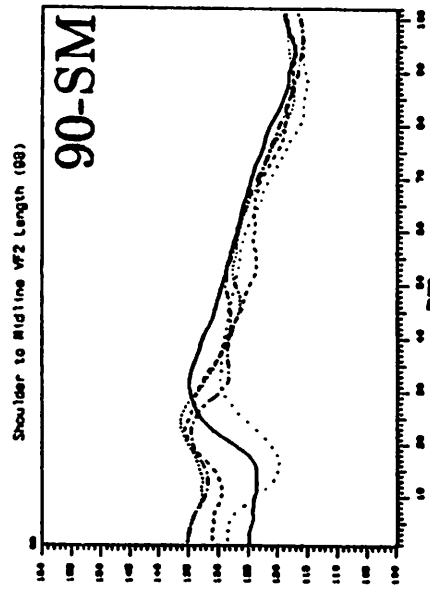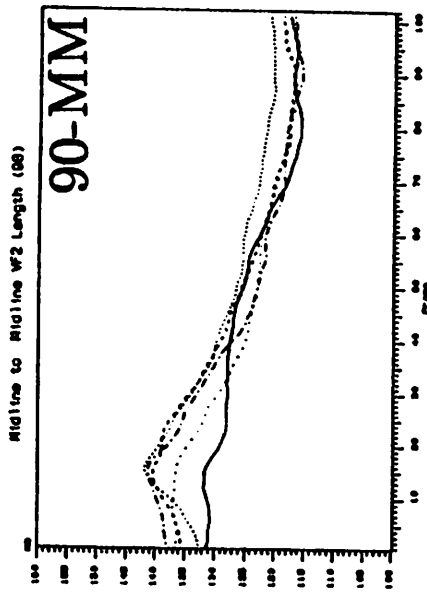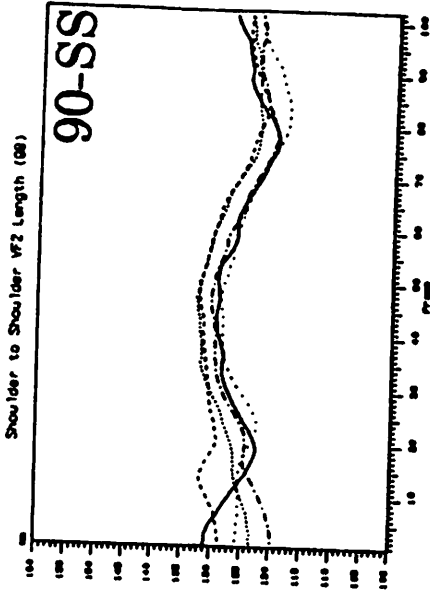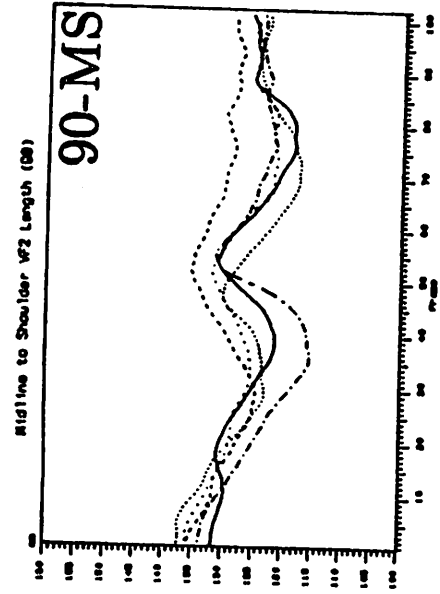
CHAPTER V

NEURAL MODEL OF PAD OPPOSITION

"The hand alone can be defined as the true organ of touch, for it alone explores or feels and thus adds to the sense of touch, activity which confers on it a unique talent ... Only the hand is at the same time touching and being touched".

<div align="right">

–Jean Brun

</div>

The coordinated control program of Figure 11 shows the general relationship between schemas and gives some indication about the type of information needed. However, it lacks the details necessary for developing a neural model. In this chapter we take a careful look at some of the schemas described in the coordinated control program, trying to be more specific about signaled information in terms of task requirements and opposition space. We draw a new coordinated control program, and describe a computer simulation of the schema to determine where to place opposition space relative to the object. The model we present is more a conceptual neural model, not specifically tied to known neural interconnections. In order to have a reference for developing a model and then to evaluate its success, we use the data from the Waterloo experiments, described in the previous chapter. As a first approximation toward developing a full model of prehension, we are initially only looking at pad opposition.

§1. Object Perception

As the arm and hand reach toward the object, there are an infinite number of approach vectors that could be taken. In the coordinated control program three perceptual schemas specify object information: one that extracts visual location, one for size recognition, and a third for orientation recognition. In our terminology, we would suggest that the size and orientation perceptual schemas extract the opposition vector V relative to the approach vector A, which has magnitude and angle (r,ϕ). The visual location schema extracts a location in an object-centered polar coordinate frame, representing the distance and the orientation for the origin of opposition space (the wrist) to be placed along an approach vector relative to the center of the opposition vector.

An object is, of course, first perceived in some two dimensional retinotopic coordinates, as seen in Figure 25. The CNS must somehow extract relevant information about that object, in this case perhaps the location of a surface point along the opposition vector. A transformation is then needed to place the object into a three dimensional coordinate system, which could be body-centered, or hand-centered, or both [Paillard 1982]. As the hand and wrist are also in this body coordinate frame, we hypothesize that an object-centered coordinate frame can be readily established, which approximates the world around the center of the chosen opposition vector of the object. The relationship between the hand and the object is then represented by two vectors: the opposition vector V and the approach vector A. The latter has an origin at the center of the opposition vector and points toward the origin of the opposition space (the wrist). This defines an object plane with normal given by the cross product of V and A, i.e., $V \times A$.

Using this framework then, the visual location perceptual schema computes the desired approach vector $A_d = (r_d,\phi_d)$ in polar form. This is the desired location for the opposition space to be placed, relative to the object. There are,
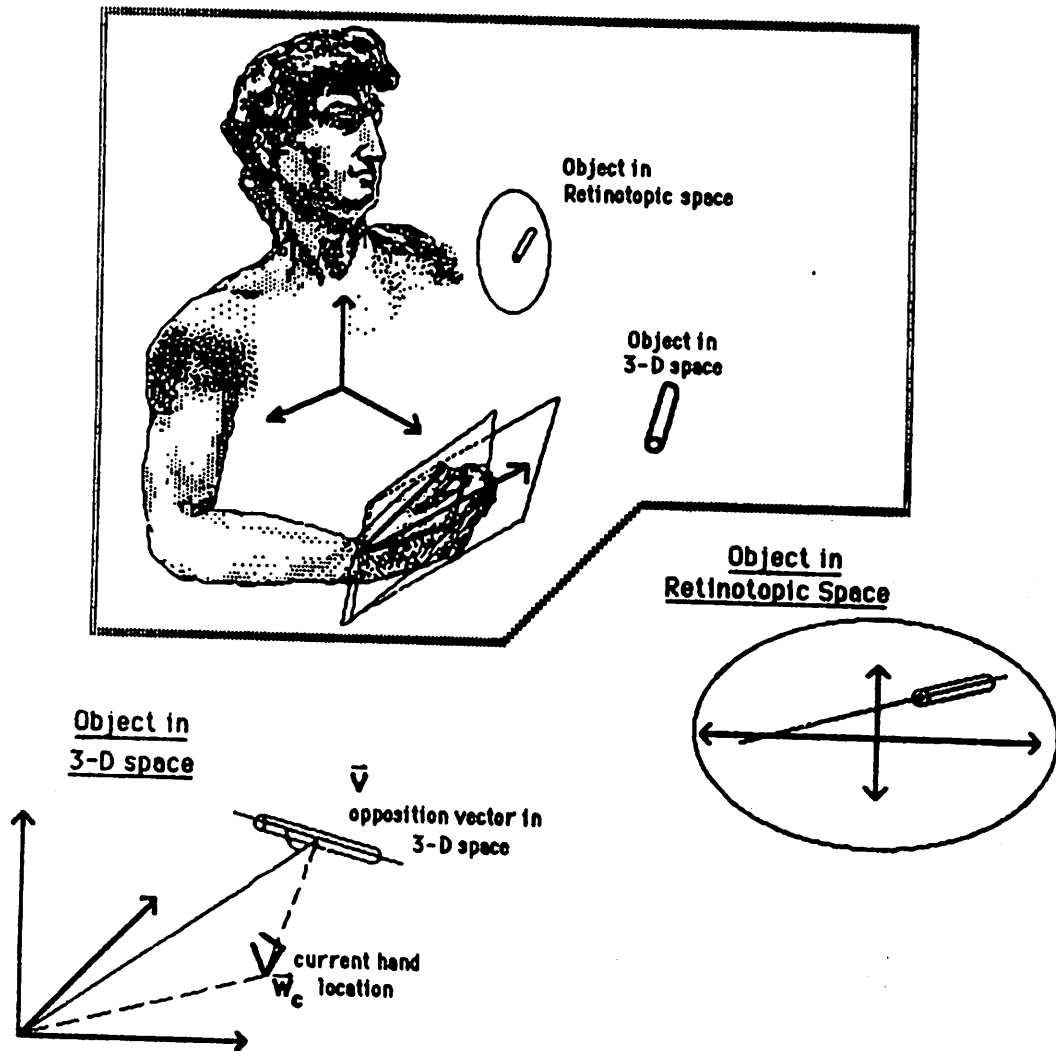
Figure 25: Object perceived relative to various reference systems.

An object is perceived retinotopically in a two-dimensional space. It must be transformed into some sort of three-dimensional space. The hand is also in a three-dimensional space. We can denote the wrist's location in the three-dimensional space by W_c, where the subscript c denotes its current location. Its distance from the object is r along the approach vector, which has an orientation ϕ relative to the opposition vector.

however, an infinite number of places for the wrist to be, in terms of distance from and orientation to the opposition vector. We hypothesize, from the functional analysis of Chapter 3, that the most useful location (r_d, ϕ_d) is one that places the object into a location within the opposition space at time of contact. At that location (r_d, ϕ_d), the Enclose Schema can then place the virtual fingers into configurations useful to the opposition task, as was shown by the experimental evidence in Chapter 4 for pad opposition. In those studies, we observed, for this subject, that ϕ at the end of the Preshape phase is generally in the right 'ballpark' $\pm\delta_{1,\phi}$ of its goal value (where the first subscript refers to which of the two δ values are being referenced). We also observed that, except for the midline to shoulder reaches, r is also in a particular 'ballpark' $\delta_{1,r}$ at the end of the Preshape phase.

We call the perceptual schema that extracts the desired wrist location (r_d, ϕ_d) the Approach Vector Selector.

§2. Mapping Task Requirements into Opposition Spaces

We can characterize the pad opposition space between the thumb and index as the set of all possible spatially-tagged normal vectors realizable by virtual finger 1 and virtual finger 2. Precisely, we can represent this mathematically as a pair of vector-valued functions of finger coordinates, one for each virtual finger. We use the notation $VF1$ and $VF2$, informally associated to the human hand in Chapter 3, in a more formal sense here for describing virtual finger positions within opposition spaces. The set of possible angles for $VF1$ is the set $ANGLES_{VF1}$, and for $VF2$, it is the set $ANGLES_{VF2}$. The set of possible lengths for $VF1$ and $VF2$ are the sets $LENGTHS_{VF1}$ and $LENGTHS_{VF2}$, respectively. Therefore, the set of possible $VF1$ coordinates is $ANGLES_{VF1} \times LENGTHS_{VF1}$ and the set of possible $VF2$ coordinates is $ANGLES_{VF2} \times LENGTHS_{VF2}$. Typical points in each set are $VF1 = (\theta_{VF1}, l_{VF1})$ and $VF2 = (\theta_{VF2}, l_{VF2})$. For virtual finger i,

there is a mapping O_i where:

$$O_i : (ANGLES_{VFi} \times LENGTHS_{VFi}) \rightarrow \Re^2$$

given by

$$(\theta_{VF1}, l_{VF1}) \mapsto (x_{VF1}(\theta_{VF1}, l_{VF1}), y_{VF1}(\theta_{VF1}, l_{VF1}))$$

$$(\theta_{VF2}, l_{VF2}) \mapsto (x_{VF2}(\theta_{VF2}, l_{VF2}), y_{VF2}(\theta_{VF2}, l_{VF2}))$$

The vector $(x_{VFi}(\theta_{VFi}, l_{VFi}), y_{VFi}(\theta_{VFi}, l_{VFi}))$ is the vector normal to the pad of VFi when VFi is at (θ_{VFi}, l_{VFi}) and where the length is equal to the magnitude of the force. The functions x and y give the Cartesion components of the force. Then the opposition space for a particular pair of virtual fingers is (O_1, O_2); i.e., a pair of vector-valued functions. A virtual finger configuration is $(VF1, VF2)$.

We would also like to describe a virtual finger configuration at a moment in time, so that we can describe the unfolding posture from its initial state, to the peak grip aperture, and finally to enclosing the object. Let $VF1_c$ denote the current configuration $(\theta_{VF1}^c, l_{VF1}^c)$ of the virtual finger 1, and let $VF2_c$ denote it for virtual finger 2. Movement of the fingers will convert the current virtual finger configuration $(VF1_c, VF2_c)$ into another virtual finger configuration. We can characterize the Preshape Schema by saying that it maps the current virtual finger configuration into a peak aperture virtual finger configuration $(VF1_p, VF2_p)$. The Enclose Schema maps the peak aperture virtual finger configuration $(VF1_p, VF2_p)$, into the desired virtual finger configuration $(VF1_d, VF2_d)$. We call $VF1 \times VF2$ the normal to the grasping plane.

The motor problem of mapping kinematic object properties to an opposition
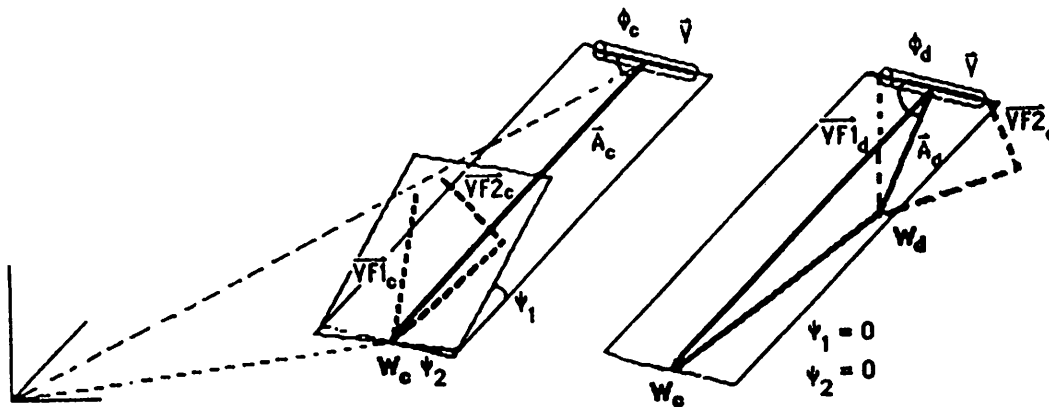
Figure 26: Positioning of an opposition space relative to the object

From the current position W_c of the hand relative to the object, a desired position W_d is chosen. The current VF configuration $(VF1_c, VF2_c)$ is transformed in the desired configuration $(VF1_d, VF2_d)$ within an opposition space.

space is seen in Figure 26. Three variables specify the initial difference between the grasping plane and the object plane:

1. ψ_1- a rotational *dof* representing pitch (adduction/abduction) at the wrist

2. ψ_2- a rotational *dof* representing roll (supination/pronation) at the wrist

3. r_c - distance from the current wrist location W_c to the center of the object at its opposition vector V along the current approach vector A_c

We suggest that the motor schemas reduce these differences in task specific manners. In Figure 27, we redisplay the coordinated control program, labeled with useful prehensile information. In the next three sections, we outline the input/output behavior of the motor schemas within this control program, noting the information they need and their contribution to the coordinated control program. Later, we offer possible neural algorithms for implementing them and the perceptual Approach Vector Selector schema.

§3. The Preshape Schema for Pad Opposition

The Preshape Schema computes the preshape opposition space solution $(VF1_p, VF2_p)$ adjusting the values of various inputs. It is provided with r_d and ϕ_d, the desired location for the wrist relative to the object, at the end of the Enclose Schema. It is also provided with the magnitude of the opposition vector, and size of the opposable surfaces. At (r_d, ϕ_d), the direction of the forces through the virtual finger 1 and virtual finger 2 pad normals are collinear with the opposition vector V, and equal in value and opposite in direction, that is, $O_1(VF1_d) = -O_2(VF2_d)$. Since the desired approach vector points from the center of the opposition vector to the desired wrist location (and the magnitude of the opposition vector is one of the inputs), the preshape schema can either compute the inverse kinematic solution for $(VF1_d, VF2_d)$ or else look it up in
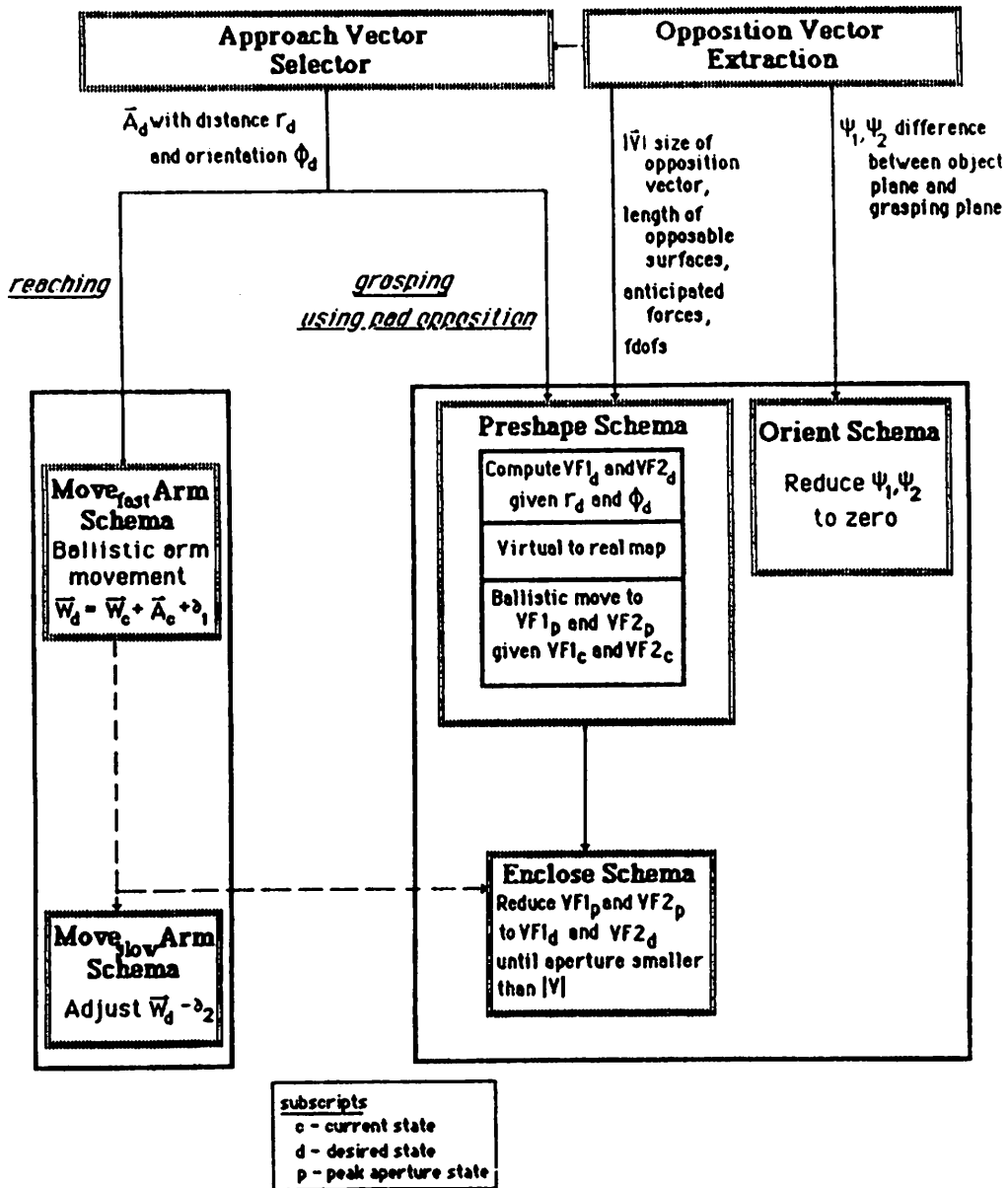
Figure 27: Updated Coordinated Control Program for Pad Opposition

The information passed between the schemas is noted in the coordinated control program. The Approach Vector Selector extracts the desired distance r_d and orientation ϕ_d for opposition space. These are passed to the Preshape Schema which selects a virtual finger configuration at peak aperture. The $Move_{fast}$ schema adds a small distance factor $\delta_{1,r}$ to r_d to avoid hitting the object. The $Move_{slow}$ schema subtracts $\delta_{2,r}$ from r_d to allow contact with the object.

a table. In order to determine the difference between the desired configuration $(VF1_d, VF2_d)$ at the end of the Enclose schema and the preshape configuration $(VF1_p, VF2_p)$ the end of the Preshape schema, an algorithm is needed which implements the ballpark concept. As a first approximation, we use the results noted in Chapter 4:

1. $VF1$ length: any length less than the desired length of $VF1_d$ that is within the set $LENGTHS_{VF1}$.

2. $VF1$ angle: any angle within a small tolerance of and less than the desired angle $VF1_d$, while still in the set $ANGLES_{VF1}$.

3. $VF2$ length: any length within a small tolerance in a range around the desired length of $VF2_d$, while still in the set $LENGTHS_{VF2}$.

4. $VF2$ angle: any angle within a small tolerance in a range around the desired angle of $VF2_d$, while still in the set $ANGLES_{VF2}$.

More formally,

$$\theta^p_{VF1} = \theta^d_{VF1} - \delta_{1,\theta_{VF1}}$$

$$l^p_{VF1} = l^d_{VF1} - \delta_{1,l_{VF1}}$$

$$\theta^p_{VF2} = \theta^d_{VF2} \pm \delta_{1,\theta_{VF2}}$$

$$l^p_{VF2} = l^d_{VF2} \pm \delta_{1,l_{VF2}}$$

To determine the number of real fingers to map into virtual fingers, the Preshape Schema uses the magnitude of the opposition vector V and the size of its two opposable surfaces. (We note that this is still a gross simplification, because it does not yet mention the anticipated forces or the functional *dofs* that we have specified necessary for a task description in Chapter 3). Finally, the Preshape Schema performs a ballistic movement from $(VF1_c, VF2_c)$ to $(VF1_p, VF2_p)$ during the $Move_{fast}$ Arm Schema.

§4.   The Orient Wrist Schema for Pad Opposition

The Orient Wrist Schema uses the difference between the grasping plane and the object's plane, and reduces to zero the difference between the planes. Out of the three *dofs* at the wrist, we are suggesting that, at least in pure pad opposition, the Orient Wrist Schema controls only two of them, in order to align the two planes. The third is controlled by the Preshape Schema for aligning opposition space relative to the center of the opposition vector. Such a distinction shows a difference in functional control versus physical control.

§5.   The Enclose Schema for Pad Opposition

When the hand is postured correctly at $(VF1_p, VF2_p)$ and the wrist transported to a general ballpark location, the Enclose schema is activated, along with the $Move_{slow}$ Arm schema. The goal during the enclose phase is to bring virtual finger 1 and 2 together by reducing the separation between them along the opposition vector V using a small buffer δ_2. Contact with the object stops the movement.

§6.   Move Arm Schemas

The Approach Vector Selector determines the final wrist location (r_d, ϕ_d). The $Move_{fast}$ Arm Schema uses this information to compute where that point is in space relative to the body coordinate frame and to move the arm to a point $(r_d + \delta_{1,r}, \phi_d \pm \delta_{1,\phi})$. As was noted in Chapter 4, this puts both the orientation component and the distance component close to that of the goal position. The $Move_{slow}$ Arm Schema will then move relative to the object, bringing the hand

into contact with the object, by trying to reach $(r_d - \delta_{2,r}, \phi_d - \delta_{2,\phi})$.

§7. Modelling the Approach Vector Selector for Pad Opposition

As mentioned above, there are an infinite number of approach vectors that the hand could take as it reaches toward the object. We have hypothesized that only a limited number of wrist locations represent useful positions. We use the word useful here in a task-related sense. We model the Approach Vector Selector using a conceptual neural network to perform the computation. It is based on cooperative/competitive models of computation [Dev 1975, Didday 1976, Amari and Arbib 1977, House 1984]. In the Amari-Arbib framework, a single element is selected from each one-dimensional array (fixed x) of a two dimensional (x,d) array of neurons. Their solution consists of a homogeneous two-dimensional excitatory neural field interacting with a one-dimensional inhibitory neuron pool. In the competition model (a single x, varying d), a single maximum is selected from a one-dimensional array. In the present study, we shall adapt the net to select a single maximum from a two-dimensional array.

Figure 28 shows how the Amari-Arbib system can be modified for an Approach Vector Selector. We use a two-dimensional excitatory field, defined here as the distance r from the object versus the orientation ϕ, which is the angle that the approach vector makes with the object's opposition vector. An input is provided to the excitatory field, which is tuned in such a way that it will be active when an input is presented and quiesce when the input dies out. The input I to the field is a map of the solution space, indicating all the locations (r,ϕ) that are reasonable places to place the wrist. Reasonable is used here in the sense that kinematic solutions exist in both $ANGLES_{VF1} \times LENGTHS_{VF1}$ and $ANGLES_{VF2} \times LENGTHS_{VF2}$. This input represents a very large solution space, because it could be defined over all possible kinematic solutions for all pos-
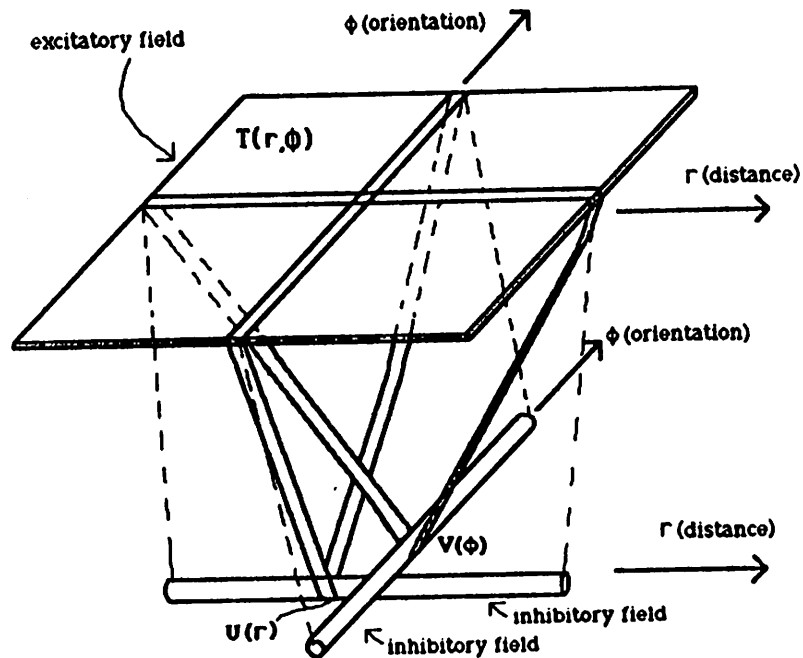
Figure 28: Modified Amari-Arbib Competition Model

Conceptualization of Amari-Arbib competition model using two inhibitory fields instead of the one used by Amari and Arbib [1977]. In this domain, the excitatory field consists of two-dimensions, the distance r from the object and the angle ϕ which the approach vector makes with the object's opposition vector.

sible graspable object sizes. In this model we are, however, interested in finding ways to efficiently represent this information. In our first attempt at a solution to this problem presented here, we restrict the input I by using summarized knowledge about the solution space. For each (r, ϕ), we count up the number of vectors in $ANGLES_{VF_i} \times LENGTHS_{VF_i}$ where the functions $O_1(VF1_d)$ and $O_2(VF2_d)$ are equal in value and opposite in direction and also collinear with the opposition vector V. We also limit the analysis to opposition vectors with a magnitude of 4 cm. While constraints like these reduce the scope of the problem, we use this analysis to explicitly represent the constraints on the hand. In future work, we can then relax them one at a time.

The full competition/cooperation model of Amari-Arbib used an inhibitory, one-dimensional pool of neurons to provide global inhibition to the system. An inhibitory pool receives an excitatory signal that is the sum of all the excitation along a narrow band centered at that location in the excitatory field, so as to "choose" a single active cell for each direction. In our case, we found it necessary to model the system with two inhibitory pools. Without all the arm and body constraints built into this initial model, we felt this a necessary step in order to get a 'winner take all' network solution. Since each wrist position (r, ϕ) already represents possibly multiple VF configurations, we felt it conceptually clearer to initially force the system into one peak value across the entire excitatory field. Later, when we can add in arm and body constraints as well, we can drop the need for two inhibitory pools.

The portion of the inhibitory pool U assigned to a particular distance receives an excitatory signal that is modulated by the sum of all excitation at that distance in the field. This inhibitory pool, in turn, sends inhibitory feedback to all elements at that distance. Thus, multiple distance estimates compete with each other in order to sustain field excitation. Similarly, orientations compete with other orientations using an inhibitory pool V. If the parameters are properly chosen,

the Amari-Arbib model predicts that the field will reach a state of equilibrium, where excitation is maintained at only one location.

Our model extends the Amari-Arbib scheme, but is similar to [House 1984], in that it uses two processes. In [House 1984], two excitatory processes were used for a model of depth perception in frogs and toads. One process represented the monocular cues of the visual field, and the other, the binocular cues. Here, in our system, both excitatory processes represent wrist positions (r, ϕ); however, the process T receives inputs from $ANGLES_{VF1} \times LENGTHS_{VF1}$ and the other process F from $ANGLES_{VF2} \times LENGTHS_{VF2}$. While this seems to break the hand into two separate pieces, it is justified by the constraints we used to set up the problem. Any approach vector, by its definition in relation to the opposition vector of the object, constrains the kinematic solutions for virtual finger 1. This in turn constrains the function O_1. While the kinematic solutions for virtual finger 2 are not as constrained as for virtual finger 1, we still want a solution where $O_1(VF1_d) = -O_2(VF2_d)$. The constraints on O_1 will therefore force constraints onto O_2 as well.

Since each point (r, ϕ) in T and F represents a position of the wrist, we would like each excitatory field to peak at the same value That peak would, of course, then represent a wrist location where VF configurations exist for both virtual fingers, such that the pads are generally aligned with each other and along the opposition vector. We can do this by means of reinforced, cross-coupled, pathways between T and F. In the House model, a location in the visual field receiving reinforcement from the other field indicated a better likelihood of that location providing a solution. In our case, a location in the solution space is reinforced if both VF1 and VF2 have kinematic solutions at that location. For example, if the wrist is placed at a location where the fingers could reach the object but the thumb could not, this would not be a good place for the wrist to be.

We define the input to T as I_T (the input to the thumb, or virtual finger

1), and the input to F as I_F (the input to the finger, or virtual finger 2). These each represent the summarized kinematic solution space for their virtual finger (i.e., a histogram counting the number of configurations satisfying $O_1(VF1_d) = -O_2(VF2_d)$ for this opposition vector, while being collinear with it). Global inhibition is used along both fields r and ϕ. In the case of T, we label the two inhibitory fields U for the distance dimension and V for the orientation dimension. For F, these two dimensions are denoted by X and Y, respectively.

The following equations characterize our use of an Amari-Arbib competition model [Amari and Arbib 1977], where we (a) couple two processes, and (b) add a second inhibitory dimension to each process.

$$\tau_T \Delta T_{ij}(t) = -T_{ij}(t) + W_0 f[T_{ij}(t)] + \sum_{k=i\pm 1} \sum_{l=j\pm 1} W_1 f[T_{kl}(t)]$$
$$+ K_{FT} f[F_{ij}(t)] + W_i I_{Tij}(t) - W_g(g[U_i(t)] + g[V_j(t)])$$

$$\tau_U \Delta U_i(t) = -U_i(t) + \frac{1}{m} \sum_{j=1}^{m} f[T_{ij}(t)]$$

$$\tau_V \Delta V_j(t) = -V_j(t) + \frac{1}{n} \sum_{i=1}^{n} f[T_{ij}(t)]$$

$$\tau_F \Delta F_{ij}(t) = -F_{ij}(t) + W_0 f[F_{ij}(t)] + \sum_{k=i\pm 1} \sum_{l=j\pm 1} W_1 f[F_{kl}(t)]$$
$$+ K_{TF} f[T_{ij}(t)] + W_i I_{Fij}(t) - W_g(g[X_i(t)] + g[Y_j(t)])$$

$$\tau_X \Delta X_i(t) = -X_i(t) + \frac{1}{m} \sum_{j=1}^{m} f[F_{ij}(t)]$$

$$\tau_Y \Delta Y_j(t) = -Y_j(t) + \frac{1}{n} \sum_{i=1}^{n} f[F_{ij}(t)]$$

The subscripts i and j in these equations refer to the ith distance away that the wrist can be from the object, and the jth orientation that the approach vector makes with the opposition vector. At the ith distance and jth orientation, there are I_{Tij} solutions for the thumb and I_{Fij} solutions for the index finger. The general form of the saturation-threshold function f used is:

$$f(T) = \begin{cases} 0 & T < h_0 \\ \sigma^2(3 - 2\sigma) & h_0 \leq T \leq h_1 \\ 1 & T > h_1 \end{cases}$$

where:

h_0 is the threshold,

h_1 is the saturation level,

and $\sigma = (T - h_0) / (h_1 - h_0)$.

The linear thresholding function g is defined as:

$$g(T) = \begin{cases} 0 & T < h_0 \\ T - h_0 & T \geq h_0 \end{cases}$$

These functions are similar to those used by House [1984] for an application of the Amari-Arbib model to depth and detour behavior of frogs and toads. Our model reflects five different terms:

1. Self-excitation of a cell. Cells are set to some initial resting value. The weight factor is W_0.

2. The weighted sum of near neighbors to a cell. In this case, we are currently using the four immediate neighbors of a cell within the excitatory field. The weight factor is W_1.

3. Excitatory input from cells in the same column of the other space. A solution in the VF1 space mutually excites solutions in the VF2 space which are at the same distance r_i and angle ϕ_j, with a gain of K_{FT}.

4. An external input, representing the 'score' of this solution. A virtual finger configuration $(\theta^d_{VFi}, l^d_{VFi})$ is a potential solution if $O_i(VFi_d)$ is oriented, within some tolerance, along the same direction as the opposition vector. An ith and jth value of I_{Tij} and I_{Fij} sums up the number of potential virtual finger configurations for virtual finger 1 and virtual finger 2, respectively, at some distance r_i and orientation ϕ_j of the approach vector. The weight factor is W_I.

5. Two global inhibitory inputs. One is summed up over the angles ϕ_j, and then subtracted from the cell's value. The other does global inhibition over the distances r_i. The weight factor is W_g.

§8. Approach Vector Selector Simulation

We performed a computer simulation of the Approach Vector Selector model, using measurements from the hand of the Waterloo subject when necessary. The equations were translated into FORTRAN, and were approximated as difference equations. The object to be grasped was always assumed to have an opposition vector 4 cm in diameter. Its orientation is, of course, relative to the wrist location, and therefore, not assumed to have a fixed angle in space.

To construct the inputs to the model, we first had to model the pad opposition space of the Waterloo subject. From measurements of his hand, we estimated the direction of the thumb and index finger pads, and did a linear interpolation, as seen in Figure 29. On the left, is an approximation of his thumb pad within the range of its movement, and on the right, is his index finger. We discretized this approximation within a 20 × 20 element space. We modeled his thumb
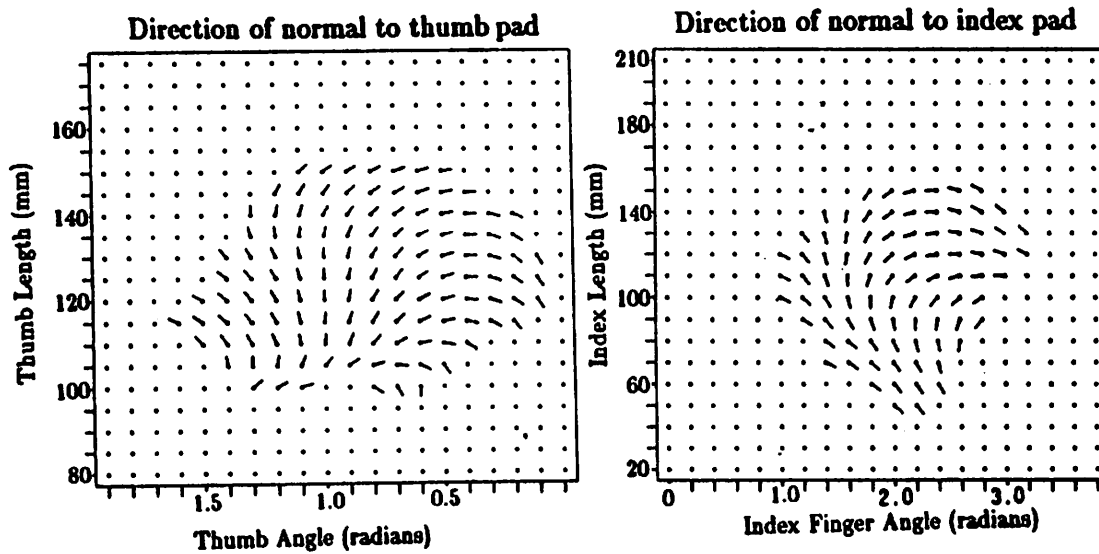
Figure 29: Approximation of Pad Opposition Space for Waterloo Subject

As a virtual finger vector changes orientation (abscissa) and length (ordinate), the direction that the pad is pointing also changes. On the left, the angle that $VF1$ makes with the palm is plotted versus the length of $VF1$, showing the direction of the thumb pad normal at a given vector configuration. On the right, the angle that $VF2$ makes with the palm is seen versus the length of $VF2$, showing the normal to the index finger pad. The abscissas are opposite in direction, reflecting the opposability of the thumb and index.

workspace $ANGLES_{VF1} \times LENGTHS_{VF1}$ and index workspace $ANGLES_{VF2} \times LENGTHS_{VF2}$ by the values noted in the figure. The values of the vector-valued functions (O_1, O_2) are shown graphically.

From the measurements taken from his hand and from estimates on the range of the *dofs* of the hand articulations [Kapandji 1982], we calculated the kinematic solution sets $ANGLES_{VF1} \times LENGTHS_{VF1}$ and $ANGLES_{VF2} \times LENGTHS_{VF2}$ and counted the number of solutions to $O_1(VF1_d) = -O_2(VF2_d)$ at various approach vector solutions for this 4 cm object. For data-processing simplicity, we limited this computation to a 20 × 20 element space, representing a discretized approximation of the world between the object and the wrist. We felt justified precalculating these as inputs to the network, as it is low level information representing the capabilities and skills of the hand. Such knowledge can be built up associative memories, and then modified as the body grows, changes, and develops. Since this model is currently not using an adaptive network, we feel justified in isolating the adaptive aspects of the problem from the constraints being modelled.

In Figure 30, we plot the results of these calculations presented as histograms, plotting distance r against orientation ϕ. In this figure, the height of the surface at each location (r_i, ϕ_j), indicates the number of kinematic solutions. On the left, the number of virtual finger 1 configurations at a given (r_i, ϕ_j) are plotted, and on the right, the number of kinematic solutions for virtual finger 2 at a given (r_i, ϕ_j) are plotted. If a VF1 kinematic solution was not matched by some VF2 kinematic solution, that VF1 solution was not included in the histogram; and vice versa for VF2. As soon as the object gets too far away, the number of solutions for the virtual finger configurations drops to zero.

For each (r_i, ϕ_j), we looked at the $O_1(VF1_d) = -O_2(VF2_d)$ constraint, using an ϵ to align them within some tolerance along the opposition vector. From the analysis of pad opposition in Chapter 3, this takes into account only the first two
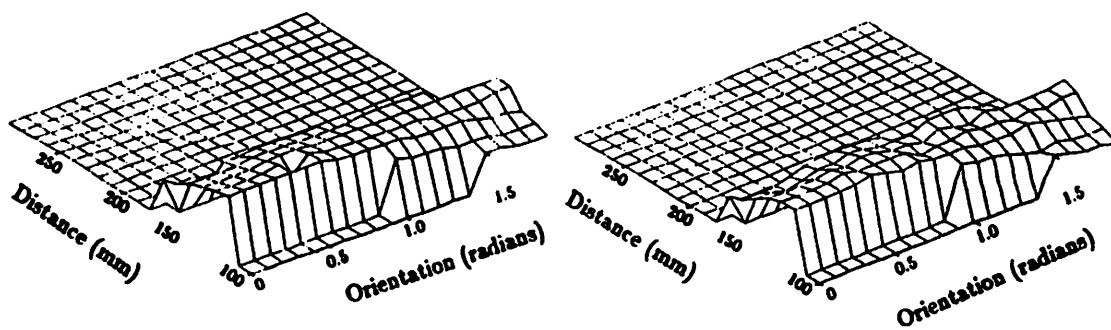
Figure 30: Possible object-centered locations where Waterloo subject could put wrist when grasping given object

Histograms showing the number of kinematic solutions within the pad opposition space of the Waterloo subject. On the left, we plot the number of solutions for $VF1_d$ at a given distance r from the object versus a given orientation ϕ that an approach vector makes with the opposition vector. On the right, we plot the same for $VF2_d$. We only include solutions where there is overlap at the given (r,ϕ) location.

goals outlined (satisfying kinematic constraints, and aligning the pad normals within some tolerance). These potential solutions were then counted to produce the histogram seen in Figure 31, representing the input to the simulation.

Although we describe the creation of this input in two separate stages, we are not suggesting that the CNS does it this way. There are two ways to look at this issue. On one hand, all the possible kinematic solutions for grasping a particular object are not very useful if they are not task related. A more useful representation is this latter one (Figure 31), because it incorporates how the object will be used in the task. However, this would then limit the usefulness of these kinematic solutions because they would then be embedded in a pad opposition representation. For now, we choose to make explicit the type of information necessary for specific prehensile movements, in order to capture the fundamental constraints acting on them.

Using the count of potential solutions as input, the Approach Vector Selector computes where is a reasonable place to put the wrist at time of contact. In Figure 32, we trace a time course of the Selector running, starting from an initial state and finishing when it has converged on a solution for the wrist position relative to the object. The network of cells is initialized to a zero excitation level, as seen in Figure 32a. On the left, the excitatory field T for VF1 is seen; on the right, the field F for VF2 is seen. Simulated activity at 11 time-constants after initialization is seen in Figure 32b, and at convergence in Figure 32c at 27 time-constants after initialization. It has converged on the solution $r_d = 140$ mm and $\phi_d = 1.4$ radians. The gradual buildup of excitation is seen. To achieve this convergence, the set of parameters seen in Table 14 was used. We found that weights on virtual finger 1 had to be higher than those on virtual finger 2 in order to get convergence.
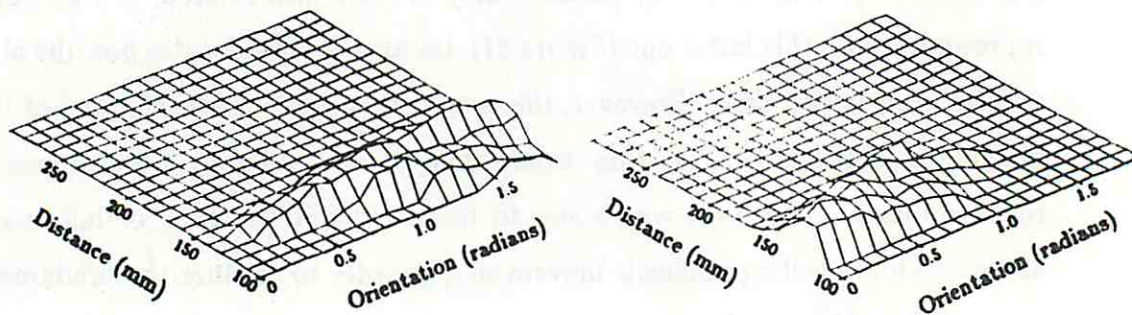
Figure 31: Object-centered locations for wrist reflecting solution constraints

Within the possible pad opposition space solutions, some solutions are not useful for the particular task. The input to the simulation reflects this, by including the kinematic solutions that satisfy the $O_1(VF1_d) = -O_2(VF2_d)$ constraint. In addition, normals to the thumb and index finger pads must be aligned with the opposition vector.
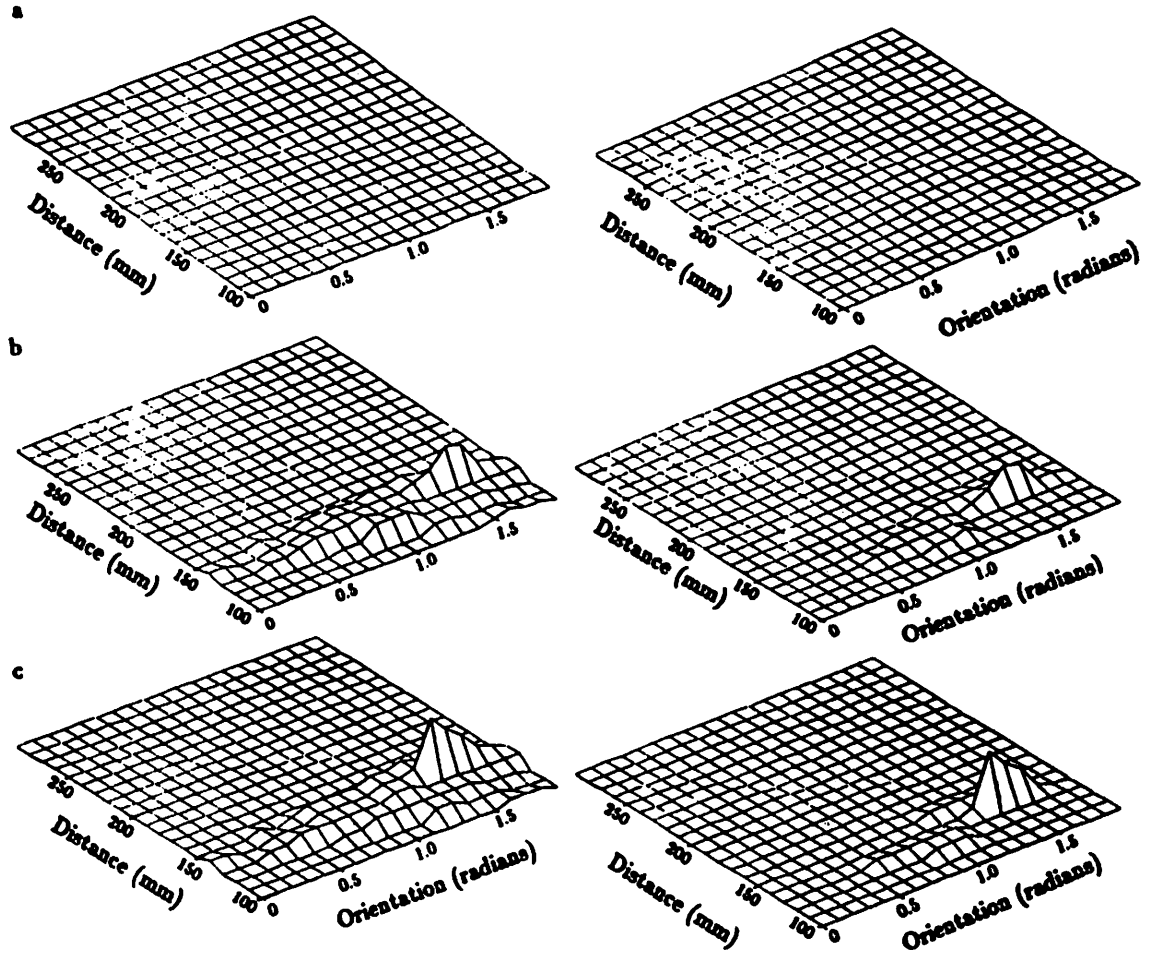
Figure 32: Approach Vector Simulation through a time course

(a) The initial state of the excitatory fields T (on the left) and F (on the right). (b) After 11 time periods, peaks are seen slowly developing (c) At convergence, a peak is seen at location $r_d = 140$ mm, $\phi_d = 1.4$ radians in each field.

	W_0	W_1	W_I	W_g	K
T	0.5	0.04	0.035	0.35	0.35
F	0.45	0.03	0.003	0.35	0.6

Table 14: Values on weighting factors used in simulation

Values for the weighting factors that allowed the simulation to converge. T and F represent the two excitory fields, for virtual finger 1 and virtual finger 2, respectively. W_0 is the weight for self-excitation, W_1 is the weight for near neighbors, K is the weight for the other space, W_I is the weight for the external input, and W_g is the weight for global inhibition.

§9. Modelling and Simulating the Preshape and Enclose Schemas

The Approach Vector Selector outputs a location (r_d, ϕ_d), which specifies where to put the wrist at contact. The $Move_{fast}$ Arm Schema will place opposition space in that vicinity, moving the wrist to a point $(r_d + \delta_{1,r}, \phi_d \pm \delta_{1,\phi})$.

The Preshape Schema uses (r_d, ϕ_d) to compute the inverse kinematic solutions for $VF1_d$ and $VF2_d$ (the desired VF configurations at the end of the enclose phase). However, the virtual fingers at peak aperture do not have to be at the $VF1_d$ and $VF2_d$ configuration, but in some ballpark configuration, $VF1_p$ and $VF2_p$. The Preshape Schema relaxes $VF1_d$ and $VF2_d$ using $\delta_{1,\theta_{VF1}}$, $\delta_{1,l_{VF1}}$, $\delta_{1,\theta_{VF2}}$, and $\delta_{1,l_{VF2}}$ as noted above.

To simulate the Preshape Schema, we waited for the Approach Vector Selector to converge on a solution (the peak in Figure 32 which refers to the solution (r_d, ϕ_d)). We then performed the inverse kinematic computations using a lookup table to find virtual finger configurations in the sets $ANGLES_{VF1} \times LENGTHS_{VF1}$ and $ANGLES_{VF2} \times LENGTHS_{VF2}$. We did not care if these satisfied the constraint $O_1(VF1_d) = -O_2(VF2_d)$, because that constraint was built into the input. Also, the Preshape Schema puts the virtual fingers into

locations only approximately near the object, so variability at the peak aperture is acceptable.

The Enclose Schema brings the virtual fingers together, by reducing the separation between $O_1(VF1_d)$ and $O_2(VF2_d)$ along the opposition vector V using a small buffer δ_2 for each variable until contact is made. We assume that, if contact is not made within that small tolerance, an error signal is sent by the Enclose Schema, as described by Arbib, Iberall, Lyons [1985].

In simulating the Enclose Schema, we were really only interested in looking at the results of the inverse kinematic computation for $VF1_d$ and $VF2_d$, based on (r, ϕ). Therefore, we did not add δ_2 values to the variables in the results we show below.

§10. Comparison of Simulation to Waterloo Empirical Results

Out of the possible solutions that the Waterloo subject could have chosen, we can see in Figure 33 the values for (r_i, ϕ_j) where he actually chose to put his wrist. The upper plots show the number of times he put his hand at a particular location, relative to the object at the peak aperture. On the left, are the number of VF1 configurations he used, and on the right are the number of VF2 configurations. In the lower plots, we see his solutions at contact with the object. Two general peaks are seen in the contact plots. A major peak is seen when the hand is about 150 mm from the object (in the 150-160 mm range), with about a 58° orientation (1-1.1 radians range), which is where most contacts occurred. A smaller peak is seen at the location where ϕ is about 40° (0.6-0.7 radians) and r is in the 150-160 mm range. This peak is created by the reaches toward the shoulder direction when the object was oriented at a 45° orientation to the subject (the R-4-45-MS). This peak is smaller because the subject chose this solution fewer times.
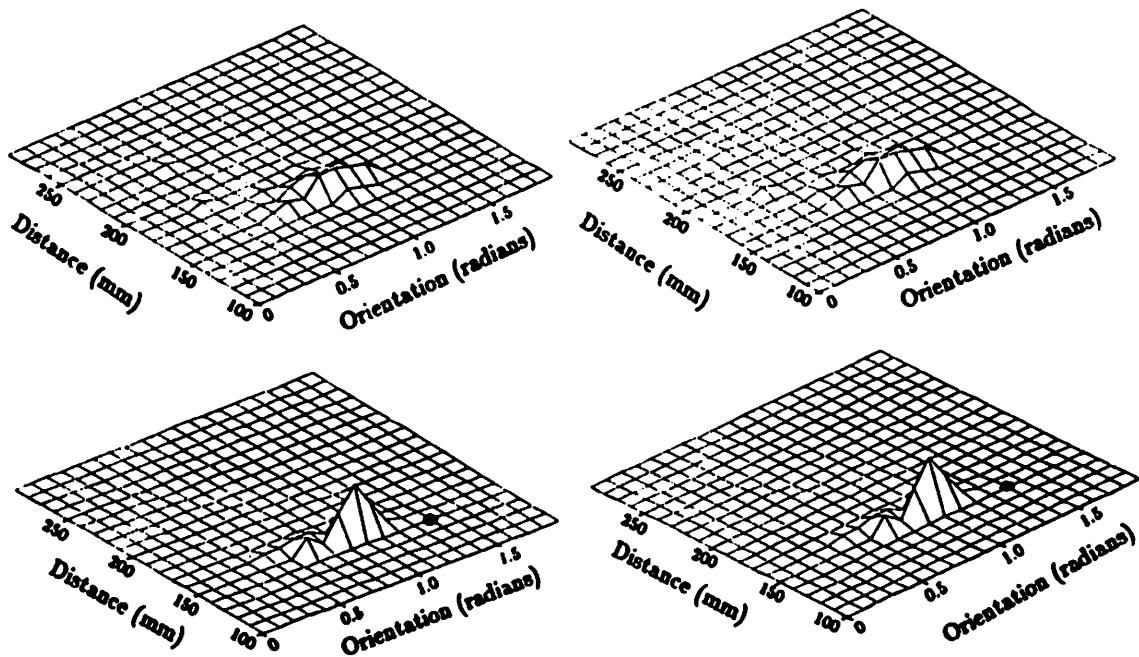
Figure 33: Approach Vector Selection Comparison of Simulation and Empirical results

From the empirical data presented in Chapter 4, we plot where the Waterloo subject actually places his wrist relative to the object. In the upper figures, we see the wrist locations at peak aperture for VF1 (on the left) and VF2 (on the right). In the lower figures are the wrist locations at contact with the dowel. From these lower figures, we can see that the subject generally put his wrist at a location $r = 150$ mm and $\phi = 1.0$ radians relative to the object. We have marked the location ($r_d = 140$ mm, $\phi_d = 1.4$ radians) where the simulation converged, noting that this is very close to the location that the subject chose.

We compare this to the results of the Approach Vector Selector simulation, by marking on Figure 33 the results ($r_d = 140$ mm, $\phi_d = 1.4$ radians) that were shown in Figure 32c. As the Approach Vector Selector is predicting where he will put his wrist at the end of the Enclose phase, we only mark the bottom two figures. Our model generally predicts his solutions, as it converged on a solution very close to the location that the subject chose.

In terms of the grasping schemas, we can map his virtual finger solutions back into his pad opposition space, as seen in Figure 34. In the upper plot, we circle (heavy line) the virtual finger configurations he used at peak aperture, with virtual finger 1 on the left and virtual finger 2 on the right. In the lower plots, we circle his chosen opposition space solutions at contact. We compare the empirical results to our simulation results by circling in a light line the results of the Preshape Schema (upper plots in Figure 34) and the results of the Enclose Schema (lower plots in Figure 34). The lower ones, as we mentioned above, are the actual goal computed, instead of the values offset by a δ_2. The simulation results tend to be closer to the center of the opposition space than the configurations chosen by the subject. In the upper plots, we see that the Preshape Schema simulation relaxes the goal configuration, and suggests VF configurations that can be used. However, since the goal configurations were at the center of the opposition space, these tend to be also.

§11. Discussion

We have presented here a model and simulation of the parts of the coordinated control program most directly related to finger movement. We have tried to seek out ways to use the hypotheses built on the empirical data of Chapter 4 to model these schemas. The major task we see in solving the grasping problem is to determine where to put the hand, actually the wrist, relative to a perceived
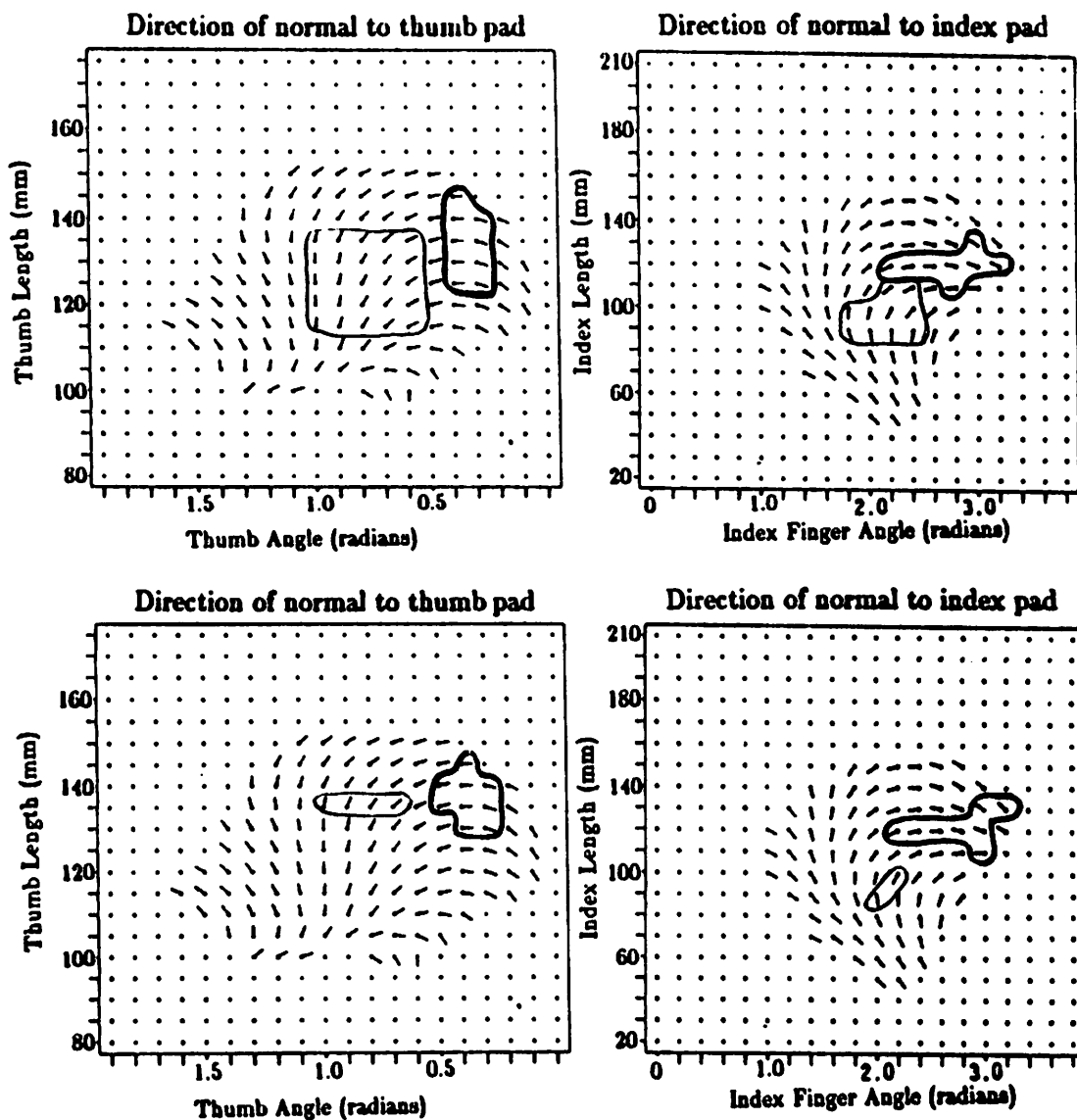
Figure 34: Opposition Space Comparison of Simulation and Empirical Results

Using the approximation of the pad opposition space of the Waterloo subject, we circle (heavy line) the solutions chosen by the Waterloo subject at peak aperture (upper plots) and at contact (lower plots). On the left the chosen VF1 configurations are noted mapped onto O_1; on the right, the chosen VF2 configurations mapped onto O_2. In contrast, we circle (light line) the solutions chosen by the Preshape Schema simulation (upper plots) and the Enclose Schema (lower plots).

object. Towards this end, we have shown that multiple processes, each focusing on some location in an object-centered space, can compete and then converge on a solution, depending on the constraints on the system. Our goal in this chapter was to show that the converged upon location is constrained in many important ways by the capabilities of the fingers.

As our system is only a first approximation, we would have to improve it along the following lines to get a closer approximation of human movement:

1. Incorporate a better model of the subject's hand. We only estimated the direction of the normals of his pads, and used anatomical texts to guess at the mobility of his joints. We also estimated what the workspace of his pad opposition space was.

2. Incorporate a more complete model of pad opposition space, using the constraint list described in Chapter 3 (kinematic constraints, pads generally aligned, minimize magnitude of forces used, minimize finger movement, maximize available *dofs*). Our model of opposition space does not yet include magnitude information about applicable forces through the pads, only direction. With a better model of the subject's hand and a more complete model of pad opposition space, our results would be more accurate.

3. Incorporate reaching constraints, taking into account the effect of arm constraints on opposition space. The data discussed in Chapter 4 shows major effects involving the relative position of the object to the body.

We believe that goal-directed motor behavior must take into account the constraints imposed on the movement: these arise from multiple sources, such as from the nature of the task, from the arm and body, from the relationship of the hand to the object, and even from the abilities of the perceptual systems. The conceptual model presented here tries to capture some of those constraints, as a first step toward making them all explicit. A plausible neural model for the more conceptual model presented here would involve neural structures, such as the cerebellum, which could learn the constraints and solve the problem more in terms of constraint propagation. This would be more natural to living systems,

where the linkages in the arms and hands are constantly changing throughout ontogeny.

One way we captured the constraints on prehensile movements was by "chunking" together the kinematic constraints; we feel that this method presents an efficient processing style of representation. It suggests to us a way for decisions to be made in the CNS at a general level, in that the decision can be made based on the number of solutions at a particular location, versus on the details of the solution. Putting the wrist at a place where lots of kinematic solutions exist in opposition space seems a useful place for the wrist to be. This is especially true if later, under tactile and/or visual guidance, corrections can be made, as long as the movement was in the right 'ballpark'. Information processing can be done on high level information. We also feel that different motor systems can learn the 'goodness' of a solution, through various learning algorithms. Low level feedback information can be compared to desired results, and better and better estimates of good solutions can be made.

In our presentation, we have shown how planning for a prehensile task can be performed by a network of 'neuron-like' processes working together. Our choice of networks acts to demonstrate the feasibility of network solutions, but does not suggest that the CNS actually performs the calculations in such a manner. Other possible network solutions could have been chosen which have been developed to demonstrate feasibile computational solutions for learning non-linear mappings for biololgical and non-biological problems. These techniques include the Boltzmann machine[Hinton and Sejnowski 1986],back-propagation [Rumelhart, Hinton and Williams 1986], and self-interested adaptive networks [Barto 1985]. A Hopfield network [Hopfield 1982, Hopfield and Tank 1986] could be used which could account for many constraints over a solution space, and then learn a solution based on minimizing an energy function. However, there are really more than one solution in this (r, ϕ) space, as there are many places one can place their

wrist relative to the object and still pick it up. Whereas the Hopfield network is deterministic, a system is needed that would take into account sequential constraints as well as the spatial constraints. As we saw in Chapter 4, and observed in Figure 33, there are effects on the solution relative to the initial conditions, as well as the final conditions. An adaptive network such as developed in [Jordan 1986] could account for these sequential effects as well, and actually begin to predict the effects later constraints have on the initial state.

In terms of the Enclose Schema, data have shown [Jeannerod 1981, Wing, Turton, and Fraser, in press, etc.] that visual information is needed for accurate enclosing of the hand about the object. Studies involving intersensory conflicts [Rock and Victor 1964, Power and Graham 1976, Warren 1982] have demonstrated that when both kinesthetic and visual information about the hand position are available but they are in conflict, the subject believes the visual information more than the proprioceptive information. These data indicate that the strong visual input is significant for the fine positioning of the hand when near the object. Paillard [1982] gives evidence for the use of vision for encoding the moving hand position relative to the object during the enclose phase. However, Jeannerod [1981] noted that in visual open-loop experiments the two phase movements still occur. Wing, Turton, and Fraser [in press] note that without visual information in the reaching movement, there is a great deal of variability. This is also true when the movement is fast. Our modelling of the Preshape Schema fits with these results, because we allow variability in the way we approximate the VF configurations and do not recompute the constraints.

Psychophysical experiments will help provide further insights into this model. Using this coordinate system for studying prehensile movements will provide more intrinsic information about movement. Understanding the constraints on the movements, and implementing them in this model will allow a more robust approach. Using adaptive learning networks [Barto 1985, Jordan 1986, etc] which

could incorporate sequential and parallel processing would be powerful additions to improving the performance of this model.

CORTICAL CONTRIBUTIONS TO PREHENSILE MOVEMENT

"But between the mind and the hand the relationship is not so simple as that of a master to a humble servant ... Gestures may continually reflect the inner feelings. (Conversely,) hands have their gifts inscribed in their very shape and design ... The mind makes the hand, the hand makes the mind."

— H. Focillon

Sensory information from the receptors in the muscles, tendons, skin, and joint capsules enters the CNS through the dorsal root ganglia of the spinal cord [see Kandel and Schwartz 1985, etc]. These cells give off collaterals, which ascend in the dorsal columns, as seen in Figure 35. Information arrives at the dorsal column nuclei, where cells (not necessarily common ones) send fibers to the cerebellum and also to the ventral posterior lateral nuclei of the thalamus, by way of the medial lemniscus system. From the thalamus, cells project onto somatosensory cortex. Cortico-cortical connections send sensory information to many cortical areas, including *motor cortex*. From various cortical areas (both frontal and parietal regions) arises the *pyramidal tract* [Phillips and Porter 1964, 1977] which descends through the pyramids on the ventral surface of the medulla [Phillips 1971]. While some of these fibers end in the dorsal column nuclei, many continue into the spinal cord, making up the *corticospinal tract* [Phillips and Porter 1964]. This tract directly connects cerebral cortical areas with spinal centers, and includes, in Primates, cortical fibers which make excitatory monosynaptic connections directly with motoneurons [Phillips and Porter 1964]. Motoneurons, in turn, send axons into the periphery, innervating the skeletal muscles. The func-
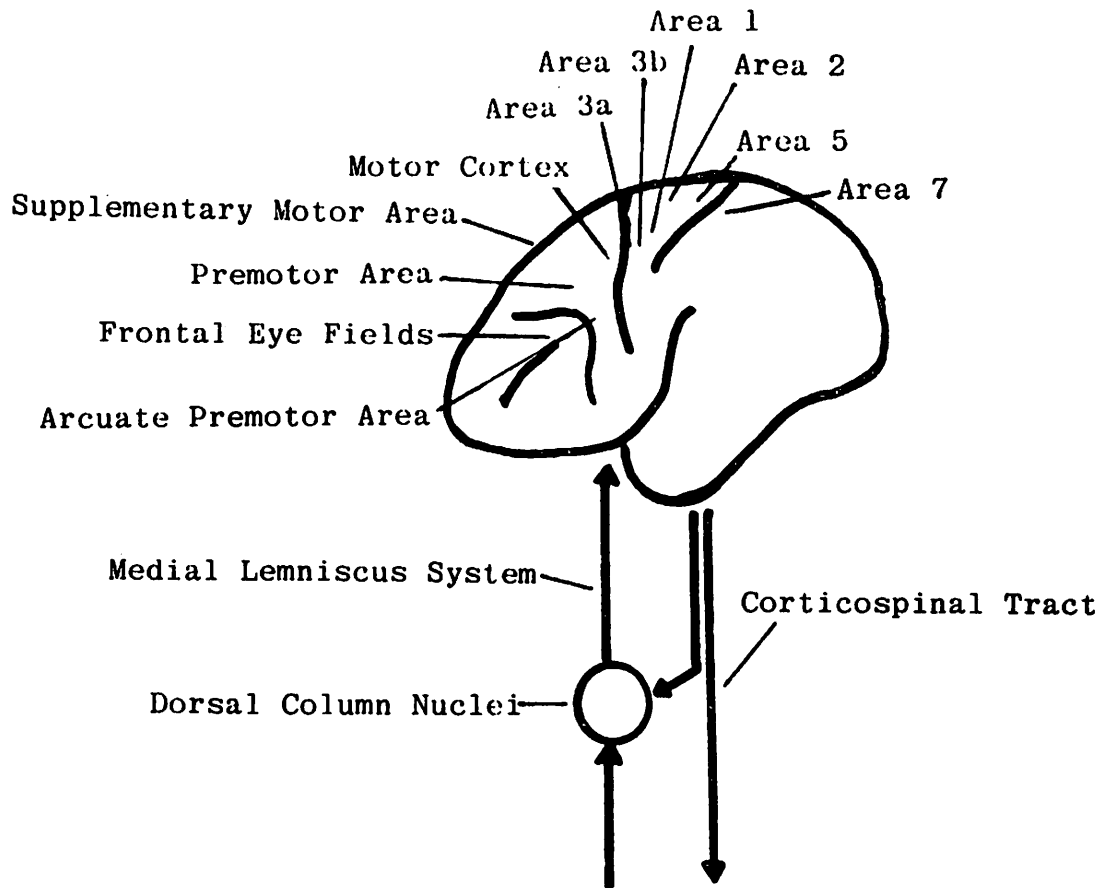
Figure 35: Ascending and Descending Pathways of the Central Nervous System

Somatosensory information reaches the cerebral cortex through the medial lemniscus system. From many cortical areas, motor signals descend through the corticospinal pathway, reaching the motoneurons in the spinal cord.

tional significance of this direct corticospinal pathway is greatly discussed in the literature [Kuypers 1964, Phillips 1971, Brinkman and Kuypers 1972, Kuypers 1973, Haaxma and Kuypers 1974, Phillips and Porter 1977, Phillips 1978, Muir and Lemon 1983], and its role in motor behavior is far from being understood.

The corticospinal tract increases in bulk as one ascends through the families of living Primates [Kuypers 1964, Phillips and Porter 1977] and while one cannot explain all movements of the forelimb and hand in terms of cortical signaling, research has shown that the corticospinal tract and motor cortex are critical parts of the motor pathway in the fine, fractionated finger movements seen in pad opposition [Tower 1940, Denny-Brown 1960, Lawrence and Kuypers 1968, Brinkman and Kuypers 1972, Kuypers 1973, etc]. The motoneurons that send axons to the distal muscles of the arm (forearm and hand) reside in the dorsolateral aspect of the ventral horn of the spinal cord, and Kuypers and Brinkman [1970] showed it is the giant pyramidal cells in layer 5 of motor cortex that project directly onto these motoneurons. Only in the Primate order are these monosynaptic connections with motoneurons made [Phillips and Porter 1977], increasing in number as one ascends the order [Phillips 1978], with a larger distribution made to motoneurons of the distal muscles [Phillips and Porter 1964, Clough et al 1968]. And in terms of the behavior, we note that prehensile movement specifically belongs to the Primate order [Napier 1961], other than isolated examples in lower orders, such as raccoon [Petras and Lehman 1966, Buxton and Goodman 1967].

In a first attempt to identify the function of the pyramidal tract, Tower [1940] performed a unilateral pyramidotomy on macaques, which resulted in stereotyped grasping involving the entire contralateral side of the body. However, use of the hand in running and climbing was unaffected. Thus, one concludes that the contribution is for specific functions of the limb, and not complete control of it. Other, extrapyramidal, tracts, arising from brain stem centers and therefore being only indirectly connected to cortex, would still survive such an operation; these

include the medial and lateral vestibulospinal tracts, the medial and lateral reticulospinal tracts, the tectospinal tract, and the rubrospinal tract. Lawrence and Kuypers [1968] performed a bilateral pyramidotomy on macaques which resulted in the loss of fractionated finger movements in both hands. Within the follow up period (up to 5 months), use of the precision grip was never recovered. Again, the monkeys could run and climb normally, although there remained a difficulty in voluntarily relaxing their grasp from food (but not during climbing or clinging). Brinkman and Kuypers [1972] showed that when a monkey has a pyramidotomy, it cannot grasp small objects between its fingers or make isolated movements of its wrist. Kuypers and his colleagues [Brinkman and Kuypers 1972, Haaxma and Kuypers 1974] therefore concluded that finely coordinated visually-guided behaviors involve the cooperative computation of cortex via the corticospinal tract (controlling the distal muscles and relatively independent finger movements) and the brainstem through other, extrapyramidal, tracts (controlling undifferentiated hand movements).

While ablation of the limb area of motor cortex only temporarily causes paralysis [Sherrington 1889, Glees and Cole 1950], the control of fine, fractionated finger movements is permanently impaired in monkeys and apes [Denny-Brown 1960, Lawrence and Kuypers 1968] and man [Walshe 1963]. Walshe also noted that a deficit remains in extension of the wrist and fingers as well. Patients with the index finger and thumb area removed in motor cortex are permanently paralyzed for fine discriminating movements [Phillips 1966]. Electrostimulation of motor cortex can evoke thumb and index finger movements at levels too low for evoking a response in any other part of the body [Liddell and Phillips 1950, Asanuma and Rosen 1972, Kwan et al 1978]. This suggests preferential accessibility of thumb and finger motoneurons by motor cortex, with stronger connections than to other muscle groups [Phillips and Porter 1964, Phillips 1971]. It matches with the observation that during a focal epileptic seizure, commonly the thumb and index finger move before other parts of the body [Jackson 1873].

The concept of hierarchical control within these pathways has dominated the theory and practice of brain research for over a century [Jackson 1873, 1889, 1931, 1932; Sherrington 1889, Shik *et al* 1966, Grillner 1975, Lundberg 1979, Evarts 1984, etc]. The hypothesis argues that primitive behaviors, emerging from the more primitive centers of the CNS, are regulated by higher cortical centers which control more complex behaviors. Sherrington [1906] described the segmental apparatus (controlling stereotypical, reflexive movements) as being subordinated to suprasegmental control (from centers above the spinal cord, both cortical and subcortical). An example of a primitive behavior is locomotion; studies on decerebrate cats [Shik *et al* 1966, Lundberg 1979, etc] and spinal cats [Grillner 1975] suggest that this behavior can be controlled by low level central pattern generators in the spinal cord. These centers generate coordinated rhythmic outputs which are activated in turn by higher centers. In more theoretical terms, a variety of hierarchical frameworks have been suggested. Jackson [1931, 1932] theorized that there were three levels: the lowest being the brain stem and spinal cord, the middle level being the precentral and postcentral sensorimotor areas, and the highest level being the prefrontal lobe.

The basic question is whether commands are sent through the central nervous system in a strictly hierarchical fashion, or else whether commands emerge with equal importance from various, more heterarchically arranged, centers. The lesion studies cited here could be used to support the hierarchical principle of organization. Without cortex, only undifferentiated hand movements are possible, while with cortex, fractionated finger movements are possible [Denny-Brown 1960, Walshe 1963, Lawrence and Kuypers 1968]. Phillips [1978] suggests that in higher Primates it is advantageous to have a system which bypasses the segmental (low-level) local reflex system, sending complex and integrated (high-level) commands directly to the motoneurons. In referring to Jackson's notion of 'more automatic' and 'less automatic' (voluntary) control [Jackson 1931, 1932], Phillips [1978] argues that the Primate hand is under more automatic (low-level) con-

trol in climbing and locomotion, and under less automatic (high-level) control for tactile exploration and prehension.

In contrast to the hierarchical organization, Mountcastle [1978] suggests that the CNS should be thought of as a distributed system, with functions distributed across its various centers. Over the last 50 years, neuroanatomical and neurophysiological techniques have slowly improved and much is now known about the CNS that was not known in Sherrington's time. Major motor and sensory areas of the Primate cerebral cortex have been identified, using careful techniques such as axoplasmic flow methods, intracellular staining, electron microscopy, and intracellular microelectrode single cell recording and stimulation. It has become clear that multiple representations of topographically organized modalities are mapped across cortex [Jackson 1931, Penfield and Rasmussen 1952, Woolsey 1958, Merzenich and Kaas 1980, Wiesendanger 1986]. The well-known 'homunculus' which maps out the human body across somatosensory and motor cortex [Penfield and Rasmussen 1952] and 'simiunculus' of the monkey cortex [Woolsey 1958] are being replaced by multiple and finer detailed maps [Kaas *et al* 1979, Strick and Preston 1979]. Mountcastle [1978] has suggested that within these maps, local neural circuits are being replicated, preserving neighborhood relations between other, topographically organized, interconnected circuits. He argues that simple aspects of function can be executed by local operations, but in general, a function is distributed across circuits, without residing in any one particular area. He offers as evidence the fact (as noted in the above studies) that lesions only degrade the performance of a function without completely destroying it, and that there is the adaptive ability, in some animals for some functions, to adjust for behavioral goals after the lesion. The cooperative interaction of the pyramidal tract with the extrapyramidal tracts [Brinkman and Kuypers 1972] might also be looked on as evidence for a distributed prehensile function. By thinking of the CNS more as modular units linked together in parallel and in serial, Mountcastle argues that information flows through different pathways, with dominance being dynamic

and changing. In terms, then, of the direction of commands, the command may come from any direction [Mountcastle, personal communication]. Mountcastle's characterization of the CNS as having 'redundancy of potential loci of command' [Mountcastle 1978, p 40] is reminiscent of McCulloch's principle of redundancy of potential command [McCulloch 1965], which states that the command should emerge from the center with the most important information.

Perhaps the resolution to the hierarchical-distributed controversy lies in a model of the CNS which is loosely hierarchical yet distributed. It is hierarchical in the sense that some centers put forth commands which are not as muscle-oriented as the commands from other centers, and also in the sense that some functions can be performed by subfunctions. But it is distributed in the sense of distributed, decentralized, localization. Cooperation between pyramidal and extrapyramidal tracts shows possible distributed computation, yet one could also argue that a spinal cord reflex is in some sense (usually!) lower in a command situation than prefrontal and premotor cortical regions (depending on the situation). However, there would be certain circumstances when the commands could flow in the reverse direction.

A schema-theoretic approach [Arbib 1981] to modelling the CNS offers a framework for performing a top down analysis of motor behavior in both hierarchical and distributed terms. To complement looking at cortical and subcortical areas individually, trying to glean their information processing contribution from an analysis of neuronal activity, Arbib suggests looking at the functional requirements of the system. By identifying functions, schemas as units of motor behavior are then defined to account for the ability of the system to perform such a function. Multiple cortical and subcortical areas contribute to a given schema, and it is in the interaction of these schemas that the motor behavior emerges. The task, then, for the brain modeller is to not only identify potential schemas which represent the motor behavior, but to also show how these schemas map into the

known neural circuitry.

In the previous chapters we have identified a possible coordinated control program for prehensile movement involving interacting schemas. In order to suggest how these schemas might map into the CNS, we first summarize the known data about sensorimotor contributions toward reaching behaviors in Primates. We then suggest how they might interact in a schema-theoretic picture of the Primate CNS.

§1. Somatosensory cortex

Primary somatosensory cortex (SI) is implicated in our study of the cortical contributions to prehension for two major reasons: (1) there is evidence of direct and reciprocal connections with motor cortex [Jones and Powell 1970, Jones, Coulter, and Hendry 1978], and (2) it contributes to the corticospinal tract (all of the parietal lobe, which includes somatosensory cortex, makes up about 40% of the fibers in the corticospinal tract in the macaque [Russell and de Myer 1961]). We currently are not looking at secondary somatosensory cortex SII, because it has bilateral inputs, whereas primary somatosensory cortex has contralateral inputs, meaning that sensory information from each hand is directed to the contralateral hemisphere in primary somatosensory cortex. Also, fewer SII cells contribute to the corticospinal tract than other cortical areas [Jones and Wise 1977].

Primary somatosensory cortex has evolved into four architectonically distinct areas in the Primate brain, identified as Brodmann areas 3a, 3b, 1, and 2, each of which containing a separate representation of the hand in higher Primates [Kaas *et al* 1979, Kaas 1982, 1983, Kaas et al 1983]. Somatosensory information enters the sensorimotor system through the medial lemniscus system and reaches somatosensory cortex by way of the ventralis posterior lateralis caudalis nuclei

(from VPL$_0$ and VL$_c$ of thalamus)

(from VPL$_c$ of thalamus)

FJ81:	[Friedman and Jones 1981]
HR76:	[Humphrey and Rietz 1976]
J75:	[Jones 1975]
JCH78:	[Jones, Coulter and Hendry 1978]
JP70:	[Jones and Powell 1970]
K78:	[Kunzle 1978]
VP78:	[Vogt and Pandya 1978]
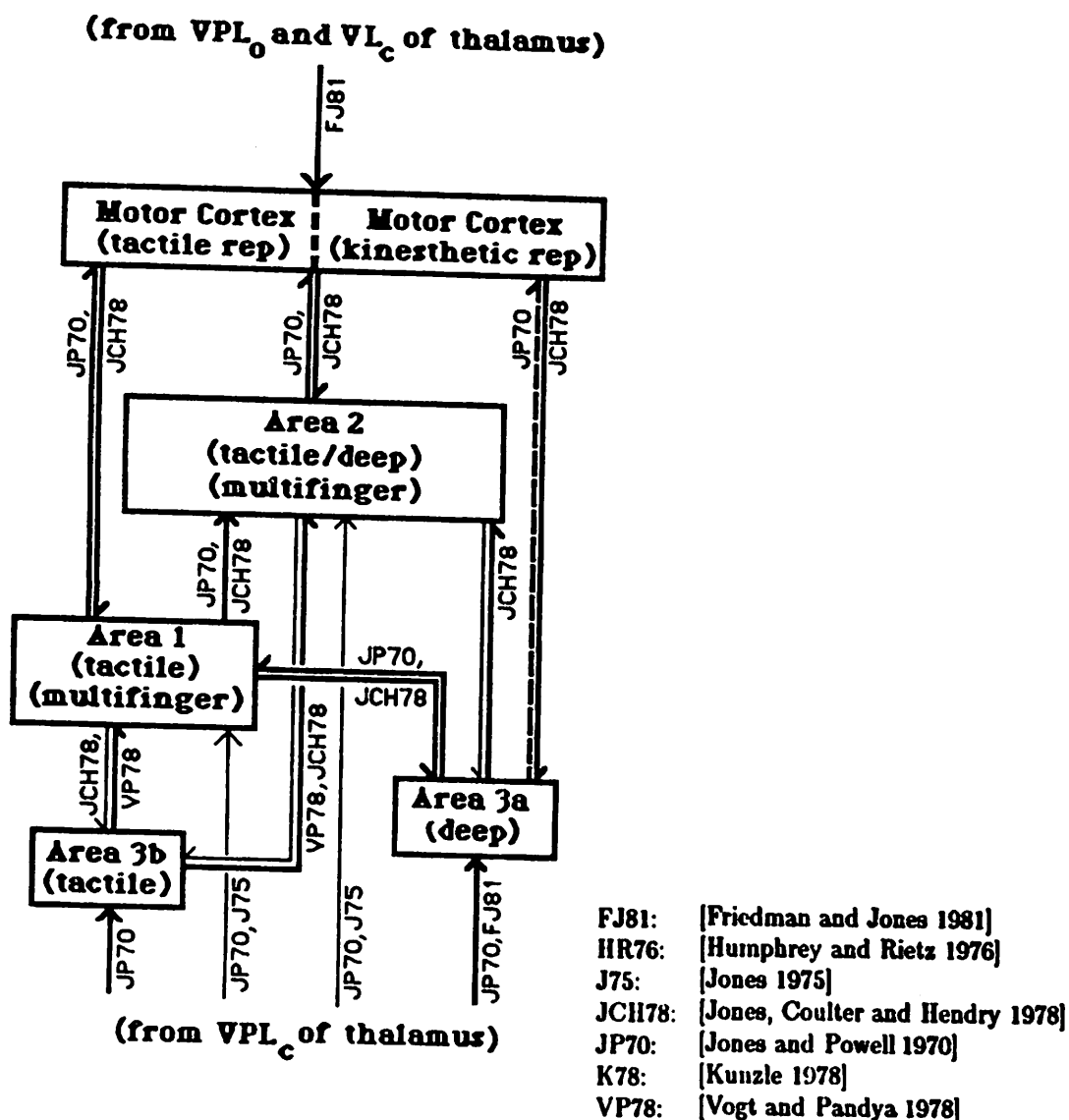
Figure 36: Pathways between Motor Cortex and Somatosensory Cortex

Known pathways within the four somatosensory cortical areas, along with their projections to motor cortex. Possible separate tactile and kinesthetic pathways might play a role in preshaping versus enclosing movements. Lighter lines indicate fewer projections. Thalamic contributions are shown, in order to show the difference between somatosensory and motor cortex thalamic inputs.

(VPLc) of the thalamus [Jones and Powell 1970, Jones 1975, Friedman and Jones 1981], as seen in Figure 36. The figure summaries the known pathways between somatosensory and motor cortex; it is based on the published results from various laboratories (noted on the labels), work generally performed on the macaque monkey. Whereas areas 3b and 3a receive dense thalamic inputs [Jones and Powell 1970, Friedman and Jones 1981], fewer thalamic inputs have been noted to areas 1 and 2 [Jones and Powell 1970, Jones 1975]. Areas 3b and 3a both were found to project to areas 1 and 2, and area 1 to project to area 2 as well [Jones and Powell 1970, Jones, Coulter, and Hendry 1978, Vogt and Pandya 1978]. As seen in the figure, a few projections were found in the opposite directions (area 1 to area 3b, area 2 to 3a, area 2 to 3b). No projections were found from area 2 to area 1, and equally dense projections were found from area 1 to area 3a. Areas 1, 2 and 3a all project reciprocally to motor cortex (though the projection from motor cortex to area 3a has yet to be confirmed), while area 3b does not [Jones and Powell 1970, Jones, Coulter, and Hendry 1978]. Projections to other parietal cortical areas and other motor centers will be noted below. This evidence for differential pathways has been suggested to represent hierarchical processing of sensory information [Evarts 1981, Vogt and Pandya 1978, Iwamura *et al* 1983a].

Jones and Powell [1970] found that area 3b responds to the stimulation of slowly adapting skin mechanoreceptors; area 3a to group I muscle afferents; area 1 to rapidly adapting skin mechanoreceptors; and area 2 to movements of the joints. Randolf and Semmes [1974] showed that ablation of area 3 impaired performance on all somatosensory discrimination tasks, whereas removing area 1 impaired texture discrimination, and area 2, shape and form discrimination. In studies of somatosensory cortex of the macaque monkey to further elucidate its functionality, Iwamura [Iwamura *et al* 1983a] identifies area 3b as containing slow and rapid adapting neurons from skin receptors with small receptive fields, as well as some deep receptors. While area 3b units respond to light skin or hair contact in their studies, area 3a responds to joint or muscle manipulation. Area

1 is activated by rapidly adapting cutaneous mechanoreceptors on the most part [Iwamura *et al* 1983b]; however, they note differences between area 1 and area 3b. They found that area 3b is somatotopically organized by individual fingers, while area 1 responses are more multifinger. This could be due to the fact that area 1 receives fewer thalamic fibers than area 3b [Jones and Powell 1970, Jones 1975].

Iwamura classified cortical units of area 2 into categories based on the type of receptor that was driving the area: simple skin units, complicated skin units, joint units, joint and skin units, and undrivable units [Iwamura and Tanaka 1978]. The complicated skin units produced a differential discharge in response to particular object features, such as cylinders or flat objects. They suggest that these various units contributed to the perception of objects by touch. Other evidence of complex perception in area 2 is preferential activity to direction of movement across the palm [Constanzo and Gardner 1980, Hyvarinen and Poranen 1978]. Based on their results of hierarchical processing and multifinger representations, Iwamura *et al* [1983b] suggest that somatosensory information is integrated within area 1. Area 2 also shows sensory integration, receiving information from the other three somatosensory areas, and also having multifinger responses [Iwamura *et al* 1980]. This matches the neuroanatomical results noted above, since both area 3a and 3b project to area 1 and to area 2, and also area 1 and 2 are not as directly connected to the periphery as area 3a and 3b [Jones and Powell 1970, Jones, Coulter, and Hendry 1978, Vogt and Pandya 1978].

In terms of prehensile functionality, we suggest that since area 3a is involved in more kinesthetic processing, it might be more active during the Preshape Schema and during the transition to the Enclose Schema, times when the hand is moving proprioceptively. At some point during the Enclose Schema, contact is made with the object, a time when the multi-modal representation in area 2 would be useful, in terms of integrating tactile and kinesthetic information about the hand. Areas

3b and 1, involved more in tactile processing, would become more active during the Enclose Schema while the fingers are actually touching the object, but again, as the fingers tighten around the object and the object glides across the skin, area 2 would certainly be crucial. With its more processed information, it could signal the relationship between the hand and the object, providing information about object shape, object location relative to the hand, and forces and torques acting on the object as it is being lifted. Area 1 and area 2, with their multifinger representation, could have already encoded sensory information from the fingers into a virtual finger representation.

As an aside, it is interesting to note that raccoons, with their enhanced prehensile skills [Petras and Lehman 1966, Buxton and Goodman 1967, Johnson 1985], also have enlarged somatosensory forepaw areas.

§2. Motor cortex

Area 4 in the Brodmann taxonomy of cerebral cortex has been designated the name of motor cortex, or MI [see Evarts 1981]. As noted above, reciprocal cortical projections are seen between motor cortex and areas 1, 2, and 3a, but not area 3b [Jones and Powell 1970, Jones, Coulter, and Hendry 1978]. There are no commissural projections in the hand area of motor cortex [Jones and Wise 1977]. The major thalamic input to motor cortex is from the ventralis posterior lateralis oralis nuclei (VPLo) and the ventralis lateralis caudalis nuclei (VLc) [Friedman and Jones 1981], as seen in Figure 36. Before we discuss the other major cortical pathways into motor cortex, we turn to an analysis of its organization, in order to complete the discussion of the interaction between somatosensory and motor cortex.

While the separate representations of somatosensory cortex have been noted

and verified by many researchers, the organization of motor cortex is still debated [Asanuma and Rosen 1972, Rosen and Asanuma 1972, Kwan *et al* 1978, Murphy *et al* 1978, Wong *et al* 1978, Strick and Preston 1978, 1979, 1982a, 1982b; Lemon 1981a, 1981b]. In research first on cats [Asanuma and Sakata 1967] and then on anaesthetized capuchin monkeys [Asanuma and Rosen 1972, Rosen and Asanuma 1972], Asanuma demonstrated the possible existence of sometimes overlapping *efferent columns* in motor cortex, far more extensive in the monkey than the cat. The diameter of these columns averaged 1 mm, and they found that zones for antagonistic finger and thumb movements never overlapped. Zones for antagonist wrist movements overlapped, thus, as they suggest, facilitating motor cortical control of coactivation of antagonist wrist movements for a stable base for fine finger movement. They also noted that stimulation of columns more rostral in motor cortex produced movements in the more proximal muscles of the forelimb [Asanuma and Rosen 1972], and that efferent columns received polymodal inputs, from both proprioceptive and cutaneous receptors [Rosen and Asanuma 1972]. Individual cells, however, responded to a specific input.

In studies on conscious macaque monkeys, Lemon [1981b] looked at neurons in motor cortex within groups, which he defined as neurons lying within 500 μm of each other within the same penetration of the electrode. He found most, but not all, groups of cells to be unimodal, results which differ from the work on anaesthetized animals [Rosen and Asanuma 1972]. He identified a central zone, receiving input from only the hand, with a thumb area more lateral, next to an index finger area, and the ulnar fingers more medial. Neurons within a group responded similarly in tasks. Outside this central region, Lemon saw groups that contained neurons receiving inputs from noncontiguous joints. He notes that neurons responding to cutaneous inputs tend to lie more caudal than the ones with proprioceptive inputs, but that, in the groups that were multi-modal, neurons responding to cutaneous inputs were more superficial than the ones responding to deep receptors.

Kwan and his colleagues [Kwan *et al* 1978, Murphy *et al* 1978, Wong *et al* 1978] found neurons with identical peripheral receptive fields grouped in vertical aggregates in motor cortex in studies on awake macaque monkeys. By stimulation of mechanoreceptors in the fingers and arm, they show that these groups receive inputs from different modalities (cutaneous, joint rotation, or both), and by stimulation of neurons in the same location, the outputs of the aggregates go to the same joint (evidence which seems to disagree with [Lemon 1981b]). They found that groups with similar input and output properties are grouped into horizontal clusters, of sizes 0.5-2.0 mm, similar to efferent columns [Asanuma and Rosen 1972], but larger than the groups Lemon was using as a measure [Lemon 1981b]. They found that these columns group into crescent shaped zones which functionally relate single joints, with a central hand zone similar to [Lemon 1981b]. These zones are nested so that contiguous forelimb joints are successively represented, with proximal joints surrounding distal joints. The zones of contiguous joints overlap, while there is no overlap between non-contiguous joints, which is different from the findings of [Lemon 1981b]. Lemon [1981a, 1981b] suggests that overlapping areas, such as these, might play a role in synergist movements, which are so obviously exhibited in the hand.

Separate maps in motor cortex have recently been identified [Strick and Preston 1978, 1979, 1982a, 1982b]. Using a squirrel monkey, which has a flat motor cortex, Strick and Preston suggest that motor cortex maintains spatially separated kinesthetic and tactile maps. The tactile map is more caudal than the kinesthetic map, agreeing with the results of [Lemon 1981b]. However, Jones *et al* [1978] made injections into somatosensory cortex (in macaques) and saw patchy labeling of several independent columns, suggesting a multiple distribution of inputs to motor cortex. In Figure 36, we show a functional description of the interconnections between two motor maps and somatosensory cortex. Whether these two motor maps are somatotopically organized in a horizontal mosaic [Strick and Preston 1978, 1979, 1982a, 1982b; Lemon 1981b], vertical mosaic [Rosen and

Asanuma 1972, Kwan *et al* 1978], or both remains to be seen. One cannot argue that the processing going on in the sensorimotor cortex of a New World monkey (the squirrel monkey) is the same as in an Old World monkey (the macaque), and research has begun to show some of the differences [Carlson and Nystrom 1986]. However, in terms of connectivity, Jones and Wise [1977] found similar reciprocal connections between motor cortex and areas 1, 2, and 3a in the squirrel monkey, as were described in Figure 36 for the macaque. In terms of multiple representations in somatosensory cortex, Carlson and Nystrom [1986] show that the squirrel monkey also has multiple cutaneous representations (area 1 and area 3b), as does the owl monkey (another New World monkey) [Kaas *et al* 1983]. It seems likely that, if area 1 receives information mostly from cutaneous receptors [Iwamura *et al* 1983a], then it would be connected to the tactile motor map. Area 3a, with inputs from deep sensors, would likely be connected to the kinesthetic motor map. Area 2, with its multimodal representation, would perhaps go to both.

Such a representation would be useful in a gating scheme, as suggested by Evarts and Tanji [1974], who showed that motor cortex reflexes could be gated on or off by the voluntary set of a monkey. We would argue that having two motor maps would facilitate this process: if proprioceptive-oriented movements are performed and therefore feedback from deep receptors is expected, the kinesthetic motor pathway through motor cortex would be primed, thus allowing a quick response to the input; if cutaneous information is expected during tactile following movements, the other motor pathway would instead be primed. The connections in Figure 36 would support a transcortical reflex loop [Phillips 1969], through somatosensory and motor cortex. Information from the receptors to somatosensory cortex would be gated to motor cortex [Evarts and Tanji 1974, Tanji and Evarts 1976], under the direction of a higher motor center (perhaps, as seen below, by the pathway from area 5 back to motor cortex).

Reciprocal connections between motor cortex and somatosensory cortex could allow motor cortex to send motor collaterals to somatosensory cortex, signaling the anticipated changes of the hand. In experiments where a human subject was deprived of awareness of position or movement in the first phalanx of the thumb [Merton 1964], the subject could move a pointer attached to his thumb over a measured distance. However, with his eyes closed, the subject could not tell if the movement actually happened. This 'sense of effort' could stem from the difference between the motor cortex output and the sensory state; without somatosensory (or visual) information, there is no verification that the movement occurred. The movement does occur, though, because the central pathways are still intact. In parietal patients making movements while blindfolded, not only is there no sense of effort, but these sorts of movements are impossible due to the lesions in these pathways, [Jeannerod et al 1984, Jeannerod 1986].

We now turn to discussing the other major cortical pathways into motor cortex. In Figure 37, we summarize the known cortico-cortical connections of major sensory/motor areas involved in reaching, noting the research which either identified the connection or verified the result. Motor cortex has reciprocal transcortical connections with major frontal motor areas, such as the supplementary motor area (SMA) [Jones and Powell 1969, Pandya and Vignolo 1971, Jones, Coulter and Hendry 1978] and the premotor area (PM) [Kuypers and Lawrence 1967, Pandya and Kuypers 1969, Kunzle 1978, Muakkassa and Strick 1979, Schell and Strick 1984]. Motor cortex also receives afferent projections from area 5 of the parietal cortex [Strick and Kim 1978, Jones, Coulter, Hendry 1978, Zarzecki, Strick, and Asanuma 1978] and sends projections back [Pandya and Kuypers 1969, Kunzle 1978, Jones, Coulter, Hendry 1978]. Motor cortex, as noted above, receives information from the somatosensory cortex [Jones and Powell 1970, Jones, Coulter, Hendry 1978]. Motor cortex sends fibers down through the corticospinal tract, accounting for about 31% of it in the macaque [Russell and de Myer 1961].

A question related to motor cortex which has been long debated [Jackson 1873, Evarts 1967, Phillips 1975, 1978; Kwan *et al* 1978, etc] is whether pyramidal tract neurons, and motor cortex, are specifically signaling muscles or else signaling more task related movements. With the development of intracortical microstimulation techniques [Asanuma and Rosen 1972], information about pyramidal tract neurons (PTNs) is slowly becoming available. Lemon and Muir [Lemon and Muir 1981, Lemon and Muir 1982, Muir and Lemon 1983] found PTNs in the macaque motor cortex which relate to activity of the intrinsic muscles of the hand during precision gripping tasks, such as pinching two spring loaded levers with the index finger and thumb pads. However, when the muscle was also active in a power task, such as squeezing an air-filled cylinder with the whole hand, the same neurons were not active. This suggests that motor cortex may be organized in terms of task specific movements, rather than in terms of muscles. On the other hand, the organization of motor cortex found by Kwan *et al* [1978] showed joint related zones, which might indicate specific muscles being represented. However, these latter data were not collected during task-related activity (nor exclusively focused on PTNs), so it is possible that the multiple representations that Kwan *et al* found are also due to task-specific movements being represented.

Not only is there a task-related distinction to activity in the motor cortex, research has shown evidence of preferential access toward the distal muscles and even to specific, more task-related, muscles. Kwan *et al* [1978] found that neurons involved in movements of the hand had generally lower thresholds than those to the arm, indicating that it may take less facilitation to produce finger movements than arm movements. Clough *et al* [1968] found that the intrinsic muscles of the baboon hand and the extensor digitorum communis muscle received the largest monosynaptic connections from corticospinal cells. Fetz and Cheney [1980] identified the effects of motor cortical cells on various muscles of the hand. They found that postspike facilitation by corticospinal neurons, in general, tends to be stronger and more widespread in the extensor muscles, while poststimulus

Peristriate Cortex

Frontal Eye Fields Areas 8,9

Area 7

Premotor Area 6a

APA

Area 5

SMA

Motor Cortex

Primary Somatosensory Cortex

Area 2

Area 1

Area 3a

Area 3b

(HK74 cut)

corticospinal tract
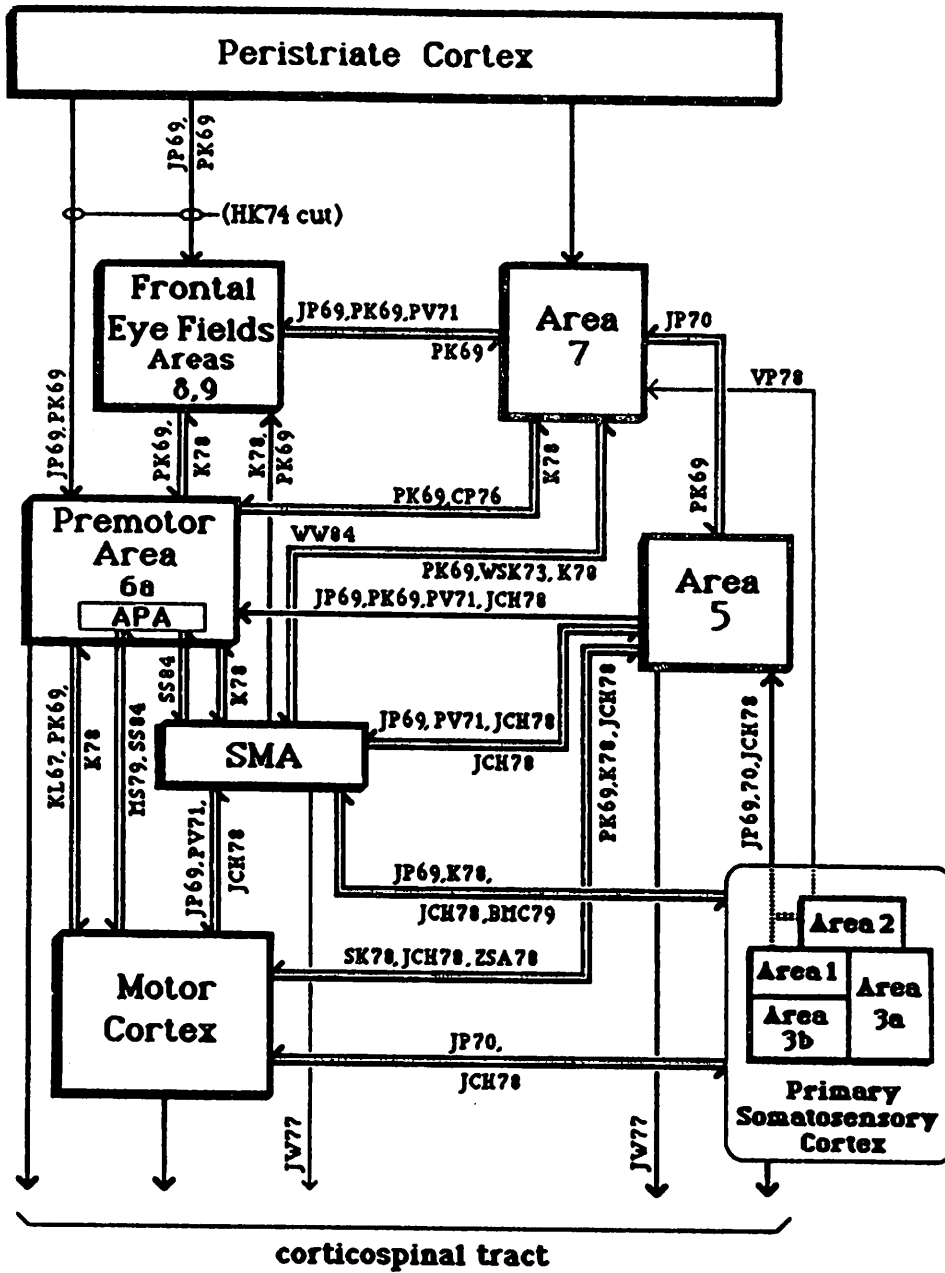
Figure 37: Neocortical Pathways Contributing to Reaching

Cortico-cortical pathways currently known within major sensorimotor areas of the Primate cerebral cortex. Labels on the path indicate the research which either identified or verified the connection. The only outputs indicated are those which contribute directly to hand and forelimb movement through the corticospinal tract. Lighter lines indicate fewer projections.

BMC79:	[Bowker, Murray and Coulter 1979]
CP76:	[Chavis and Pandya 1976]
HK74:	[Haaxma and Kuypers 1974]
JCH78:	[Jones, Coulter and Hendry 1978]
JP69:	[Jones and Powell 1969]
JP70:	[Jones and Powell 1970]
JW77:	[Jones and Wise 1977]
K78:	[Kunzle 1978]
KL67:	[Kuypers and Lawrence 1967]
MS79:	[Muakkassa and Strick 1979]
PK69:	[Pandya and Kuypers 1969]
PV71:	[Pandya and Vignolo 1971]
SK78:	[Strick and Kim 1978]
SS84:	[Schell and Strick 1984]
VP78:	[Vogt and Pandya 1978]
WSK73:	[Wiesendanger, Seguin and Kunzle 1973]
WW84:	[Wiesendanger and Wiesendanger 1984]
ZSA78:	[Zarzecki, Strick and Asanuma 1978]

(Legend for Figure 37)

and postspike suppression is found in flexor muscles. Phillips [1971] argues that the opening of the hand (beginning of the preshape phase) as well as precision grasping depends, therefore, on this direct corticospinal pathway.

The functional significance of this direct access of motor cortex to the extensors [Fetz and Cheney 1980] is an important issue in looking at motor cortex's contribution to the Preshape Schema and Enclose Schema. One could argue that the fingers are generally extending during the Preshape Schema when free movement is occurring, at which time the opening up of the hand could be controlled via cooperation between the corticospinal tract and the extrapyramidal pathways [Brinkman and Kuypers 1972]. The motor cortex contribution would be for signaling particular motor units, producing more pronounced extension of certain fingers (fractionation); the extrapyramidal contribution would be the facilitation of hand extension in general. We note that patients with posterior parietal lesions [Jeannerod et al 1984, Jeannerod 1986] or lemniscal damage [Jeannerod 1986] can still consistently, although just slightly, extend their fingers without visual feedback. In this sense, motor cortex and somatosensory cortex could act as a filter, sitting between higher motor centers (task related virtual finger commands) and lower spinal centers (real finger movements). These lower spinal centers would, however, be receiving other aspects of the command through other paths.

Another possible interpretation of the functional significance of extensor facilitation relates to the action of the flexors and extensors themselves in movements. It has been noted that, in the human hand, the extrinsic flexors and extensors coactivate during free motion flexion [Long 1981]. We do not know if this is also true of the baboon hand, and so the question remains whether the functional effect relates to just finger extension, and not to both flexion and extension.

Another question about motor cortex addresses the informational content of pyramidal tract neurons [Evarts 1968, 1981; Georgopoulos et al 1983, 1984, 1986; Kalaska et al 1983]. Georgopoulos et al [1983, 1984, 1986; Kalaska et al 1983] sug-

gest a *vector sum* model for motor cortex, where populations of cells contribute to the overall direction of a movement. By looking at 241 neurons in tasks where monkeys move a manipulandum from one location to another, they find the neuronal discharge to be directionally tuned. A neuron votes with a certain strength on how close a particular movement is to the direction to which it has been tuned. By computing the vectorial sum of these neurons, they show it is within 11° of the actual movement direction. However, Evarts [1968, 1981] argues that motor cortex could be sending force information to motoneurons. In studies of repetitive single joint rotations [Evarts 1968], Evarts correlates pyramidal tract neuron discharge with a controllable reflex noted in the EMG. If an unexpected load is placed on the wrist by the experimenter, motor cortex increases in discharge, but only if the increase is necessary to counteract the load. If the load will help in the direction that the movement was being made, no increase is seen. These are single joint studies, however, and constrained movements, a task perhaps better suited to force control. The task in the Georgopoulos paradigm is perhaps better suited to direction control. Free space motions, as seen in the Preshape Schema, would not have to counteract loads of the type seen in [Evarts 1968].

Applying this to the hand movement, area 2 could provide information about the current spatial state of the fingers in terms of VF configurations. Within motor cortex, this could be subtracted from the desired state of the fingers (information provided to motor cortex by other cortical systems), thus producing a direction signal as the output from motor cortex, satisfying the informational processing noted by [Georgopoulos *et al* 1983, 1984; Kalaska *et al* 1983]. This direction signal could also result from a cutaneous signal as well: the current cutaneous state of the fingers (in area 1 and/or 2) could be subtracted from the desired cutaneous state of the fingers. If, instead, the task required control of the forces, area 2 could still provide information about the state of forces acting on the joints, and this could be subtracted from the desired force state, as in the Evarts experiments where the animal was 'set' for force control. Thus, it would seem

that there are two distinct low level transcortical reflexes through motor cortex: a kinesthetic-dominated system or a tactile-dominated system, both outputting direction of movement or direction of force application. Each system would be 'programmable' other motor systems, with schemas selecting the desired system as they are activated in the performance of a task.

A necessary requirement for such a scheme is the inhibition of the unwanted ascending sensory information, allowing for the gating of only the desired sensory information [Evarts and Tanji 1974]. A possible location for this is at the dorsal column nuclei level. Sensory fibers ascending through the medial lemniscus system synapse at the dorsal column nuclei, as do descending fibers from area 5 [Catsman-Berrevoets and Kuypers 1976]. This latter area, as described below, could be involved in this selectively letting through the anticipated task-related sensory information. In general free space movements, such as preshaping the hand, tactile information is unwanted, and therefore should be inhibited, letting kinesthetic information through. However, when expecting contact, as when enclosing the hand around an object, the information from the cutaneous mechanoreceptors could be gated to the flexors to further enhance the contact. Such data has been noted in the literature [Garnett and Stephens 1981, Kanda and Desmedt 1983]. Johansson and Westling have shown [Johansson and Westling 1984, Westling and Johansson 1984] that, even though a person perceives that they have stably grasped an object that they are about to lift, slight movement still occurs, below the person's level of awareness. Johansson and Westling have also shown that this microslip information is actually being transmitted by the receptors. This fine contact information can be the type being gated to the motoneurons.

The multiple, seemingly non-somatotopic, representations of the digits in motor cortex [Kwan *et al* 1978, Strick and Preston 1982a, 1982b] could be due to a virtual finger representation. In Figure 38, we show an adapted version of the
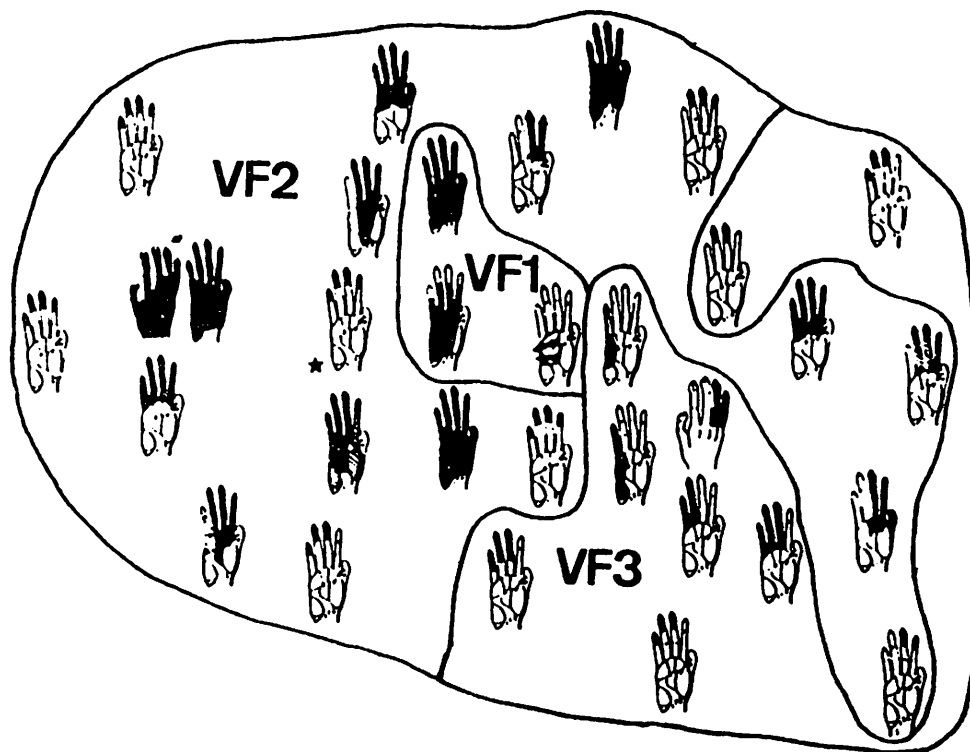
Figure 38: Caudal Representation of Kinesthetic Motor Map, adapted from [Strick and Preston 1982]

Hypothetical mapping of virtual fingers in squirrel monkey motor cortex. Each icon represents a typical receptive field of the neurons responding at that location, and we suggest each might represent a virtual finger. We have grouped the mappings into virtual finger categories. The smaller area for virtual finger 1 suggests fewer VF1 mappings and thus limited prehensile ability. The upper half of the figure caused movement in the fingers; the lower half of the figure caused movement at the wrist. One can see that there is no obvious relationship between the inputs and the outputs.

Strick and Preston [1982b] kinesthetic map of the receptive fields of the responding neurons. Strick and Preston use a hand icon to represent a typical receptive field of a neuron found at a given location. We argue that the icons could each be looked at as a virtual finger mapping. For example, if the pads of all four fingers (the icon on far left edge of figure) are mapped into VF2, then a touch felt at any one of the four finger pads would be a touch to VF2. In order to decide whether an icon represented a VF1, VF2, or VF3 mapping, we used the following general algorithm in adapting their figure:

1. we assume that palm and thumb areas are involved in VF1 functions, and note that these are seen generally in the central portion of Figure 38. An example VF1 mapping is one of the central icons, where the palm and volar surfaces of the fingers mapped into VF1; touching any skin in this area would mean that VF1 is being touched.

2. we assume that the index finger is involved in VF2 functions. For the VF2 area, we have circled all icons which include receptive fields anywhere on the index finger with or without other fingers. An example VF2 mapping would involve the volar surfaces of all four fingers (one of the icons seen on the left) By this algorithm, it is unclear what is the correct virtual finger assignment for icons involving the index, the palm, and the thumb. We argue that, since the squirrel monkey does not have true thumb opposability [Bishop 1964, Phillips 1971], one of its grasping styles involves a thumb to palm opposition. In our representation, the thumb and the palm are mapped into VF1, and therefore it seems that the monkey is trying to use two VF1s, instead of a VF1 and a VF2. We will leave this issue for now by saying that it is conceivable that a VF1 mapping and a VF2 mapping could be identical, but it is not up to motor cortex to resolve the conflicts.

3. we assume that combinations not involving the thumb or index are involved in VF3 functions. These tend to congregate along the bottom and right side

in Figure 38.

A squirrel monkey, being a New World monkey, has limited prehensile capability [Bishop 1964, Phillips 1971]. Having a pseudo-opposable thumb, it uses a limited type of side opposition for picking up small objects. The small representation for virtual finger 1 is most likely due to these reasons. Other Primates, especially humans, would have many more virtual finger mappings. The rhesus monkey (*Macaca mulatta*) has a hand that is somewhat similar to the human hand, although there are notable differences in both the intrinsic muscles and extrinsic muscles [Abbott 1970]. (For example, the extensor digitorum communis inserts into the middle phalanx in the rhesus hand, and into the distal phalanx in the human hand, thus affecting how far the fingers can open.)

The selection of a particular virtual finger mapping would then be done by other systems in the CNS. We argue that this would allow the mapping to be performed by lateral inhibition at the motor cortex level. While it is also necessary to account for consistent mappings that do not try to use the same real finger in two different virtual fingers, this hypothesis is still limited to the sensory side. Further neurophysiological studies which record from motor cortex during fractionated and non-fractionated finger movements are needed, where experimenters look carefully at the spatial differences in inputs from various motor centers, such as the supplementary motor area and the premotor area. By changing the number of real fingers used in a virtual finger, we would hope to see differential responses in motor cortex.

In conclusion, the 'grasp' motor command does not begin in motor cortex, as stimulation of motor cortex does not cause a patient to believe he willed a movement that he did not do [Phillips 1966]. Movements of the hand do not even need motor cortex [Walshe 1963, Denny-Brown 1960, etc]. However, the control of fractionated finger movement through the medial lemniscus/corticospinal pathway could possibly represent a multidimensional transcortical reflex loop that is

played upon by other cortical systems. To quote Jackson [1889], 'There are, we shall say, thirty muscles of the hand; these are represented in the nervous centres in thousands of different combinations-that is, as very many movements; it is just as many chords, musical expressions and tunes can be made out of a few notes.' We would argue that these chords are our primitive motor schemas – each with tunable parameters – and the items in this repertoire can be modified on the basis of experience.

§3. Posterior Parietal Cortex

Besides the inputs from motor cortex, area 5 of the posterior parietal cortex receives projections from area 1 and area 2 of the somatosensory cortex, as noted in Figure 37 [Jones and Powell 1969, 1970; Jones, Coulter and Hendry 1978]. It has reciprocal projections with the SMA [Jones and Powell 1969, Pandya and Vignolo 1971, Jones, Coulter, Hendry 1978], and area 7 [Pandya and Kuypers 1969, Jones and Powell 1970], and it sends fibers to the premotor area [Pandya and Kuypers 1969, Jones and Powell 1969, Pandya and Vignolo 1971, Jones, Coulter, Hendry 1978]. Area 5 sends fibers into the corticospinal tract, with somatosensory cortex contributing about 40% of the fibers in the macaque [Russell and de Myer 1961]. It most likely does not, however, contribute to the fibers making monosynaptic connections with motoneurons.

In the sense that the pyramidal tract is involved in adapting movements to spatial attributes of stimuli [Denny-Brown 1966], the contribution of area 5 to prehension could be significant. With its input from area 2, which Iwamura and Tanaka [1978] showed responsive to particular shapes of objects, and input from peristriate cortex with visual information about the object, one could infer its possible contribution to prehensile movements. It would have access to information about the current shape of the virtual fingers and also information about

the shape of a visually perceived object, both useful in a Preshape Schema for preshaping the hand based on object properties. Tactile information supplied by area 2 during the Enclose Schema would allow area 5 to confirm the pattern of the object shape on the skin and use the information to further drive the closing of the hand.

Ablations of area 5 cause a form of tactile avoidance, causing the animal to extract its hand from the object [Denny-Brown 1966]. Apraxic patients with posterior parietal lesions find it impossible to conceptualize the separateness of their hand from an object, a condition known as 'body-part as object [Goodglass and Kaplan 1963]. When a normal person is asked to show how to brush their teeth with an imagined toothbrush, he shapes his hand as if holding the brush. An apraxic patient uses his finger for the brush. We see this as an issue in the first step of the virtual finger mapping to real fingers: the number and placement of the virtual fingers needed in performing the task must be determined relative to the particular object. Perhaps a virtual hand is conceptualized to match the task requirements, and it is then the contribution of area 5 to selectively map that virtual hand into the real hand. Being multi-modal, with indirect inputs from visual pathways and somatosensory pathways [Pandya and Kuypers 1969, Jones and Powell 1970, Jones, Coulter and Hendry 1978], it could determine useful visually perceived prehensile information, such as the length of the opposable surfaces of the object. It could translate this information directly into signals for mapping real fingers into virtual fingers. Of course, the length of the opposable surface does not completely characterize the problem, as we saw in the 'place cylinder task'. The anticipated weight of the object, perceived from its visual texture as well as its overall size, could be computed in the visual pathway to area 5, and then be included in the real to virtual finger mapping processing.

Sensory information is needed to determine the current position of the virtual fingers. The type of sensory information used by the Preshape Schema seems

to usually be kinesthetic information. However, as shown by [Jeannerod et al 1984], posterior parietal patients without kinesthetic information will use visual information when it becomes available. Without area 5 to gate somatosensory information to motor cortex, preshaping by kinesthetic input cannot occur. The gating of visual sensory information to motor cortex would be done elsewhere.

Area 7, with its strong input from the visual cortical areas 17, 18 and 19, is more involved with perceiving visually-determined object properties. It has reciprocal connections with the frontal eye field area 8 [Pandya and Kuypers 1969, Jones and Powell 1969, Pandya and Vignolo 1971], the premotor area [Pandya and Kuypers 1969, Chavis and Pandya 1976, Kunzle 1978], as well as to parietal area 5 [Pandya and Kuypers 1969, Jones and Powell 1970], as seen in Figure 37. It is also reciprocally connected with SMA [Pandya and Kuypers 1969, Wiesendanger, Strick and Kuypers 1973, Kunzle 1978, Wiesendanger and Wiesendanger 1984]. A light projection was found from area 2 of the somatosensory cortex into area 7 [Vogt and Pandya 1978].

Aspects of visually perceived objects could be represented in area 7, such as the location and orientation of the object's multiple opposition vectors. By providing visual information about the object to cortical centers, the best opposition vector could be extracted which would then feed into an approach vector selector. The grasp command could come from area 7, as suggested by Mountcastle [Mountcastle et al 1975]. This, most likely, would be based on motivational signaling from other cortical and subcortical areas.

Visual information from the retina processed through the geniculate and extrageniculate pathways feed into a visually defined representation of the external world. Integration of the somatotopic map and external world, placing the body in the world, is perhaps represented in posterior parietal areas 5 and 7, as suggested by Mountcastle et al [1975]. This representation was called *extrapersonal space*.

§4. Premotor Cortex and the Arcuate Premotor Area

The boundaries and functional significance of area 6 of the cerebral cortex are strongly debated in the literature [see Evarts, Wise, and Shinoda 1984, Wise 1984]. Its medial part, the SMA, has been identified as containing a separate somatotopic representation [Woolsey 1958], and will be discussed in the next section. The lateral part (area 6a) is called the Premotor area, or PM, but whether this is in itself is one unit or many is still in question [see Wise 1984]. While many researchers suggest a role for PM of orienting the trunk and limbs for reaching movements [see Humphrey 1979], it has been noted that there is a strong output from the caudal bank of the arcuate sulcus into the hand area of motor cortex [Muakkassa and Strick 1979, Godschalk *et al* 1981, Godschalk *et al* 1985]. This area, a small region around the genu of the arcuate sulcus, is called the Arcuate Premotor area, or APA.

The premotor cortex reciprocally projects to motor cortex [Kuypers and Lawrence 1967, Pandya and Kuypers 1969, Kunzle 1978], as seen in Figure 37, although not directly to the hand area [Kunzle 1978]. The arcuate premotor area reciprocally projects into arm-hand region of motor cortex [Muakkassa and Strick 1979, Schell and Strick 1984]. Besides the connections noted in the previous sections between premotor cortex and parietal areas, reciprocal connections exist with the frontal eye field area 8 (through area 9) [Pandya and Kuypers 1969, Kunzle 1978] and with SMA [Kunzle 1978]. Schell and Strick [1984] determined that the APA also reciprocally connects with SMA. Area 6 as a group sends fibers into the corticospinal tract, contributing about 29% in the macaque [Russell and de Myer 1961].

Rizzolatti [Rizzolatti *et al* 1983, Gentilucci *et al* 1983] has suggested a finer definition of extrapersonal space, separating the world into what is within reach and what is not. *Peripersonal space*, the representation of the world within reach,

was suggested to exist in area 6 of the neocortex. Body parts, such as the location of the wrist, could be represented in a peripersonal space. Rizzolatti further suggest that pericutaneous maps exist, relative to the skin, which would suggest to us a current hand map could exist in area 6, perhaps in the APA.

In reaching behaviors, orienting information is needed in order to prevent the Enclose schema from starting to flex the fingers too early. This suggests a role for the APA in directing the Enclose Schema to not become active, no matter what other inputs, until the opposition space is correctly oriented.

Ablation of the peri-arcuate cortex (caudal and rostral banks of arcuate sulcus) causes temporary deficits in visually guided orientation of the fingers [Moll and Kuypers 1977]. However, the rostral bank of the arcuate sulcus is more related to the frontal eye field area 8 than to the APA. In order to determine the contribution of the APA to hand movement, studies of this sort are needed which focus more directly on just the APA. More importantly, non-evasive studies, such as electrostimulation and recording, would help determine its role in behaving animals.

A possible contribution of the APA could be in the facilitation of the preshaping movements, since it is within area 6. Using the current virtual finger shape information from area 5, it could direct the Preshape schema to gate desired VF configurations from area 5 to motor cortex. Motor cortex, in turn, would subtract the current VF configurations from the desired one, thus producing a direction signal, of the sort noted in the studies of Georgopoulos [Georgopoulos et 1983, 1984]. Such a scenario would predict a direct connection between the APA and area 5, although such a connection has yet to be found.

§5. Supplementary Motor Area

The supplementary motor area (SMA, or MII) reciprocally projects to frontal areas, such as the motor cortex [Jones and Powell 1969, Pandya and Vignolo 1971, Jones, Coulter and Hendry 1978] and the premotor area [Kunzle 1978], as seen in Figure 37. Schell and Strick [1984] show reciprocal connections between SMA and APA of the premotor cortex. It also sends fibers to the frontal eye fields [Pandya and Kuypers 1969, Kunzle 1978]. Reciprocal projections are seen with parietal areas also, such as area 5 [Jones and Powell 1969, Pandya and Vignolo 1971, Jones, Coulter and Hendry 1978] and area 7 [Pandya and Kuypers 1969, Wiesendanger, Seguin and Kunzle 1973, Kunzle 1978, Wiesendanger and Wiesendanger 1984]. It projects to area 3a of the somatosensory cortex and receives fibers back from area 1, 2, and 3a [Jones, Coulter and Hendry 1978]. SMA sends fibers into the corticospinal tract, with all of area 6 as a group contributing about 29% in the macaque [Russell and de Myer 1961].

It has been suggested that the SMA's influence on motor cortex is inhibitory [Humphrey 1979]. In ablation studies of the SMA [Travis 1955], a deficit was found, resulting in a behavior where the animal could no longer let go of objects (an effect called tactile following). This was attributed to the release of the instinctive grasp reflex, in that it occurs only if motor cortex is not removed along with the SMA. This suggests a role for the SMA as part of the Preshape Schema, perhaps acting to inhibit motor cortex from enclosing around the object too early. Receiving desired virtual finger shape information from area 5, the SMA could use that to direct the Preshape Schema, along with the APA. The Enclose Schema is inhibited until the hand is preshaped and arm oriented correctly.

§6. Frontal Eye Fields

Area 8 (see Figure 37), with its inputs from peristriate cortex [Jones and Powell 1969, Pandya and Kuypers 1969] and area 7 [Jones and Powell 1969, Pandya and Kuypers 1969, Pandya and Vignolo 1971], collects visual information about objects. It returns fibers to area 7 [Pandya and Kuypers 1969]. As noted in sections above, area 8 also receives fibers from SMA and is reciprocally connected with the premotor area (through area 9) [Pandya and Kuypers 1969, Kunzle 1978]. While area 8 is specifically named the frontal eye fields, we will lump it with area 9 for simplicity, since the connection between the premotor area and area 8 is made through area 9 [Kunzle 1978].

The frontal eye fields monitor eye movements, and seem to be able to suppress reaching movements until the trunk is oriented correctly [Humphrey 1979]. We suggest it could be involved in the prehensile pathway as the approach vector selector. It collects processed information from other cortical areas, as well as motivational information from other cortical and subcortical structures. Using this information, it could plan where to put the hand. Area 7 could be the requester, asking it to determine the best approach vector. Its output would then be the desired wrist location, which could then be sent in turn to premotor cortex for orienting the arm and trunk.

Neuroanatomical studies of the connections between the frontal eye fields and the arcuate premotor area would help in determining how extensive their interaction is. We also suggest that recording experiments be performed on unanaesthetized animals performing reaching and grasping tasks. In the tasks, the size and distance of the objects to be grasped can be varied, in order to build up a picture of the object representation.

§7. Subcortical Contributions

In Figure 39, we present some of the immediate subcortical connections made with the cortical sensorimotor centers. In the figure, we do not attempt to show the interconnections between these subcortical areas, and we only show some of the extrapyramidal pathways to the spinal cord. It is interesting to note in this figure the incredible interweaving of cortical and subcortical areas, showing the immense difficulty that neurophysiologists have in trying to sort out the neural correlates to behavior. In the following subsections, we briefly try to point out some features of this figure, and suggest some of the implications of these pathways.

§7.1 Basal Ganglia and Substantia Nigra

Three groups of nuclei, the caudate nucleus, the putamen, and the globus pallidus collectively are known as the basal ganglia [see Kandel and Schwartz 1985]. The caudate and putamen together are called the striatum. The striatum receives afferents from motor cortex, the frontal eye fields, the premotor cortex, and the SMA [Astruc 1971, Jones et al 1977]. The putamen also receives fibers from area 5 and 7 [Jones et al 1977]. The internal segment of the globus pallidus (GPi) projects to the ventralis lateralis pars oralis (VLo), a thalamic subdivision known to reciprocally project to the SMA [Kuo and Carpenter 1973, Schell and Strick 1984, Strick 1985]. Of the two zones of the substantia nigra, the pars reticulata (SNpr) projects to to the ventralis lateralis pars medialis (VLm) portion of the thalamus [Carpenter, Nakano, Kim 1976, Schell and Strick 1984, Strick 1985], an area known to project to the premotor cortex [Akert 1964, Kalil 1975]. Disorders in the basal ganglia have been noted to reduce the speed of movements, change muscle tone, and cause involuntary movements [see Kandel and Schwartz 1985]. It has been suggested that the basal ganglia have a role in the initiation and

to spinal cord
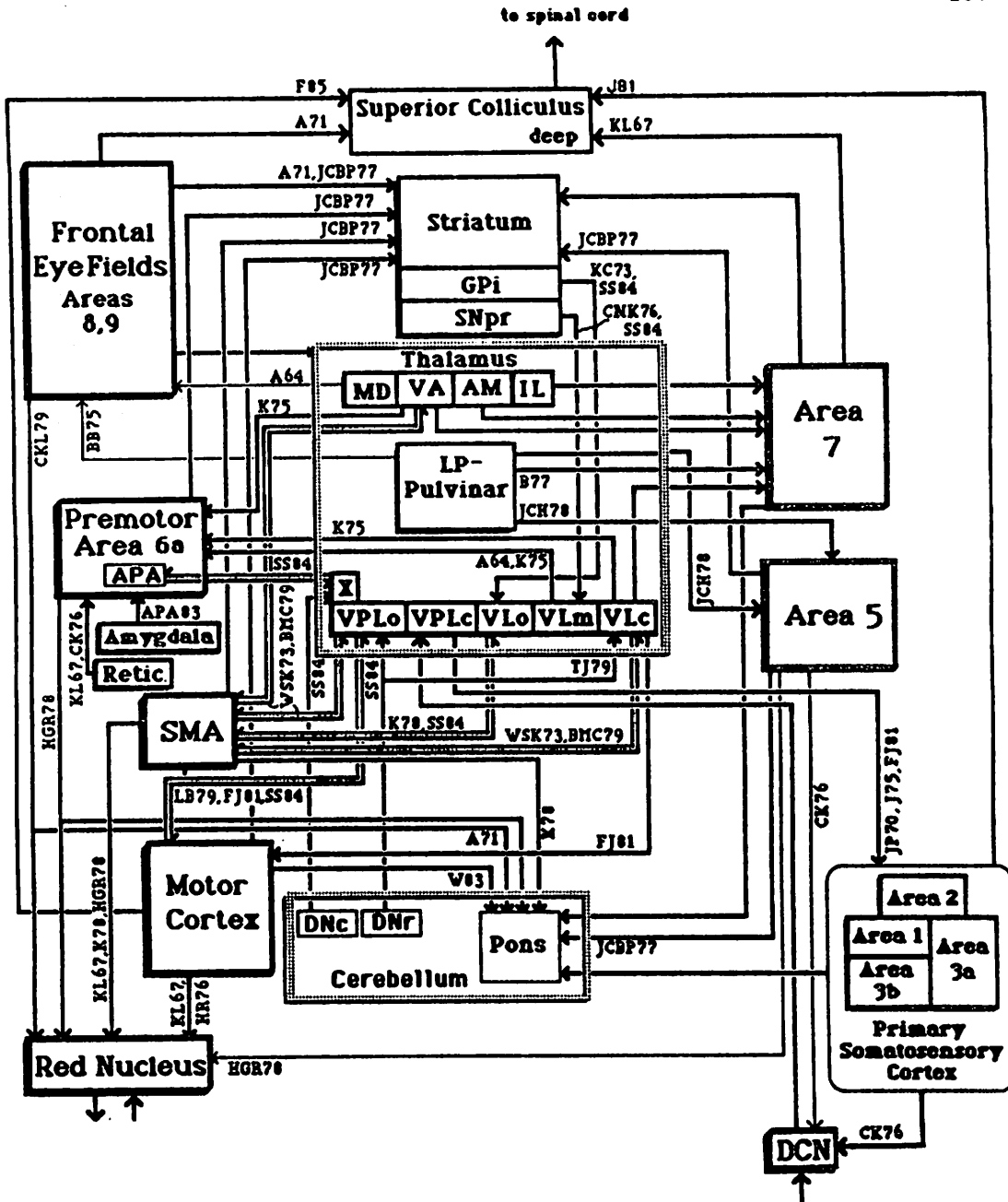
Figure 39: Subcortical Connections to Cortical Areas involved in Reaching

Subcortical inputs currently known to major sensorimotor areas of the Primate cerebral cortex. Labels on the path indicate the research which either identified or verified the connection. The only outputs indicated are those which contribute directly to hand and forelimb movement through the rubrospinal and tectospinal tracts. Lighter lines indicate fewer projections.

A64:	[Akert 1964]
A71:	[Astruc 1971]
APA83:	[Avendaño, Price, and Amaral 1983]
B77:	[Bayledier 1977]
BB75:	[Bos and Benventao 1975]
BMC79:	[Bowker, Murray and Coulter 1979]
CK76:	[Catsman-Berrevoets and Kuypers 1976]
CKL79:	[Catsman-Berrevoets, Kuypers, and Lemon 1979]
CNK76:	[Carpenter, Nakano, Kim 1976]
FJ81:	[Friedman and Jones 1981]
F85:	[Fries 1985]
HGR78:	[Humphrey, Gold and Reed 1978]
HR76:	[Humphrey and Rietz 1976]
J75:	[Jones 1975]
J81:	[Jones 1981]
JCH78:	[Jones, Coulter and Hendry 1978]
JCBP77:	[Jones, Coulter, Burton, and Porter 1977]
JP70:	[Jones and Powell 1970]
K75:	[Kalil 1975]
K78:	[Kunzle 1978]
KC73:	[Kuo and Carpenter 1973]
KL67:	[Kuypers and Lawrence 1967]
LB79:	[Lemon and Burg 1979]
SS84:	[Schell and Strick 1984]
TJ79:	[Thach and Jones 1979]
W83:	[Wiesendanger 1983]
WSK73:	[Wiesendanger, Seguin and Kunzle 1973]

(Legend for Figure 39)

control of movement. In studies done on awake monkeys, DeLong [1974] noted changes in activity in the globus pallidus and substantia nigra (pars reticulata) to occur before changes in motor cortex and cerebellum. In later studies, DeLong et al [1984] found that basal ganglia activity related to specific parameters of movement, and suggest its role is in the integration of information from various cortical areas.

§7.2 Thalamus

The thalamus, as a major relay center for sensorimotor signals has three main groups of nuclei: the medial, lateral, and anterior nuclei [see Kandel and Schwartz 1985].

Area 7 of the posterior parietal cortex receives inputs from various thalamic nuclei, including the intralaminar nuclei (IL), the ventralis anterior (VA), the anterior medialis (AM), and the LP lateral posterior (LP)-pulvinar complex. Surprisingly, area 5 does not seem to receive as many thalamic inputs. The VA is reciprocally connected with SMA [Wiesendanger, Seguin and Kunzle 1973, Bowker, Murray and Coulter 1979] and it also projects to premotor area [Kalil 1975], providing a parallel, subcortical, pathway between area 7, PM, and SMA.

The frontal eye fields seem to have only light projections with the thalamus, receiving from the pulvinar [Bos and Benevento 1975] and from the mediodorsal nucleus (MD) [Akert 1964]. As area 5 and the frontal eye fields do not seem to directly connect, there could be an indirect connection through the pulvinar.

The premotor area receives from the VA, the ventralis lateralis pars caudalis (VLc) and and pars medialis (VLm) [Kalil 1975]. Schell and Strick [1984] note that area X reciprocally connects with the APA, and that area X also receives inputs from deep cerebellar nuclei. The VLc also projects to motor cortex [Friedman and Jones 1981] and it is reciprocally connected with the SMA [Wiesendanger,

Seguin and Kunzle 1973, Bowker, Murray and Coulter 1979]. A major input into the VLc is from the deep cerebellar nuclei [Thach and Jones 1979]. This also represents a parallel, subcortical pathway, this time connecting the SMA, PM, and motor cortex. Both motor cortex and the SMA are reciprocally connected with ventralis posterior lateralis pars oralis (VPLo) [Wiesendanger, Seguin and Kunzle 1973, Bowker, Murray and Coulter 1979, Lemon and Burg 1979, Friedman and Jones 1981, Schell and Strick 1984], which also receives from the deep cerebellar nuclei [Schell and Strick 1984].

Somatosensory cortex receives projections from ventralis posterior lateralis pars caudalis (VPLc), which is the thalamic termination of the medial lemniscus system.

§7.3 Red Nucleus

The red nucleus receives projections from the frontal eye fields [Catsman-Berrevoets, Kuypers, and Lemon 1979], the premotor area [Humphrey, Gold and Reed 1978], the SMA [Kuypers and Lawrence 1967, Kunzle 1978, Humphrey, Gold and Reed 1978], motor cortex [Humphrey and Rietz 1976], and a light projection from area 5 [Humphrey, Gold and Reed 1978]. The corticorubral tract parallels the corticospinal tract, and research has noted that non-fractionated finger movement is possible through corticorubral projections to distal muscles from motor cortex [Humphrey and Rietz 1976].

§7.4 Cerebellum and Pons

The pontine nuclei receive inputs from every cortical area discussed in this thesis, the details of which is reviewed by Wiesendanger et al [1979]. The deep cerebellar nuclei send projections to the thalamus, as noted above.

With its enormous number of neurons, the lateral hemispheres of the cerebel-

lum are most likely involved in the execution of the reaching movements, providing a temporal pattern of agonist-antagonist activation [Allen and Tsukahara 1974]. In studies on macaque monkeys performing isometric pinching tasks using their thumb and forefinger, Smith *et al* [1985] found that the interpositus and dentate nuclei increase activity during the task. They suggest these nuclei are involved in cocontraction of agonist and antagonist muscles. Cocontraction of agonist and antagonist muscles are seen in finger flexion [Long 1981].

§7.5 *Superior Colliculus*

The superior colliculus receives projections from motor cortex [Fries 1985], the frontal eye fields [Astruc 1971], somatosensory cortex [Jones 1981], and area 7 [Kuypers and Lawrence 1967]. Fries [1985] suggest superior colliculus input could bring hand under foveal control for visuomotor coordination before execution of fine manipulatory movements.

§8. Cortical Contributions to Opposition Space

In Figure 40, we summarize the contributions of cortical areas to pad opposition. For simplicity's sake, we do not attempt to add in the subcortical interactions, although a true schema picture would show both cortical and subcortical areas distributed through all the schemas. In this first approximation, we can give no more than a very coarse description of the cortical contributions. This picture should be used to indicate what we think are the major contributions of these areas to prehensile movement. We try to show how sensorimotor areas can contribute dynamically to both the Preshape and the Enclose Schemas.

Area 7, using motivational cues from other cortical and subcortical systems, sends out the cortical grasp command along with anticipated task features (weight
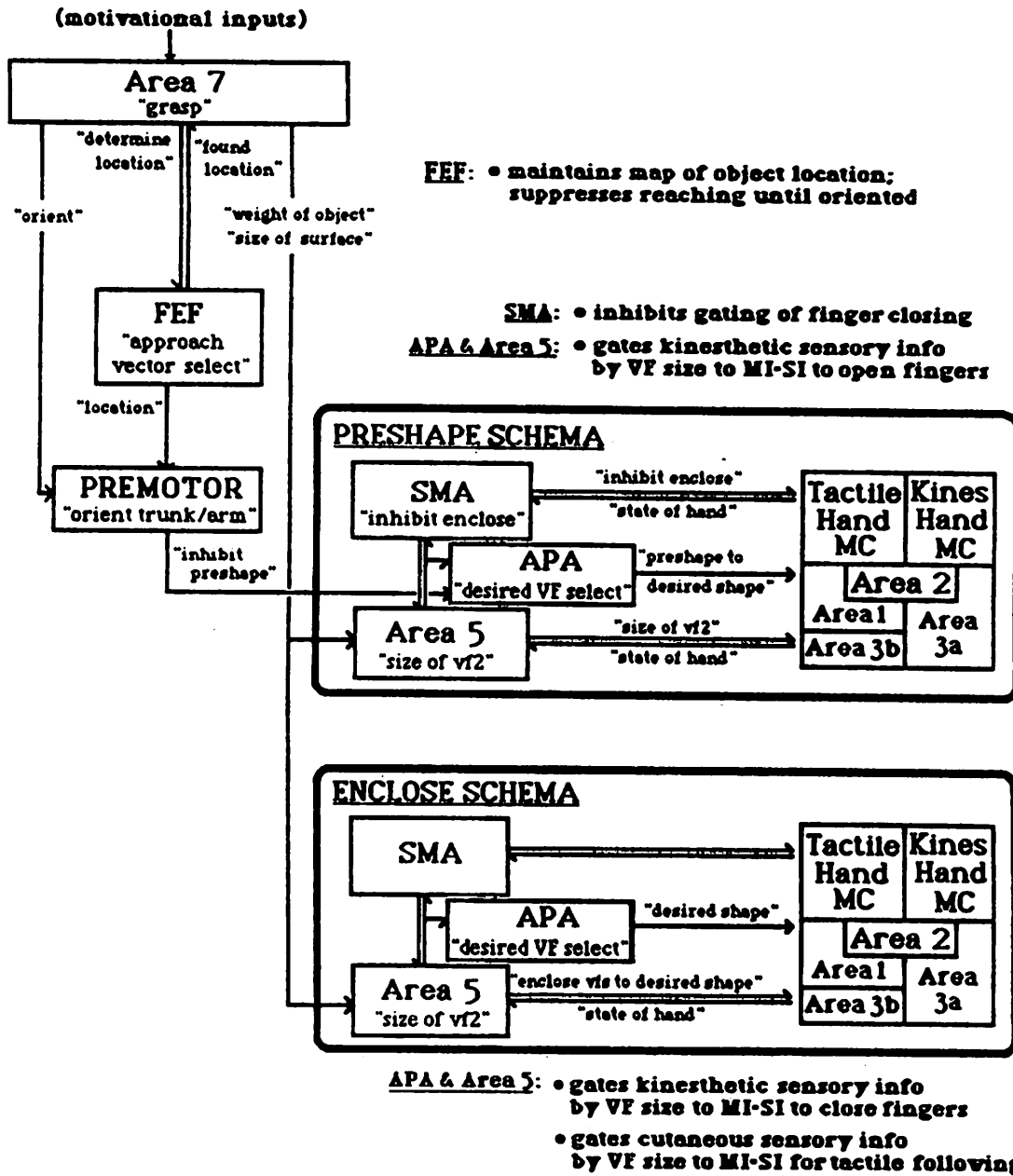
Figure 40: Hypothetical mapping of Coordinated Control Program onto CNS

Pad opposition is a subset of the prehensile repertoire of the CNS. We identify the types of roles various cortical areas might have in prehensile movements, but especially in pad opposition. Subcortical contributions are not included.

of object, size of surface, etc) to area 5. It also sends commands to cue the approach vector selector perceptual schema (mostly in the frontal eye fields) and the Orient Trunk and Move Arm Schemas (mostly in the Premotor Area). These schemas start working when the desired wrist location is known, produced by the FEF. Current state information,, not shown, would influence the FEF to take into account the current body and arm orientation. The FEF maintains a map of object locations, along with premotor areas (extrapersonal and peripersonal space), and suppresses reaching until the body is oriented. The desired wrist location (in an object-centered coordinate system) is sent to the Preshape Schema, which is then released from inhibition. The Preshape Schema involves the activity of various cortical (and subcortical) areas, working together to gate the correct sensory information along motor pathways. Motor cortex (MI) and somatosensory cortex (SI) collectively act as a system which can either respond to kinesthetic stimuli or to tactile stimuli, performing virtual-to-real and real-to-virtual finger mappings. The APA, possibly containing knowledge about opposition space, would use the desired wrist location to compute the desired preshape state, based on the virtual finger size information from area 5. These could work, in a distributed fashion, to gate kinesthetic sensory information from somatosensory cortex to the motor cortex, thus 'turning on' the kinesthetic MI-SI system. The contribution of area 5 would be in the specification of virtual finger requirements, thus perhaps choosing a reasonable solution of virtual finger mappings, given the constraints of the task. The APA directs the preshaping of the virtual fingers, commands which are turned into real fingers within motor cortex. Another cortical area in the Preshape Schema is the SMA, which ensures success of the preshape by possibly inhibiting the Enclose Schema through inhibition of the tactile MI-SI system. This continues until the wrist is correctly oriented and located. When this happens, inhibition is released and the Enclose Schema closes the fingers. The APA contributes its knowledge about opposition space still, while area 5 gates kinesthetic sensory information to motor cortex during the closing of the

hand. When contact is made, area 5 can then change gating modes, and now gate the cutaneous sensory information to motor cortex for tactile following of the object.

We suggest that the Preshape Schema and the Enclose Schema both work by gating the correct sensory information to motor cortex. Using this gating mechanism, the current state is subtracted from the desired state, producing a differential signal to the muscles. The APA, SMA, and area 5 basically work together, in a distributed fashion, to describe virtual finger requirements and to program the motor cortex-somatosensory cortex (MI-SI) dual system. Either the kinesthetic MI-SI system or the tactile MI-SI system is chosen, depending on the task and on the part of the task being performed. The MI-SI system can then basically set up a filter to tell the dorsal column nuclei what sensory information (tactile or kinesthetic) to let through. The MI-SI system also performs the real-to-virtual finger mapping on sensory information arriving in SI, and the virtual-to-real finger mapping on the motor commands coming from the APA-Area5-SMA system.

A recurrent theme in the literature is the issue of feedback loops. While it has been noted for 100 years that spinal reflexes exist [Sherrington 1889], the possible existence of transcortical reflexes pose an interesting hypothesis for prehensile movement. The mammalian brain, as noted by Warren [1974] is to 'flexibly interact with changing patterns of environmental events'. Transcortical reflexes, with their many possible change points, seem highly flexible and useful, especially in prehensile movements. Basmajian [1963] trained subjects with biofeedback to selectively discharge motor units of the abductor brevis pollicis. Within one half of a day, many subjects were able to track the potentials through sound or visual input, even able to do it without the feedback.

We note two subcortical reflex loops acting in conjunction with at least two possible transcortical reflex loops in prehensile movements. The first one is the

spinal cord reflex. The next one, the dorsal column nuclei reflex, we noted as a possible way to gate only anticipated sensory information to somatosensory cortex. The third one, the somatosensory/motor cortex loop (MI-SI), we noted as a way of gating different somatosensory channels to motor cortex. Finally, we see the APA-Area5-SMA connection as a loop, where, again, anticipated sensory information can be gated to motor pathways. However, the sensory information and motor commands are more highly processed in this loop, acting in virtual finger terms to direct the MI-SI system.

§9. Summary

While muscles are the devices which actually cause movement, it is the overlying nervous system which make the muscles work. While alpha motoneurons innervating those muscles represent the 'final common path' [Sherrington 1889], the character of the outputs from the central nervous system which gives Primate movement its subtlety is highly complex. A distributed system is presented here for prehensile movements, which tries to account for Primate flexibility and capability, using what is currently known about the central nervous system. A coordinated control program is mapped onto cortical areas, showing the interaction of perceptual and motor schemas. Task-related information, such as opposition space and virtual fingers, has been located among various structures, allowing the system to perform task-specific behaviors. We suggest a critical area for needed information is the Arcuate Premotor Area, which we feel contains representations for opposition space. We also see that it is important to look at the APA, SMA and area 5 together as a unit for gating tactile or kinesthetic information through the transcortical somatosensory/motor cortex loop. Further neurophysiological research is needed which can prove or disprove the model put forth. Tasks performed by awake, unanaesthetized monkeys using combinations of real fingers

may shed light on the notion of virtual finger mappings. We feel that the analysis presented here sets forth a conceptual model which neurophysiologists can use for studying goal-oriented motor behavior. Virtual finger and an opposition space representation seem close enough to 'excitable' cortex, so that interested experimentalists could test some of our hypotheses.

CHAPTER VII

CONCLUSIONS AND SUGGESTIONS FOR FURTHER RESEARCH

The hand can become a claw, a fist, a horn or spear or sword or any other weapon or tool. It can be everything because it has the ability to grasp anything and hold anything.

-Aristotle

Research in artificial intelligence has demonstrated the efficacy of attention focusing mechanisms for goal directed behavior. In terms of natural intelligence, the CNS is presented with an infinite number of sensations when dealing with even one object. In order to successfully interact with such an object, only information specific to the interaction is desirable. Important perceptions for prehensile movements involve: what surfaces can be grasped given a particular intention, what are the characteristics of those surfaces, and what will happen when they are grasped. In attempting to capture this information in a computational model of prehensile movements, we call these features the *task requirements* and list them, in a first approximation, as a set of opposable surfaces, an opposition vector between pairs of opposable surfaces, the functional degrees of freedom about an opposition vector, and a set of anticipated forces arising relative to an opposition vector. We feel that this is a powerful task representation, because it not only captures physical features of the object, but also how the person intends to use the object within the task. In effect, it sets up the context for all subsequent movements, and we can use this representation as a goal structure to plan those movements.

The human hand, having anatomical and physical constraints, applies oppo-
sitions around objects along three basic axes using the fingers in groupings called
virtual fingers. Prehensile postures reflect the combined use of one or more of
these oppositions, as if the hand were three hands in one. Each type of opposition
has particular functional capabilities, involving the direction and magnitude of
the applied force, the direction and range of available movement, and the amount
of control possible. Each functional capability we call an *opposition space*, and
we use a coordinate system to describe the prehensile postures of the opposition
spaces. We feel that this is a significant contribution to motor behavior research,
because opposition spaces are defined intrinsically based on the architecture of
the hand. This representation has the power to describe goals for the movements,
and also allows one to understand how a controller might work functionally. Using
task requirements as an input and opposition spaces as an output, a functional
mapping can be made explicit so that a computational model of a controller
can be built. The major emphasize we have made here in this dissertation is
to capture the sources of constraints on these prehensile movements. Our task
requirements capture a set of task constraints, and opposition space captures a
set of hand constraints. With this analysis, a more refined level of description of
a coordinated control program has been achieved.

While we do not claim to have explained all of movement or listed all sources
of constraints, it was our goal of this research to gain some small understanding of
the central nervous system. In our review of the neurophysiological literature, we
have noted the important contribution that neocortex makes to prehensile move-
ments. This contribution is suitably modelled as a distributed somatotopically
organized planning system acting within constraints and directing sensorimotor
systems. We noted the importance of different types of sensory information in
the different aspects of prehensile movements.

We suggest that the motor cortex and somatosensory cortex collectively act

as a system which can either respond to kinesthetic stimuli or to tactile stimuli, performing virtual-to-real and real-to-virtual finger mappings. The Preshape Schema and the Enclose Schema both work then by gating the correct sensory information to motor cortex In free-space movements, like preshaping, kinesthetic sensory information from somatosensory cortex would be gated by higher cortical areas (such as the APA-Area5-SMA areas) to the motor cortex, thus 'turning on' the kinesthetic system. When contact with an object is expected, these same areas (now working within the Enclose Schema) would gate the cutaneous sensory information to motor cortex for tactile following of the object. High level preshape and enclose commands are given in virtual finger representations, with the real-to-virtual finger mapping done in somatosensory cortex and virtual-to-real finger mapping done in motor cortex.

We believe that the way to understanding the informational processing capability of neocortex is to look for simple yet effective ways to integrate sensory information with motor control. We have suggested here a schema model that both makes explicit the informational content of cortical signaling, and that also suggests mechanisms for quickly transmitting that information. We have tried here to suggest neural correlates of the coordinated control program, and even suggest mechanisms for the control and representation of virtual fingers.

We have looked carefully into the grasping schemas, which we believe map task requirements into opposition spaces so that functionally effective forces can be brought to bear around a perceived object for a given task. In order to apply those forces, the hand must be positioned at a distance and orientation from the opposition vector where a solution in opposition space exists. An assertion we have made here is that detailed information is not necessary for decisions; instead, summarized kinematic knowledge can be used for making movements into the right 'ballpark'. Tactile information can then be used to further adjust the hand shape for enclosing the object into the grasp. As the hand grows and

changes, kinematic knowledge can be updated when mismatches occur. Instead of maintaining detailed kinematic solutions for all possible distances and orientations from an object, we have modelled the system so that it makes decisions based on maps of where lots of solutions exist. We have demonstrated a neural network solution, which could allow these grouped possible solutions to compete, converging when a group of solutions within opposition space is found in both the VF1 space and the VF2 space.

This study used many estimates and simplifications, chosen to help up work out the feasibility of such a model of human prehension. For example, we were not able to look at the force output within opposition space for any of the oppositions. More sophisticated instrumentation and experimentation is needed which will provide a more complete characterization of the force profiles of opposition space, in terms of maximum force output, and median force output (i.e., what is the force range in which the system is *actually* working?). We also feel some problems are associated with using IREDs attached to a person's skin. They move around as the person moves, and thus their data readings are not too reliable.

Because of these limitations, we were also not able to look at the goal structure of palm opposition or side opposition. The long term goal of this research is to do the complete mapping from task requirements, as seen in Figure 41. Given a set of task requirements, what are the combinations of oppositions that emerge in the resultant hand posture? While the mappings are shown in dark lines, with possibly more than one opposition emerging, constraints are shown in dashed lines. It is due to these constraints, coming from a variety of sources, that a particular mapping will emerge. Here, in this dissertation, we were only able to look at the mapping from one opposition vector to pad opposition, and only look at a limited set of constraints.

The goal of this research is to encourage links between robotics and neuroscience research. Neurophysiologists can help prove or disprove the models
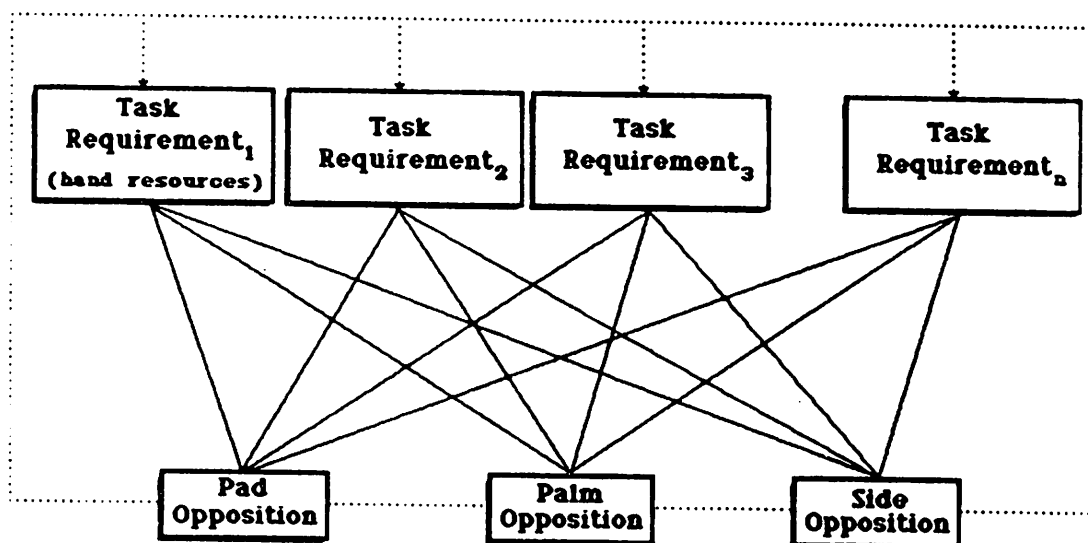
Figure 41: Mapping from Task Requirements to Opposition Spaces

The preshaped posture reflects combinations of one or more opposi-
tions. The emergent mapping depends on the constraints (shown in
dashed lines) acting on the system. The goal of this research is to be
able to start with a task description and map that into the functionality
of the hand, or the opposition spaces, based on system constraints.

presented by looking at their data in terms of opposition space and virtual fingers. Sensory neurophysiologists and psychologists can look at object perceptions suggested here. They can verify the use of sensory information within a task and also opposition space based coordinates in kinesthetic processing. Motor physiologists and psychologists are encouraged to use the opposition space coordinate system in their experiments, to both valid this model and to see what other correlations can be made. Roboticists developing dextrous robot hands might gain insight both for designing those hands as well as for controlling them. The human hand, with over 25 degrees of freedom, represents a level of complexity beyond the capacity of mechanical hands and their controllers. Understanding how the human hand works will both help in the design of future robotic and prosthetic hands, and also help in the understanding of the human brain at its most basic intellectual capacity.

REFERENCES

Abbott, R. A. (1970): The Comparative Myology of the Hands of the Human and the Rhesus Monkey, M.S. Thesis, Dept Phys Educ, Health and Recreation, Florida State Univesity.

Aggarwal, J. K., Davis, L. S., Martin, W. W. and Roach, J. W. (1981): Survey: Representation Methods for Three-Dimensional Objects. In: *Progress in Pattern Recognition, vol 1*, L. N. Wanal and A. Rosenfeld, eds, NY: North-Holland Pub, 377-391.

Akert, K. (1964): Comparative Anatomy of Frontal Cortex and Thalamofrontal Connections. In: *The Frontal Granular Cortex and Behavior*, J. M. Warren and K. Akert (Eds.), NY: McGraw-Hill, 372-394.

Allen, G. I. and Tsukahara, N. (1974): Cerebrocerebellar Communication Systems, *Physiol Rev*, 54: 957-1006.

Amari, S. and Arbib, M. A. (1977): Competition and Cooperation in Neural Nets. In: *Systems Neuroscience*, J. Metzler (Ed.), NY: Academic Press, 119-165.

Amontons, G. (1699): De la resistance causee dans les machines, *Memoires de l'Academie Royale des Science*, 206-227.

Anderson, C. T. (1965): Wrist Joint Position Influences Normal Hand Function. Unpublished Master's Thesis, University of Iowa.

Arbib, M. A. (1972): *The Metaphorical Brain. An Introduction to Cybernetics as Artificial Intelligence and Brain Theory*, NY: Wiley-Interscience.

Arbib, M. A. (1981): Perceptual Structures and Distributed Motor Control. In: V. B. Brooks, (Ed.) *Handbook of Physiology-The Nervous System, II. Motor Control*, Bethesda, MD: American Physiological Society, 1449-1480.

Arbib, M. A., Iberall, T., and Lyons, D. (1985): Coordinated Control Programs for Movements of the Hand. In: *Hand Function and the Neocortex*, A. W. Goodwin and I. Darian-Smith (Eds.), Berlin: Springer Verlag, 111-129. (available as *COINS Technical Report 83-25*, Dept of Computer Science, University of Mass, Amherst, Mass.)

Arbib, M. A., Iberall, T., and Lyons, D. Schemas Which Integrate Vision and Touch. In: *Vision, Brains, and Cooperative Computations*, M. A. Arbib and A. Hanson (Eds.), in press.

Aristotle, *The Animal Parts*, IV, 10.

Asanuma, H. and Rosen, I. (1972): Topographical organization of cortical efferent zones projecting to distal forelimb muscles in the monkey. *Exp Brain Res*, 14: 243-256.

Asanuma, H. and Sakata, H. (1967): Functional Organization of a Cortical Efferent System Examined with Focal Depth Stimulation in Cats. *J Neurophys.*, 30: 35-54.

Astruc, J. (1971): Corticofugal connections of Area 8 (Frontal Eye Field) in *Macaca mulatta*, *Brain Res*, 33:241-256.

Avendaño, C. J., Price, L., and Amaral, D. G. (1983): Evidence for an Amygdaloid Projection to Premotor Cortex but not to Motor Cortex in the Monkey, *Brain Research*, 264: 111-117.

Barto, A. G. (1985): Learning by Statistical Cooperation of Self-interested Neuronlike Computing Elements, *Human Neurobiol*, 4:229-256.

Basmajian, J. V. (1963): Control and training of individual motor units. *Science*, 141: 440-441.

Bayledier, C. (1977): Pulvinar-lateroposterior Afferents to Cortical Area 7 in Monkeys demonstrated by Horseradish Peroxidase Tracing Technique, *Exp Brain Res*, 27: 501-507.

Becker, J. C., Thakor, N. V., Gruben, K. G. (1986): A Study of Human Hand Tendon Kinematics with Applications to Robot Hand Design, *Proc 1986 IEEE Intl Conf on Robotics and Automation*, April 7-10, San Fran, 1540-1545.

Becker, R. A. (1954): *Introduction to Theoretical Mechanics*, McGraw Hill, NY.

Bell, C. (1832): *The Hand; Its Mechanism and Vital Endowments, as Evincing Design and Illustrating the Power, Wisdom and Goodness of God (English Edition), Preceded by an account of the author's discoveries in the Nervous System*, by Alexander Shaw, London: George Bell and Sons.

Bishop, A. (1964): Use of the hand in lower primates. In: *Evolutionary and genetic biology of primates, vol 2*, Buettner-Janusch, ed. NY: Academic Press.

Bos, J. and Benevento, L. A. (1975): Projections of the Medial Pulvinar to Orbital Cortex and Frontal Eye Fields in the Rhesus Monkey (*Macaca Mulatta*), *Exp Neurol*, 49: 487-496.

Bowden, F. P. and Tabor, D. (1950): *Friction and Lubrication of Solids*, Oxford: Clarendon Press.

Bowker, R. M., Murray, E. A., and Coulter, J. D. (1979): Intracortical and thalamic connections of the supplementary sensory and supplementary motor areas in the monkey, *Soc. Neurosci. Abstr*, 5: 704.

Brinkman, J. and Kuypers, H. G.J. (1972): SplitBrain monkeys: Cerebral Control of Ipsilateral and Contralateral Arm, Hand, and Finger Movements, *Science* 176 (4034): 536-539.

Brooks, R. A. (1981): Symbolic reasoning among 3-D models and 2-D images, *Artificial Intell*, 17:285-348.

Brun, J. (1963): em La Main et l'Esprit, Paris: Presses Universitaires de France.

Bunnell, S. (1942): Surgery of the Intrinsic Muscles of the Hand other than Producing Opposition of the Thumb. *J Bone Jt Surg*, 24: 1-32.

Bunnell, S. (1944): *Surgery of the Hand*. Phil: J. B. Lippincott Co.

Buxton, D.F and Goodman D. C. (1967): Motor function and the corticospinal tracts in the dog and raccoon. *J Comp neurol*, 129: 341-360.

Carlson, M. and Nystrom, P. (1986): Significance of Topography in Primary Somatic Sensory Cortex (SI) for Tactile Discrimination Capacity in Old and New World Primates. *Soc Neurosci Abstr* 12(2): 1429.

Carpenter, M. B., Nakano, K., and Kim, R. (1976): Nigrothalamic Projections in the Monkey Demonstrated by Autoradiographic Technics, *J Comp Neurol*, 165: 401-416.

Catsman-Berrevoets, C. E. and Kuypers, H. G.J. M. (1976): Cells of origin of cortical projections to dorsal column nuclei, spinal cord and bulbar medial reticular formation in the rhesus monkey, *Neurosci. Letters*, 3: 245-252.

Catsman-Berrevoets, C. E., Kuypers, H. G.J. M., and Lemon, R. N. (1979): Cells of origin of the frontal projections to magnocellular and parvocellular red nucleus and superior colliculus in cynomolgus monkey. An HRP study. *Neurosci. Lett.*, 12: 41-46.

Chao E. Y., Opgrande J. D., Axmear, F. E. (1976): Three Dimensional Force Analysis of Finger Joints in Selected Isometric Hand Functions, *J Biomechanics*, 9: 387-396.

Chavis, D. A. and Pandya, D. N. (1976): Further observations on corticofrontal connections in the rhesus monkey, *Brain Res.*, 117: 369-386.

Clough, J. F.M, Kernell, D. and Phillips, C.G (1968): The distribution of monosynaptic excitation from the pyramidal tract and from primary spindle afferents to emotoneurons of the baboon's hand and forearm, *J Physiol. (London)*, 198: 145-166.

Comaish, S. and Bottoms, E. (1971): The Skin and Friction: Deviations From Amonton's Laws, and the Effects of Hydration and Lubrication, *Br J Derm*, 84: 37-43.

Constanzo, R. M. and Gardner, E. P. (1980): A Quantitative Analysis of Responses of Direction-sensitive Neurons in Somatosensory Cortex of Awake Monkeys, *J Neurophysiol*, 43: 1319-1341.

Cooney, W. P., and Chao, E. Y. S. (1977): Biomechanical Analysis of Static Forces in the Thumb during Hand Function, *J Bone Joint Surgery*, 59A(1): 27-36.

Cutkosky, M. R. and Wright, P. K. (1986): Modeling Manufacturing Grips and Correlations with the Design of Robotic Hands. *IEEE International Conference on Robotics and Automation*, San Francisco, Calif, April 7-10, 1533-1539.

deKleer, J., Doyle, J., Steele, G. L. and Sussman, G.J. (1977): AMORD: Explicit Control of Reasoning, *Proc Symp Artificial Intelligence and Programming Languages* (SIGART Newsletter, 64), August, 116-125.

DeLong, M. R. (1974): Motor Functions of the Basal Ganglia: Single-unit Activity During Movement. In: *The Neurosciences: Third Study Program*, F. O. Scmitt and F. G. Worden (Eds.), Cambridge: MIT Press, 319-325.

DeLong, M. R., Alexander, G. E., Georgopoulos, A. P. Crutcher, M. D., Mitchell, S. J. and Richardson, R. T. (1984): Role of Basal Ganglia in Limb Movements, *Human Neurobiol*, 2: 235-244.

Denny-Brown, D. (1960): Motor mechanism-Introduction: The general principles of motor integration. In: *Handbook of Physiology*. Amer Physio Soc, vol 2, 781-796.

Denny-Brown, D. (1966): *The Cerebral Control of Movement*. Liverpool: Liverpool University Press.

Dev, P. (1975): Perception of depth surfaces in random-dot steriograms: a neural model. *Int J Man-Machine Studies* 7: 511-528.

Didday, R. L. (1976): A model of visuomotor mechanisms in the frog optic tectum, *Math Biosci*, 30: 169-180.

Eccles, J. C. (1977): *The Understanding of the Brain, Second Edition*, NY: McGraw-Hill.

Evarts, E. V. (1967): Representation of Movement and Muscles by Pyramidal Tract Neurons of the Precentral Motor Cortex. In: *Neurophysiological Basis of Normal and Abnormal Motor Activities*, M. D. Yahr and D. P. Purpura (Eds.), NY: Raven Press, 215-253.

Evarts, E. V. (1968): Relation of pyramidal tract activity to force exerted during voluntary movement, *J. Neurophysiol*, 31: 14-27.

Evarts, E. V. (1981): Role of motor cortex in voluntary movement in primates, in

Handbook of Physiology - The Nervous System, II. Motor Control, (V. B. Brooks, ed), Bethesda, MD: American Physiological Society, 1083-1120.

Evarts, E. V. (1984): Hierarchies and Emergent Features in Motor Control. In: *Dynamic Aspects of Neocortical Function*, G. M. Edelman, W. E. Gall, W. M. Cowan (Eds.), NY: John Wiley and Sons, 557-579.

Evarts, E. V.,Shinoda, Y, and Wise, S. P. (1984): *Neurophyiological Approaches to Higher Brain Functions*, NY: Wiley-Interscience.

Evarts, E. V. and Tanji, J. (1974): Gating of motor cortex reflexes by prior instruction. *Brain Res*, 71: 479-494.

Fearing, R. S. (1983): Touch Processing for Determining a Stable Grasp, Dept of Elec Eng and Computer Science, MIT, Cambridge, Mass.

Fearing, R. S. (1986): Simplified Grasping and Manipulation with Dextrous Robot Hands, *IEEE J Robotics and Automation*, RA-2(4): 188-195.

Fetz, E. E. and Cheney, P. D. (1980): Postspike facilitation of forelimb muscle activity by primate corticomotoneuronal cells. *J Neurophysiol*, 44: 751-772.

Fischer, G. W. (1969): A Treatise on the Topographical Anatomy of the Long Finger and a Biomechanical Investigaion of its Interjoint Movement, Ph.D Thesis, University of Iowa, Iowa.

Focillon, H. (1947): Eloge de la main. In: *Vie des Formes*. Paris: Presses Universitaires de France.

Friedman, D. P. and Jones, E. G. (1981): Thalamic Input to Areas 3a and 2 in Monkeys. *J Neurophys*, 45(1): 59-85.

Fries, W. (1985): Inputs from Motor and Premotor Cortex to the Superior Colliculus of the Macaque Monkey, *Beh Brain Res*, 18: 95-105.

Garnett, R. and Stephens, J. A. (1981): Changes in the recruitment threshold of motor units produced by cutaneous stimulation in man. *J Physiol* (Lond), 311: 463-473.

Gentilucci, M., Scandolara, C., Pigarev, I. N., and Rizzolatti, G. (1983): Visual Responses in the Postarcuate Cortex (Area 6) of the Monkey that are Independent of Eye Position, *Exp Brain Res*, 50: 464-468.

Georgopoulos, A. P., Caminiti, R., Kalaska, J. F., Massey, J. T. (1983): Spatial Coding of Movement: A Hypothesis Concerning the Coding of Movement Direction by Motor Cortical Populations. In: *Neural Coding of Motor Performance*, J. Massion, J. Paillard, W. Schultz, and M. Wiesendanger, (Eds.), NY: Springer-Verlag, 327-336.

Georgopoulos, A. P., Kalaska, J. F., Crutcher, M. D., Caminiti, R., and Massey, J. T. (1984): The Representation of Movement Direction in the Motor Cortex: Single Cell and Population Studies. In: *Dynamic Aspects of Neocortical Function*, G. M. Edelman, W. E. Gall, and W. M. Cowan (Eds.), NY: John Wiley and Sons, 501-524.

Georgopoulos, A. P., Schwartz, A. B., and Kettner, R. E. (1986): Neuronal Population Coding of Movement Direction, *Science*, 233: 1416-1419.

Glees, P. and Cole, J. (1950): Recovery of Skilled Motor Functions After Small Repeated Lesions of Motor Cortex in Macaque. *J Neurophys*, 13: 137-148.

Glicenstein J. and Dardour J. C. (1981): The Pulp: Anatomy and Physiology. In: *The Hand, vol 1*, R. Tubiana (Ed.), Phila: W. B. Saunders and Co., 116-120.

Godschalk, M., Lemon, R. N., Nijs, H. G.T, and Kuypers, H. G.J. M. (1981): Behaviour of Neurons in Monkey Peri-arcuate and Precentral Cortex Before and During Visually Guided Arm and Hand Movements, *Exp Brain Res*, 44: 113-116.

Godschalk, M., Lemon, R. N., Kuypers, H. G.J. M., and Van Der Steen, J. (1985): The Involvement of Monkey Premotor Cortex Neurones in Preparation of Visually Cued Arm Movements, *Behav Brain Research*, 18.

Goodglass, H. and Kaplan, E. (1963): Disturbance of Gesture and Pantomime in Aphasia, *Brain*, 86: 703-720.

Griffiths, H. E. (1943): Treatment of the Injured Workman, *Lancet*, i: 729.

Grillner, S. (1975): Locomotion in Vertebrates: Central Mechanisms and Reflex Interaction. *Physiol. Rev.*, 55: 247-304.

Haaxma, R. and Kuypers, H. G.J. (1974): Role of Occipito-frontal Cortico-Cortical Connections in Visual Guidance of Relatively Independent Hand and Finger Movements in Rhesus Monkeys, *Brain Res.*, 71(2-3): 361-366.

Hanafusa, H. and Asada, H. (1982): Stable Prehension by a Robot Hand with Elastic Fingers. In: M. Brady, J. M. Hollerbach, T. L. Johnson, T. Lozano-Perez, M. T. Mason (Eds.), *Robot Motion: Planning and Control*, Cambridge: MIT Press, 323-336.

Hayes-Roth, F. and Lesser, V. R. (1977): Focus of Attention in the Hearsay-II Speech Understanding System, *CMU CS report*, Carnegie-Mellon University, Pittsburgh, Pa.

Hazelton, F. T., Smidt, G. L., Flatt, A. E., and Stephens, R. I. (1975): The Influence of wrist position on the force produced by the Finger flexors, *J. Biomechanics*, 8: 301-306.

Hinton, G. E. and Sejnowski, T. J. (1986): Learning and Relearning in Boltzmann Machines. In: *Parallel Distributed Processing: Explorations in the Microstructure of Cognition. Volume 1: Foundations*, D. E. Rumelhart, J. L. McClelland and the PDP Research Group (Eds.), 282-317.

Hollerbach, J. M. (1982): Workshop on the Design and Control of Dextrous Hands. *A.I. Memo 661*, A.I. Laboratory, M.I.T., Cambridge, Mass.

Hollerbach, J. M. and Flash, T. (1982): Dynamic Interactions Between Limb Segments During Planar Arm Movements, *Biological Cybernetics*, 44: 67-77.

Hopfield, J. J. (1982): Neural networks and physical systems with emergent collective computational abilities. *Proc Nat Acad Science*, 79: 2554-2558.

Hopfield, J. J. and Tank, D. W. (1986): Computing with Neural Circuits: A Model. *Science*, 233: 625-633.

House, D. H. (1984): Neural models of depth perception in frogs and toads, *COINS Tech Report 84-16*, Univ of Massachusetts, Amherst, Mass.

Humphrey, D. R. (1979): The Cortical Control of Reaching. In: *Posture and Movement*, D. R. Humphrey and Talbot (Eds.), NY: Raven Press, 51-112

Humphrey, D. R. and Rietz, R. (1976): Cells of origin of corticorubral projections

from the arm area of primate motor cortex and their synaptic actions in the red nucleus, *Brain Res*, 110: 162-169.

Humphrey, D. R., Gold, R. and Reed, D.J. (1978): Origins of Cortical and Cerebellar Projections to the Red Nucleus in the Monkey, *Soc. Neurosci. Abstr*, 4: 297.

Hyvarinen, J. A. and Poranen, A. (1978): Movement-sensitive and direction and orientation-selective cutaneous receptive fields in the hand area of the post-central gyrus in monkeys. *J Physiol*, 283: 523-537.

Iberall, T. (1986): The Representation of Objects for Grasping. *Proc Eighth Cognitive Science Society Conf*, August 15-17, Amherst, Mass, 547-561.

Iberall, T., Bingham G. and Arbib, M. A. (1986): Opposition Space as a Structuring Concept for the Analysis of Skilled Hand Movements. In: *Generation and Modulation of Action Patterns*, H. Heuer and C. Fromm (Eds.), Berlin: Springer-Verlag, 158-173. (available as *COINS Technical Report 85-19*, Dept of Computer Science, University of Mass, Amherst, Mass.)

Iberall, T. and Lyons, D. (1984): Towards Perceptual Robotics. *Proc 1984 IEEE Intl Conf Systems, Man, Cybernetics*, Halifax, Nova Scotia, Oct. 9-12, 147-157. (available as *COINS Technical Report 84-17*, Dept of Computer Science, University of Mass, Amherst, Mass.)

Iberall, T. and Lyons, D. (1985): Perceptual Robotics: Towards a Language for the Integration of Sensation and Perception in a Dextrous Robot Hand. In: *Languages for Automation*, S. Chang, (Ed.). NY: Plenum Press, 415-427.

Iwamura, Y., and Tanaka, M. (1978): Postcentral neurons in Hand Region of area 2: their possible role in the form discrimination of tactile objects, *Brain Research*, 150: 662-666.

Iwamura, Y., Tanaka, M. and Hikosaka, O. (1980): Overlapping Representation of Fingers in the Somatosensory Cortex (Area 2) of the Conscious Monkey. *Brain Research*, 197: 516-520.

Iwamura, Y., Tanaka, M., Sakamoto, M., and Hikosaka, O. (1983a): Functional Subdivisions Representing Different Finger Regions in Area 3 of the First Somatosensory Cortex of the Conscious Monkey, *Exp Brain Res.*, 51: 315-326.

Iwamura, Y., Tanaka, M., Sakamoto, M., and Hikosaka, O. (1983b): Converging Patterns of Finger Representation and Complex Response Properties of Neurons in Area 1 of the First Somatosensory Cortex of the Conscious Monkey, *Exp Brain Res*, 51: 327-337.

Jackson, J. H. (1873): On the anatomical and physiological localization of movements in the brain. *Lancet* i: 162.

Jackson, J. H. (1889): On the comparative study of diseases of the nervous system. *Brit Med J*, 2: 355-362.

Jackson, J. H. (1931): *Selected writings of John Hughlings Jasckson, vol 1*, J. Taylor (Ed.), London: Hodder and Stoughton.

Jackson, J. H. (1932): *Selected writings of John Hughlings Jasckson, vol 2*, J. Taylor (Ed.), London: Hodder and Stoughton.

Jacobsen, S. C., Wood, J. E., Knutti, D. F., Biggers, K. B., Iversen, E. K. (1984): The Utah/M.I.T. Dextrous Hand: Work in Progress, *Inter J Robotics Research*, 4(3): 21-50.

Jeannerod, M. (1981): Intersegmental Coordination During Reaching at Natural Visual Objects. In: *Attention and Performance, IX*, J. Long, and A. Baddeley, (Eds.), Hillsdale: Erlbaum, 153-168.

Jeannerod, M. (1984): The Timing of Natural Prehension Movements, *Journal of Motor Behavior*, 16(3): 235-254.

Jeannerod, M. (1986): The Formation of Finger grip during prehension. A cortically mediated visuomotor pattern. *Beh Brain Research*, 19: 99-116.

Jeannerod, M. and Biguer, B. (1982): Visuomotor Mechanisms in Reaching within Extrapersonal Space. In: *Advances in the Analysis of Visual Behavior*, D. J. Ingle, M. A. Goodale, and R. J. W. Mansfield, (Eds.), Cambridge: MIT Press, 387-409.

Jeannerod, M., Michel, J., and Prablanc, C. (1984): The Control of Hand Move-

ments in a Case of Hemianaesthesia Following a Parietal Lesion, *Brain*, 107: 899-920.

Johansson, R. S. and Vallbo, A. B. (1983): Tactile Sensory Coding in the Glabrous Skin of the Human Hand, *Trends in Neuroscience*, 6(1): 27-37.

Johansson, R. S. and Westling, G. (1984): Influences of Cutaneous Sensory Input on the Motor Coordination During Precision Manipulation. In: *Somatosensory Mechanisms*, C. Von Fuler and O. Franzen (Eds.), London: MacMillian, 249-260.

Johnson, J. I. (1985): Thalamocortical Organization in the Raccoon: Comparison with the Primate. In: *Hand Function and the Neocortex*, A. W. Goodwin and I. Darian-Smith (Eds.), Berlin: Springer Verlag, 294-312.

Jones, E. G. (1975): Varieties and distribution of nonpyramidal cells in the somatic sensory cortex of the squirrel monkey. *J Comp Neurol*, 160: 205-268.

Jones, E. G. (1981): Anatomy of Cerebral Cortex: Columnar input-output Relations. In: *The Organization of the Cerebral Cortex*, F. O. Schmitt, F. G. Worden, G. Adelman, and S. G. Dennis (Eds.), Cambridge: MIT Press, 199-235.

Jones, E. G., Coulter, J. D., Burton, H., and Porter, R. (1977): Cells of Origin and Terminal Distribtuion of Corticostriatal Fibers Arising in the Sensory-motor Cortex of Monkeys. *J. Comp. Neurol.*, 173: 53-77.

Jones, E. G., Coulter, J. D. and Hendry, S. H. C. (1978): Intracortical connectivity of architectonic fields in the somatic sensory, motor and parietal cortex of monkeys, *J. Comp. Neurol.*, 181: 291-348.

Jones, E. G. and Powell, T. P. S. (1969): Connections of somatic sensory cortex of the Rhesus monkey. I. Ipsilateral cortical connections, *Brain*, 92: 477-502.

Jones, E. G. and Powell, T. P. S. (1970): An anatomical study of converging sensory pathways within the cerebral cortex of the monkey, *Brain*, 93: 793-820.

Jones, E. G., and Wise, S. P. (1977): Size, laminar and columnar distribution of efferent cells in the sensory-motor cortex of monkeys, *J. Comp. Neurol* 175: 391-438.

Jordan, M. I. (1986): Serial order: A Parallel Distributed Processing Approach, *ICS Report 8604*, Institute for Cognitive Science, University of Calif, San Diego,

La Jolla, Calif.

Kaas, J. II. (1982): The Segragation of Function in the Nervous System: Why do Sensory Systems Have So Many Subdivisions?, *Sensory Phys* 7: 201-240.

Kaas, J. H. (1983): What if Anything is SI? Organization of the First Somatosensory Area of Cortex, *Physiol Reviews*, 63(1): 206-231.

Kaas, J. II., Nelson, R. J., Sur, M., Lin, C. S. and Merzenich, M. M. (1979): Multiple Representations of the Body within the Primary Somatosensory Cortex of Primates. *Science*, 204: 521-523.

Kaas, J. II., Merzenich, M. M. and Killacky, II. P. (1983): The Reorganization of Somatosensory Cortex Following Peripheral Nerve Damage in Adult and Developing Mammals, *Ann. Rev. Neurosci*, 6: 325-356.

Kalaska, J. F., Georgopoulos, A. P., and Caminiti, R. (1983): Cortical mechanisms of two-dimensional aimed arm movements. VIII. Cell discharge in motor cortex and area 5 varies with movement direction, not with final position of the arm, *Soc. Neurosci. Abstr*, 9:491.

Kalil, K. (1975): Thalamo-cortical Projections of the VA and VL in the Rhesus Monkey, *Neurosci Abstr*, 1: 171.

Kanda, K. and Desmedt, J. E. (1983): Cutaneous Facilitation of Large Motor Units and Motor Control of Human Fingers in Precision Grip. In: J. E. Desmedt, ed, *Motor Control Mechanisms in Health and Disease*, NY: Raven Press, 253-261.

Kandel, E. R. and Schwartz, J. H.,eds (1985): *Principles of Neural Science, 2nd Edition*, NY: Elsevier/North Holland.

Kapandji 1. A. (1982): *The Physiology of the Joints. Volume One. Upper Limb*, Fifth Edition, Edinburgh: Churchill Livingstone.

Kraft, G. and Detels, P. (1972): Position of Function of the Wrist, *Arch Phys Med Rehab*, 53: 272-275.

Kunzle, H. (1978): An autoradiographic analysis of the efferent connections from premotor and adjacent prefrontal regions (areas 6 and 9) in Macaca fasicularis, *Brain, Behav. Evol.*, 15: 185-234.

Kuo, J. S., Carpenter, M. B. (1973): Organization of Pallidothalamic Projections in the Rhesus Monkey, *J Comp Neurol*, 151: 201-236.

Kuypers, H. G. J. M. (1964): The Descending Pathways to the Spinal Cord, Their Anatomy and Function. *Prog. Brain Res.*, 11: 178-202.

Kuypers, H. G. J. M. (1973): The anatomical organization of the descending pathways and their contributions to motor control especially in primates. In: *New Developments in Electromyology and Clinical Neurophysiology*, J. E. Desmedt (Ed.), 3, Basel: S Kruger, 38-68.

Kuypers, H. G. J. M. and Brinkman, J. (1970): Precentral projections to different parts of the spinal intermediate zone in the Rhesus monkey *Brain Res*, 24: 29-48.

Kuypers, H. G. J. M. and Lawrence, D. G. (1967): Cortical Projections to the Red Nucleus and the Brain Stem in the Rhesus Monkey, *Brain Res.*, 4: 151-188.

Kwan, H. C., MacKay, W. A., Murphy, J. T., and Wong, Y. C. (1978): Spatial organization of precentral cortex in awake primates. II. Motor outputs, *J Neurophysiology*, 41(5): 1120-1131.

Landsmeer, J. M. F. (1962): Power Grip and Precision Handling, *Ann. Rheum. Dis*, 21: 164-170.

Lawrence, D. G. and Kuypers, H. G. J. M. (1968): The functional organization of the motor system in the monkey. I. The effects of bilateral pyramidal lesions. *Brain*, 91:

LeGros-Clark (1959): *The Antecedents of Man*, Edinburgh: Edinburgh University Press.

Lemon, R. N. (1981a): Functional properties of monkey motor cortex neurones receiving afferent input from the hand and fingers, *J Physiol*, 311: 497-519.

Lemon, R. N. (1981b): Variety of functional organization within the monkey motor cortex, *J Physiol*, 311: 521-540.

Lemon, R. N. and van der Burg, J. (1979): Short-latency Peripheral Inputs to Thalamic Neurones Projecting to the Motor Cortex in the Monkey, *Exp Brain Res*, 36: 445-462.

Lemon, R. N. and Muir, R. B. (1981): Direct facilitation of intrinsic hand muscle activity by motor cortex neurones in the conscious monkey, *J Physiol*, 320: 74P.

Lemon, R. N. and Muir, R. B. (1982): Responses of hand and forearm muscles to pyramidal tract stimulation during voluntary hand movements in the monkey (Macaca nemestrina), *Journal of Physiology*, 338: 31P.

Lemon, R. N. and Muir, R. B. (1983): Responses of hand and forearm muscles to pyramidal tract stimulation during voluntary hand movements in the monkey (Macaca nemestrina), *J Physiol*, 338: 31P.

Lewis, O.J. (1977): Joint Remodelling and the Evolution of the Human Hand. *J Anat*, 123(1): 157-201.

Liddell, E. G. and Phillips, C. G. (1950): Thresholds of cortical representation, *Brain*, 73: 125-140.

Long, C. (1981): Electromyographic Studies of Hand Function. In: *The Hand*, vol 1, R. Tubiana (Ed.) Phila: W. B. Saunders and Co, 427-440.

Long, C., Conrad, P. W., Hall, E. A., Furler, S. L. (1970): Intrinsic-Extrinsic Muscle Control of the Hand in Power Grip and Precision Handling, *The Journal of Bone and Joint Surgery*, 52A(5): 853-867.

Lozano-Perez, T. and Winston, P. H. (1977): LAMA: A Language for Automatic Mechanical Assembly, *Proc 5th Intl Jt Conf Artificial Intelligence*, Cambridge, Mass, August, 710-716.

Lundberg, A. (1979): Integration in a Propriospinal Motor Centre Controlling the Forelimbs in the Cat. In: *Integration in the Nervous System*, H. Asanuma and V. J. Wilson (Eds.), Tokyo: Igaku-Shoin, 47-64.

Lyons, D. (1985): A Simple Set of Grasps for a Dextrous Hand, *COINS Technical Report 85-37*, Dept of Computer and Information Science, Univ of Massachusetts, Amherst, Mass.

MacKenzie, C. L. and Martenuik, R. G. (1985): Motor Skill: Feedback, Knowl-

edge, and Structural Issues, *Canadian J Psychology*, 39(2): 313-337.

MacKenzie, C. L., Marteniuk, R. G., Dugas, C., Liske, D. and Eickmeier, B. Three dimensinal Movement Trajectories in Fitts' task: Implications for Control, in press.

Marteniuk, R. G., MacKenzie, C. L., Jeannerod, M., Athenes, S. and Dugas, C.: Constraints on Human Arm Movement Trajectories, in press.

Marzke, M. W. (1983): Joint Functions and Grips of the *Australopithecus afarensis* Hand, with Special Reference to the Region of the Capitate, *J Human Evolution*, 12, 197-211.

Mason, M. (1982): Manipulator Grasping and Pushing Operations, *AI-TR-690*, A.I. Laboratory, M.I.T., Cambridge, Mass.

McBride, E. D. (1942): *Disability Evaluation. Third Edition*, Phila: J. B. Lippincott Co.

McCulloch, W. S. (1965): *Embodiments of Mind.* Cambridge: The MIT Press.

Merzenich, M. M. and Kaas, J. H. (1980): Principles of Organization of Sensory-Perceptual Systems in Mammals, *Progress in Psychobiology and Physiological Psychology*, 9: 1-42.

Merton, P. A. (1964): Human position sense and sense of effort, *Symp Soc Exp Biol*, 18: 387-400.

Minsky, M. (1974): A Framework for Representing Knowledge. *MIT AI Lab Memo 306*, MIT.

Minsky, M. (1986): *A Society of Mind*, NY: Simon and Schuster.

Moll and Kuypers (1977): Premotor cortical ablations in monkeys. Contralateral changes in visually guided reaching behavior, *Science*, 198: 317-319.

Moore, D. F. (1972): *The Friction and Lubrication of Elastomers*, NY: Pergamon Press.

Moore, D. F. (1975): *Principles and Applications of Tribology*, NY: Pergamon Press.

Mountcastle, V. B. (1978): An Organizing Principle for Cerebral Function: The Unit Module and the Distributed System. In: *The Mindful Brain: Cortical Organization and the Group-Selective Theory of Higher Brain Function*, G. M. Edelman and V. B. Mountcastle (Eds.), Cambridge: The MIT Press, 7-50.

Mountcastle, V. B., Lynch, J. C., Georgopoulos, A., Sakata, H., Acuna, C. (1975): Posterior Parietal Association Cortex of the Monkey: Command Functions for Operations within Extrapersonal Space, *J Neurophysiol*, 38: 871-908.

Muakkassa, K. F. and Strick, P. L. (1979): Frontal lobe inputs to primate motor cortex. Evidence for four somatotopically organizaed 'premotor' areas. *Brain Research*, 177: 176-182.

Muir, R. B., and Lemon, R. N. (1983): Corticospinal Neurons with a Special Role in Precision Grip, *Brain Research*, 261: 312-316.

Murphy, J. T., Kwan, H. C., MacKay, W. A., and Wong, Y. C. (1978): Spatial organization of precentral cortex in awake primate. III. Input output coupling, *J Neurophysiology*, 41(5): 1132-1139.

Musgrave, J. H. (1971): How Dextrous was Neanderthal Man? *Nature*, 233, Oct 22, 538-541.

Napier, J. (1956): The Prehensile Movements of the Human Hand, *Journal of Bone and Joint Surgery*, 38B(4): 902-913.

Napier, J. R. (1961): Prehensility and opposability in the hand of primates. *Symp Zool Soc, London* 5: 115-132.

Neisser, U. (1976): *Cognition and Reality: Principles and Implications of Cognitive Psychology*, San Francisco: W. Freeman.

Okada, T. (1982): Computer Control of Multijointed Finger System for Precise Object-handling, *IEEE Tran Sys, Man, Cyber*, SMC-12(3), 289-299.

Paillard, J. (1982): The Contribution of Peripheral and Central Vision to Visually Guided Reaching. In: *Analysis of Visual Behavior*, D.J. Ingle, M. A. Goodale, and R.J. W. Mansfield (Eds.), Cambridge: MIT Press, 367-385.

Pandya, D. P. and Kuypers, H. G.J. M. (1969): Cortico-cortical connections

in the rhesus monkey, *Brain Res.*, 13: 13-36.

Pandya, D. P. and Vignolo, L. A. (1971): Intra- and interhemispheric projections of the precentral, premotor and acruate areas in the rhesus monkey, *Brain Res.*, 26: 217-233.

Paul, R. (1981): *Robot Manipulators: Mathematics, Programming, and Control.* Cambridge: MIT Press.

Penfield, W. and Rasmussen, T. (1952): *The Cerebral Cortex of Man*, NY: Macmillian.

Petras, J. M. and Lehman, R. A. W. (1966): Corticospinal fibers in the raccoon, *Brain Res*, 3:195-197.

Phillips, C.G (1966): Changing Concepts of the Precentral Motor Area. In: *Brain and Conscious Experience*, J. C. Eccles (Ed.), NY: Springer-Verlag, 389-421.

Phillips, C.G (1969): Motor apparatus of the baboon's hand, *Proc R Soc London Ser B*, 173: 141-174.

Phillips, C. G.(1971): Evolution of the Corticospinal Tract in Primates with Special Reference to the Hand, *Proc 3rd Int Congr Primat*, vol 2, Basel: S Karger.

Phillips, C. G. (1975): Laying the ghost of 'muscles versus movement'. *Can J Nuerol Sci.*, 2: 209-218.

Phillips, C. G.(1978): Significance of the Monosynaptic Cortical Projection To Spinal Motoneurones in Primates. In: *Cerebral Motor Control in Man: Long Loop Mechanisms*, J. E. Desmedt (Ed.), Basel: S Karger, 1-9.

Phillips, C. G. and Porter, R. (1964): The pyramidal projection to motoneurones of some muscle groups of the baboon's forelimb, *Prog Brain Res*, 12: 222-242.

Phillips, C. G. and Porter, R. (1977): *Corticospinal Neurones: Their Role in Movement*, London: Academic Press.

Popplestone, R.J, Ambler, A. P. and Bellos, I. M. (1980): An Interpreter for a Language for Describing Assemblies, *Artificial Intelligence*, 14: 79-107.

Power, R. P. and Graham, A. (1976): Dominance of Touch by Vision: Generalization of the Hypothesis to a Tactually Experienced Population, *Perception*, 5: 161-166.

Pryce, J. C. (1980): The Wrist Position Between Neutral and Ulnar Deviation that Facilitates the Maximum Power Grip Strength, *J Biomechanics*, 13: 505-511.

Quilliam, T. A. (1978): The Structure of Fingerprint Skin. In: *Active Touch*, G. Gordon (Ed.), Oxford: Pergamon Press Ltd, 1-18.

Quillian, M. R. (1968): Semantic memory. In: *Semantic information processing*, M. Minsky (Ed.), Cambridge: MIT Press, 227-270.

Randolf, M and Semmes, J. (1974): Behavioral consequences of selective subtotal ablations in the postcentral gyrus of *Macaca mulatta*. *Brain Res*, 70: 55-70.

Rizzolatti, G., Matelli, M., and Pavesi, G. (1983): Deficits in Attention and Movement following the Removal of Postarcuate (area 6) and prearcuate (area 8) cortex in Macaque Monkeys, *Brain*, 106: 655-673.

Rock, I. and Victor, J. (1964): Vision and Touch: An Experimentally Created Conflict between the Two Senses, *Science*, 143: 594-596.

Rothwell, J. C., Traub, M. M., Day, B. L., Obeso, J. A., Thomas, P. K., and Marsden, C. D. (1982): Manual Motor Performance in a Deafferented Man, *Brain*, 105, 515-542.

Rumelhart, D. E., Hinton, G. E., and Williams, R. J. (1986): Learning Internal Representations by Error Propagation. In: *Parallel Distributed Processing: Explorations in the Microstructure of Cognition. Volume 1: Foundations*, D. E. Rumelhart, J. L. McClelland and the PDP Research Group (Eds.), 318-362.

Russell, J. R. and deMyer, W. (1961): The quantitative origin of pyramidal axons of Macaca rhesus, with some remarks on the slow rate of axolysis, *Neurology*, 11: 98-108.

Salisbury, J. K. (1982): Kinematic and Force Analysis of Articulated Hands, *STAN-CS-82-921*, Dept of Computer Science, Stanford University, Stanford, Calif.

Schank, R. and Colby, K. eds (1973): *Computer Models of Thought and Language*, San Francisco: W. H. Freeman.

Schell, and Strick, P. L. (1984): Origin to Thalamic Inputs to APA and SMA, *J Neurosci*, 4: 539-560.

Schlesinger, G. (1919): Der Mechanische Aufbau der Kunstlichen Glieder. In: *Ersatzglieder und Arbeitshilfen*, M. Borchardt *et al* (Eds.), Berlin: Springer.

Sherrington, C. S. (1889): On Nerve-tracts Degenerating Secondarily to Lesions of the Cortex Cerebri (Preliminary), *J Physio. (Lond.)*, 10: 429-432.

Sherrington, C. S. (1906): *The Integrative Action of the Nervous System*, NY: Scribners.

Shik, M. L., Severin, F. V. and Orlovsky, G. N. (1966): Control of Walking and Running by means of Electrical Stimulation of the Mid-brain. *Biophysics*, 11: 756-765.

Shortliffe, E. H. (1976): MYCin A rule-based computer program for advising physicians regarding antimicrobial therapy selection. Computer-Based Medical Consultations: MYCIN. American Elsevier, NY.

Simon, H. A. (1977): Artificial Intellignece Systems That Understand. *Proc Intl Jount Conf on Artificial Intelligence*, 1059-1073.

Slocum, D. B. and Pratt, D. R. (1946): Disability Evaluation for the Hand, *J Bone Jt Surgery*, 28: 491.

Slovly, R. C. (1967): A Study of the Power Grip Strength and How it is Influenced by Wirst Joint Position, Unpublished Master's Thesis, University of Iowa.

Smith, A. M., Bourbonnais, D. and Blanchette, G. (1981): Interaction between Forced Grasping and a Learned Precision Grip after Ablation of the Supplementary Motor Area, *Brain Res.*, 222: 395-400.

Smith, A. M., Frysinger, R. C., and Bourbonnais, D. (1983): Interaction Between Motor Commands and Somatosensory Afferents in the Control of Prehension. In: *Motor Control Mechanisms in Health and Disease*, J. E. Desmedt (Ed.), NY: Raven Press, 373-385.

Smith, A. M., Wetts, R. and Kalaska, J. F. (1985): Activity of Dentate and Interpositus Neurons During Maintained Isometric Prehension. In: *Hand Function and the Neocortex*, A. W. Goodwin and I. Darian-Smith (Eds.), Berlin: Springer Verlag, 248-258.

Strick, P. L. (1985): How Do the Basal Ganglia and Cerebellum Gain Access to the Cortical Motor Areas?, *Beh Brain Res*, 18: 107-123.

Strick, P. L. and Kim, C. C. (1978): Input to Primate Motor Cortex from Posterior Parietal Cortex (Area 5). I. Demonstration by Retrograde Transport. *Brain Res.*, 157: 325-330.

Strick, P. L., and Preston, J. B. (1978): Multiple Representation in the Primate Motor Cortex, *Brain Res.*, 154: 366-370.

Strick, P. L., and Preston, J. B. (1979): Multiple Representation in the Motor Cortex: A New Concept of Input-Output Organization for the Forearm Reprsentation. In: *Integration in the Nervous System*, H. Asanuma and V. J. Wilson (Eds.), Tokyo: Igaku-Shoin, 205-221.

Strick, P. L., and Preston, J. B. (1982a): Two Representations of the Hand in Area 4 of a Primate. I. Motor Output Organization, *J Neurophys*, 48(1): 139-149.

Strick, P. L., and Preston, J. B. (1982b): Two Representations of the Hand in Area 4 of a Primate. II. Somatosensory Input Organization, *J Neurophys*, 48(1): 150-159.

Tanji, J., and Evarts, E. V. (1976): Anticipatory Activity of Motor Cortex Neurons in Relation to Direction of an Intended Movement, *J. Neurophysiol*, 39: 1062-1068.

Tanji, K., and Kurata (1979): *Neurosci Lett*, 12: 201-206.

Thach, W. T. and Jones, E. G. (1979): The Cerebellar Dentatothalamic Connection: Terminal Field, Lamellae, Rods and Somatotopy. *Brain Res*, 169: 168-172.

Thomine (1981): The Skin of the Hand. In: *The Hand, vol 1*, R. Tubiana (Ed.) Phila: W. B. Saunders and Co, 107-115.

Tower, S. S. (1940): Pyramidal lesion in the monkey. *Brain*, 63: 36-90.

Travis, A. M. (1955): Neurological Deficiencies Following Supplementary Motor Area Lesions in *Macaca mulatta, Brain*, 78: 155-173.

Tubiana, R. (1981): The Architecture and Functions of the Hand. In: *The Hand, vol 1*, R. Tubiana (Ed.), Phila: W. B. Saunders and Co, 19-93.

Tuttle, R. H. (1969): Qualitative and functional studeis on the hand of the Anthropoidea. I. The Hominodiea. *J Morph*, 128: 309-364.

Vijaykumar, R. and Arbib, M. A. (1986): A Task-level Robot Planner for Assemply Operations, *COINS TR 86-31*, University of Massachusetts, Amherst, Mass.

Walshe, F. M. R. (1963): *Diseases of the nervous system*, 10th ed, Edinburgh: Livingstone.

Warren, D. H. (1982): The Development of Haptic Perception. In: *Tactual Perception: A Sourcebook*, W. Schiff and E. Foulke (Eds.), Cambridge: Cambridge University Press, 82-129.

WATSMART Technical Description, Northern Digital, Waterloo, Canada, 1985.

Welker, W. I. and Seidenstein, S. (1959): Somatic sensory representation in the cerebral cortex of the raccoon (Procyon loter). *J Comp Neurol*, 111: 469-501.

Wells, R., Ranney, D. and Keeler, A. (1985): The Interaction of Muscular and Elastic Forces During Unloaded Finger Movements: A Computer Graphics Model. In: *Biomechanics: Current Interdisciplinary Research*, S. M. Perrin and E. Schneider (Eds.), Dortrecht. Netherlands: Martinus Nijhof Publishers, 743-748.

Westling, G. and Johansson, R. S. (1984): Factors Influencing the Force Control During Precision Grip, *Exp Brain Res*, 53: 277-284.

Wiesendanger, M. (1983): Cortico-Cerebellar Loops. In: *Neural Coding of Motor Performance*, J. Massion, J. Paillard, W. Schultz, and M. Wiesendanger, (Eds.), NY: Springer-Verlag, 41-53.

Wiesendanger, M. (1986): Redistributive function of the motor cortex, *Trends in Neuroscience*, 9(3): 120-125.

Wiesendanger, M., Seguin, J.J and Kunzle, H. (1973): The supplementary motor area - A control system for posture? In: R. B. Stein, K. G. Pearson, R. S. Smith,

and J. B. Redford, (Eds.), *Control of Posture and Locomotion*, NY: Plenum Press, 331-346.

Wiesendanger, M. and Wiesendanger, R. (1984): The Supplementary Motor Area in the Light of Recent Investigations. In: *Sensory-Motor Integration in the Nervous System*, O. Creutzfeldt, R. F. Schmidt, W. D. Willis (Eds.), Berlin: Springer-Verlag, 382-392.

Wiesendanger, R., Wiesendanger, M., and Ruegg, D. G. (1979): An Anatomical Investigation of the Corticopontine Projection in the Primate (Macaca Fascicularis and Saimiri Sciureus). II. The Projection from Frontal and Parietal Assocation Areas. *Neuroscience*, 4: 747-765.

Wilkes, G. L., Brown, I. A. and Wildnauer, R. H. (1973): The Biomechanical Properties of Skin, *CRC Crit Rev in Bioengineering*, 1(4): 453-495.

Wing, A. M., Fraser C. (1983): The Contribution of the Thumb to Reaching Movements, *Quarterly J of Exp Psychology*, 35A: 297-309.

Wing, A. M., Turton, A., and Fraser, C. Grasp Size and Accuracy of Approach in Reaching, in press.

Wise, S. P. (1984): The Nonprimary Motor Cortex and its Role in the Cerebral Control of Movement. In: *Dynamic Aspects of Neocortical Function*, G. M. Edelman, W. E. Gall, and W. M. Cowan (Eds.), NY: John Wiley and Sons, 525-555.

Wong, Y. C., Kwan, H. C., MacKay, W. A., and Murphy, J. T. (1978): Spatial organization of precentral cortex in awake primates. I. Somatosensory inputs, *Journal of Neurophysiology*, 41(5): 1107-1119.

Wood Jones, F. (1920): *The Principles of Anatomy as Seen in the Hand.* Churchill, London.

Woodworth, R. S. (1899): The Accuracy of Voluntary Movements. *Psychol Rev Monograph Suppl.* 3: 114.

Woolsey, C. N. (1958): Organization of somatic sensory and motor areas of the cerebral cortex. In: *Biological and Biochemical Bases of Behavior*, H. F. Harlow and C. N. Woolsey (Eds.), Madison: Univ Wisconsin Press, 63-81.

Zarzecki, Strick and Asanuma (1978): Input to primate motor cortex from posterior parietal cortex (area 5). II. Identification by antidromic activation, *Brain Res.*, 157: 331-335.